Responses to reviewers' comments for manuscript

Variation in chemical composition and volatility of oxygenated organic aerosol in different rural, urban, and mountain environments

Wei Huang[1], Cheng Wu[2,3], Linyu Gao[4], Yvette Gramlich[2,5], Sophie L. Haslett[2,5], Joel Thornton[6], Felipe D. Lopez-Hilfiker[7], Ben H. Lee[6], Junwei Song[4], Harald Saathoff[4], Xiaoli Shen[4,8], Ramakrishna Ramisetty[4,9], Sachchida N. Tripathi[10], Dilip Ganguly[11], Feng Jiang[4], Magdalena Vallon[4], Siegfried Schobesberger[12], Taina Yli-Juuti[12], Claudia Mohr[2,5,13,14,*]

[1]Institute for Atmospheric and Earth System Research / Physics, Faculty of Science, University of Helsinki, 00014, Helsinki, Finland

[2]Department of Environmental Science, Stockholm University, 11418, Stockholm, Sweden

[3]Now at: Department of Chemistry and Molecular Biology, University of Gothenburg, 41296, Gothenburg, Sweden

[4]Institute of Meteorology and Climate Research, Karlsruhe Institute of Technology, 76344, Eggenstein-Leopoldshafen, Germany

[5]Bolin Centre for Climate Research, Stockholm University, 11418, Stockholm, Sweden

[6]Department of Atmospheric Sciences, University of Washington Seattle, Washington 98195, United States

[7]Tofwerk AG, 3600 Thun, Switzerland

[8]Now at: Department of Earth, Atmospheric, and Planetary Sciences, Purdue University, West Lafayette, Indiana 47907, United States

[9]Now at: TSI Instruments India Private Limited, 560102, Bangalore, India

[10]Department of Civil Engineering, Indian Institute of Technology Kanpur, 208016, Kanpur, India

[11]Centre for Atmospheric Sciences, Indian Institute of Technology Delhi, 110016, New Delhi, India

[12]Department of Technical Physics, University of Eastern Finland, 70211, Kuopio, Finland

[13]Now at: Department of Environmental Systems Science, ETH Zürich, 8006 Zürich, Switzerland

[14]Now at: Laboratory of Atmospheric Chemistry, Paul Scherrer Institute, 5232 Villigen, Switzerland

**Correspondence to*: Claudia Mohr (claudia.mohr@psi.ch)

We thank all the reviewers for their evaluation of the manuscript, and for their constructive feedback. Replies to the individual comments are directly added below in italics in green, and changes in the manuscript in italics in blue. Please note that only references that are part of the replies to the comments are listed in the bibliography at the end of this document. References in copied text excerpts from the manuscript are not included in the bibliography. Page and line numbers refer to the revised manuscript text.

Reviewer 1 ***(responses in italics)***

Organic aerosols are a major contributor to total aerosol mass concentrations and have implications for both human health and climate change. However, the formation of these aerosols is a complex supersaturation-driven process, involving highly dynamic vapor-particle interactions. Therefore, constraining the volatility of condensable vapors and the associated particles is critical for understanding the underlying oxidative chemistry and for better representation of organic aerosols in air quality models.

This paper presents data from ambient measurements of the chemical composition and thermogram of organic aerosols in various environments using the online and offline FIGAERO-CIMS methods. In addition, the authors estimated the particle volatility using a volatility parametrization and compared it with the thermal desorption profile in the lumped thermogram. The research topic of this paper is novel, the dataset is comprehensive, and the measurement techniques are state-of-the-art. Overall, this is a relevant study that fits within the scope of the ACP. However, the way the results are interpreted and discussed needs major revision to improve scientific rigor and to make it clearer to non-specialist readers. Here are my major comments:

We thank the reviewer for the constructive assessments of our manuscript. We appreciate your recommendation for publication in ACP and your time and consideration. We have carefully considered your suggestions and questions and addressed them in our revised manuscript. The point-to-point responses to the comments are given below.

1. While the dataset is comprehensive and covers various environments, I'm not convinced that it does not have a global representation. I would suggest that the authors remove text such as "across the globe" and "global dataset".

We understand the reviewer's concern and have removed the corresponding text as suggested throughout the manuscript.

2. Volatility calculation: It is not clear whether the authors used one parametrization for all data, or different parametrizations for data in different environments (or rather, for different types of compounds). If it's the former, I would suggest that the authors redo some of the calculations, because molecular formulas with the same number of carbon and oxygen atoms can have very different volatilities due to different functionalities (e.g., -OH and -OOH reduce volatility by the same amount). This could be a source of discrepancy between the calculated volatility and the thermal desorption profile. The authors can refer to this paper for further information (https://doi.org/10.1038/s41561-022-00922-5).

We have used the same parametrization for all data and have clarified that in the manuscript in Line 176. As parametrizations are developed based on different datasets comprising different compounds with different functionalities, different parametrizations can yield different results for the same dataset (e.g., Graham et al., 2023). However, for ambient datasets, to conclude the structure and functional groups from the molecular composition given by the mass spectrometer measurements will always remain speculative, at best, and requires ancillary data and measurements. We therefore believe that using the same parametrization for all datasets is the approach with the least bias. This is to some extent in agreement with the study by Nie et al. (2022) suggested by the reviewer. Nie et al. (2022) used different parametrization methods to calculate the volatility of gaseous oxygenated organic molecules (OOMs) detected by nitrate-CIMS, after identifying and classifying the OOMs based on their potential precursors using a novel workflow proposed in their paper. However, they also state that this workflow cannot be used to classify particle/aqueous-phase products, since the assumptions behind the classification are mostly based on gas-phase oxidation knowledge, and the data we present in our manuscript are from the particle phase.

We agree however with the reviewer that a comparison of different parametrizations could be instructive. Graham et al. (2023) did exactly this, investigating in depth the application of four different parametrizations to their chamber datasets on biogenic VOCs oxidized with either ozone or the nitrate radical and exposing the complexity of such an approach. They found that none of the four parametrizations investigated performed perfectly for all different biogenic terpene+NO_3 systems. For example, the Mohr et al. (2019) parametrization, tuned for -OOH functional groups, was found to work better for α-pinene+O_3 system, and thus it was speculated that the reaction products of α-pinene+O_3 have relatively more -OOH functional groups. The Daumit et al. (2013) parametrization assumes all oxygen atoms except those from -NO_3 are from -OH and =O functional groups and was found to work better for the α-pinene+NO_3 reaction products. These results underline again the complexity (and with that also the limitations) of assessments of the volatility (especially at the quantitative level) through parametrizations using the molecular composition as input, and even more so for complex ambient data from different locations and periods.

In order to clarify that, we have now added a comparison of results from the parametrization initially used in the manuscript (modified Li et al. (2016) method (Isaacman-VanWertz and Aumont, 2021;Daumit et al., 2013)) to results from using the parametrization by Donahue et al. (2011) (Figure R1a) if making a simple assumption about predominant aliphatic/aromatic OOMs at urban sites in winter (i.e., UST-w, UKA-w, and UDL) and predominant isoprene OOMs in MCC-t and RAB (Nie et al., 2022). The $\log_{10}C_{sat}$ (T) shows a similar trend for both parametrizations; however, the C_{sat} (T) using the Donahue et al. (2011) parametrization is on average 4 to 8 orders of magnitude lower, with the largest difference for UKA-w and smallest for UDL (Figure R1b). The discrepancies seem to be correlated with the average number of oxygen atoms (nO) in the bulk aerosol of the different environments (Pearson's R: 0.85; Figure R1b), confirming the influence of different functional groups on parametrization results. Our discussion of volatility results in this manuscript is therefore mostly qualitative. We also note that the correlation coefficients between thermal desorption-derived volatility and molecular composition-derived volatility for the two different parametrizations are comparable (Figure R1c).

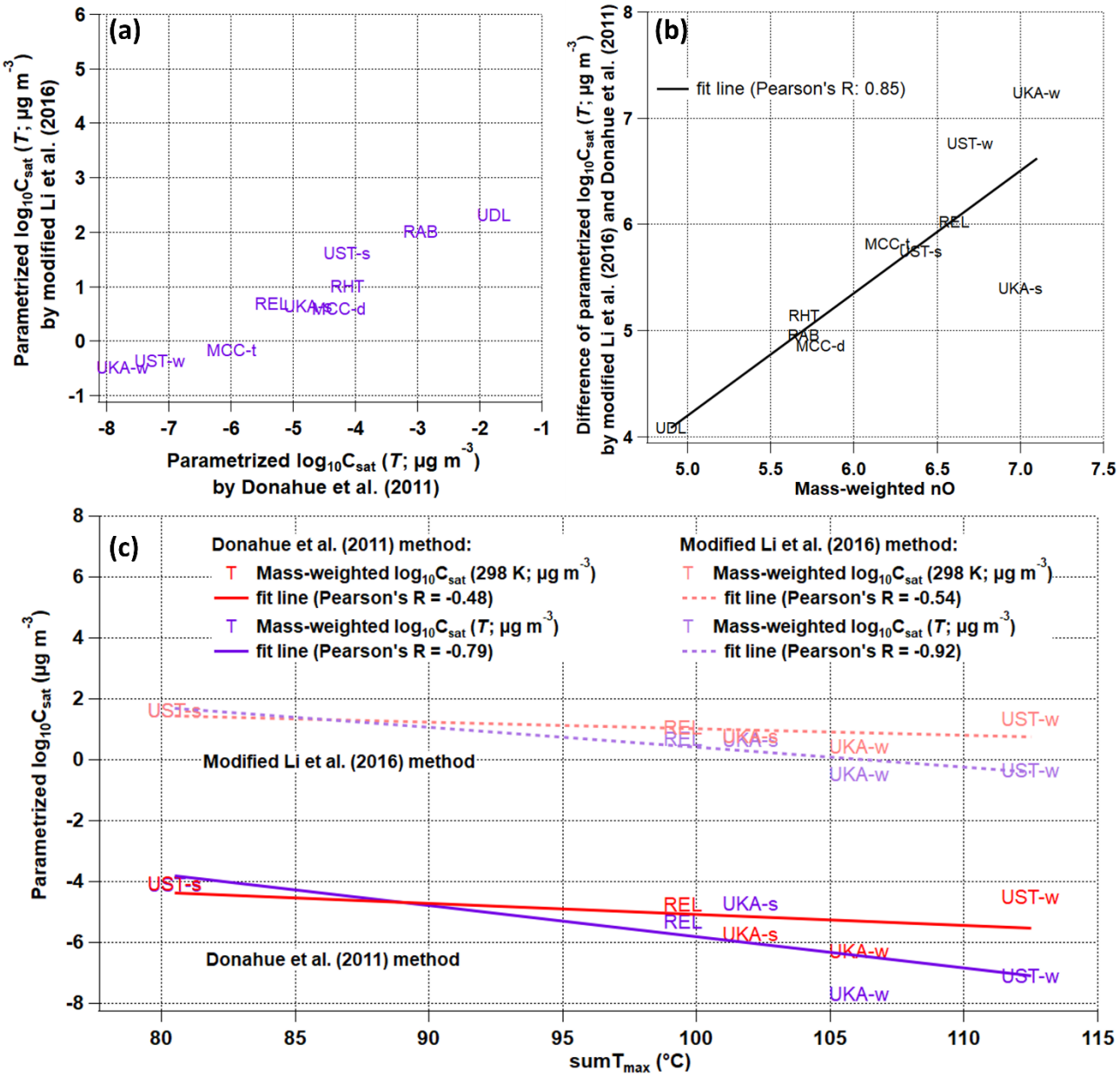

Figure R1. (a) *Comparison of the campaign-average mass-weighted $log_{10}C_{sat}$ (T) values using the modified Li et al. (2016) parametrization method (Daumit et al., 2013;Isaacman-VanWertz and Aumont, 2021) and the Donahue et al. (2011) method.* ***(b)*** *Comparison of the difference of campaign-average mass-weighted $log_{10}C_{sat}$ (T) values using the modified Li et al. (2016) parametrization method (Daumit et al., 2013;Isaacman-VanWertz and Aumont, 2021) and the Donahue et al. (2011) method with the mass-weighted number of oxygen atoms (nO).* ***(c)*** *Comparison of the campaign-average mass-weighted $log_{10}C_{sat}$ values and $sumT_{max}$ values for different locations and seasons (only datasets where the exact same FIGAERO setup was used), with mass-weighted $log_{10}C_{sat}$ (298 K) in red and mass-weighted $log_{10}C_{sat}$ (T) in purple; the colored lines are the fit lines for the corresponding markers.*

We have added Figure R1 as Figure S1 (all other SI figures are now Figure S2-S10) as well as more discussion in Lines 176, 184, 202, and 531 of the revised manuscript:

Line 176: "C_{sat} (298 K) was calculated using the approach by Li et al. (2016) as in equation (1) for all sites in order to not introduce more bias".

Line 184: "A recent study however found that the parametrization of C_{sat} for nitrate groups is highly uncertain (Graham et al., 2023). Even for different biogenic terpene+NO_3 systems, none of the four parametrizations Graham et al. (2023) investigated performed perfectly for all systems, as parametrizations which are developed based on different datasets comprising different compounds with different functionalities can yield different results for the same dataset (e.g., Graham et al., 2023). For example, the Mohr et al. (2019) parametrization method, which was tuned for -OOH functional groups, was found to work better for α-pinene+O_3 system and thus it was speculated that the α-pinene+O_3 system has more -OOH functional groups. The Daumit et al. (2013) parametrization method, which assumes all oxygen atoms except those from -NO_3 are from -OH and =O functional groups, was found to work better for α-pinene+NO_3 system and thus the α-pinene+NO_3 system is speculated to have more -OH and =O groups (Graham et al., 2023). These results underline again the complexity (and with that also the limitations) of assessments of the volatility (especially at the quantitative level) through parametrizations using the molecular composition as input, as already shown for laboratory measurements (Graham et al., 2023), and even more so for complex ambient data from different locations and periods."

Line 202: "We have added a comparison of the results from using the parametrization by Donahue et al. (2011) (Figure S1a) if making a simple assumption about predominant aliphatic/aromatic OOA at urban sites in winter (i.e., UST-w, UKA-w, and UDL) and predominant isoprene OOA in MCC-t and RAB (Nie et al., 2022). The $log_{10}C_{sat}$ (T) shows a similar trend for both parametrizations; however, the C_{sat} (T) using the Donahue et al. (2011) parametrization is on average 4 to 8 orders of magnitude lower, with the largest difference for UKA-w and smallest for UDL (Figure S1b). The discrepancies seem to be correlated with the average number of oxygen atoms (nO) in the bulk aerosol of the different environments (Pearson's R: 0.85; Figure S1b), confirming the influence of different functional groups on parametrization results. Our discussion of volatility results in this study is therefore mostly qualitative."

Line 531: "Although C_{sat} values can be biased by orders of magnitude using other parametrization methods (Graham et al., 2023), the general slope and trend is similar to the calibration curves or to that using other parametrization methods such as Donahue et al. (2011) method (Figure S1)."

3. Carbon number analysis: The author did not justify that nC alone can tell us much about the emission source, especially when comparing data from different environments. For example, nC for the urban sites is greater than that for the rural sites, but then nC for the MCC-d (anthropogenic influence) is less than that for the MCC-t (biogenic influence). Actually, I don't really see a pattern in the nC analysis. I would suggest that the authors condense the discussion and focus more on the oxidation state.

The average number of carbon atoms (nC) affects the parametrized C_{sat} and can be used to indicate potential precursor sources (Huang et al., 2019a), but we agree with the reviewer that a pattern is hard to distinguish. The air masses arriving at Chacaltaya (MCC) present a diverse mixture from various sources. This includes anthropogenic emissions from the near-by La Paz–El Alto metropolitan area, biogenic emissions from a range of biomes such as tropical rain forest and grasslands/savannas, and volcanic emissions (Bianchi et al. 2022). The contributions from these sources vary significantly between the transition and the dry seasons (Aliaga et al. 2021). The reasons for the smaller nC for MCC in the dry season (MCC-d) with higher anthropogenic influence compared to that in the transition season (MCC-t) with higher biogenic influence and the other urban sites are 1) the distance from the urban emissions and difference in car fleet and combustion conditions for MCC-d; 2) the impact of volcanic SO_2 emissions, as well as oxidation products of toluene for MCC-d (also seen in the slightly higher contributions of C_7 compounds in Figure S2)

(Bianchi et al., 2022;Zha et al., 2023b); and 3) the impact of monoterpene oxidation products for MCC-t (also seen in the slightly higher contributions of C_{8-10} compounds other than C_5 compounds for MCC-t in Figure S2).

For clarification, we have modified the discussion in Lines 214 and 229 of the revised manuscript as following:

Line 214: "We focus our analysis of the bulk molecular composition of OOA from the different locations here on the average number of carbon (nC) and oxygen atoms (nO) as they affect the parametrized C_{sat}, and give an indication of potential precursor sources (Huang et al., 2019a) and oxidation processes, respectively."

Line 229: "The air masses arriving at Chacaltaya present a diverse mixture from various sources, which vary significantly between the transition and the dry seasons (Aliaga et al. 2021). While air masses arriving at Chacaltaya during the dry season are more affected by volcanic SO_2 emissions as well as anthropogenic compounds such as toluene (also seen in the slightly higher contributions of C_7 compounds in Figure S2) (Bianchi et al., 2022;Zha et al., 2023b), air masses reaching Chacaltaya during the transition season have more influence from e.g. the Amazon Basin (Aliaga et al., 2021;Zha et al., 2023b); hence, a higher contribution of monoterpene ($C_{10}H_{16}$) and especially isoprene (C_5H_8) oxidation products is expected (also reflected in the clear peak of C_5 compounds and the second hump of C_{8-10} compounds in Figure S2) (Zha et al., 2023a)."

4. Mass contribution of organonitrates: Lacking explanations. Why do remote mountain sites have such a high CHON fraction? I don't think "in accordance with their proximity to forested areas" explains it. And why "possibly due to the less efficient production rates of CHON"?

The higher CHO contributions at the rural sites (79.9±5.2%) compared to the mountain (66.2±5.5%) and urban sites (72.6±4.3%) are in accordance with their proximity to forested areas, as stated in Line 304. The less efficient production rates of CHON or their faster loss rates caused by hydrolysis due to high RH apply only for the rural station in the southeastern U.S. (RAB; 5.6±2.6%), as stated in Line 305 and several earlier publications (Lee et al., 2020;Hu et al., 2011;Lee et al., 2016;Pye et al., 2015).The reason for the mountain site MCC to have such a high CHON fraction could be related to the inorganic nitrogen pollution being transported up there from the polluted boundary layer of La Paz–El Alto metropolitan area (Bianchi et al., 2022), as well as the long range transport of CHON species from the Amazon Basin (Zha et al., 2023a). Besides, CHON contributes more (23.9±4.1%) in the dry season (MCC-d) than in the transition season (MCC-t, 18.7±5.9%), as a result of enhanced transport of anthropogenic pollutants from the La Paz–El Alto metropolitan area during the daytime in the dry season (Bianchi et al., 2022;Aliaga et al., 2021;Zha et al., 2023b).

Given this, we have removed text like "remote" or changed it to "mountain" for the mountain MCC site description throughout the manuscript. For clarification, we have added more discussion in Line 304 of the revised manuscript:

"The nitrogen-containing compounds (CHON) contribute 18.7–31.8% to the total OOA mass, except at the rural station in southeastern U.S. (RAB; 5.6±2.6%). This low contribution could be due to the less efficient production rates of CHON and/or their faster loss rates caused by hydrolysis under the high RH conditions there (83.1±15.2%; Table S1) (Lee et al., 2020;Hu et al., 2011;Lee et al., 2016;Pye et al., 2015). At the mountain site Chacaltaya, Bolivia, CHON contributes more (23.9±4.1%) in the dry season (MCC-d) than in the transition season (MCC-t, 18.7±5.9%), as a result

of enhanced transport of anthropogenic pollutants from the nearby La Paz–El Alto metropolitan area during the daytime in the dry season (Bianchi et al., 2022;Aliaga et al., 2021;Zha et al., 2023b)."

5. Tmax: "given the large spread in Tmax for …or over a whole campaign." I understand that the authors couldn't quantify the discrepancies between different instruments and operating conditions, but I think the authors should at least discuss how much uncertainty is associated with these discrepancies since the authors are doing the intercomparison after all.

We would like to clarify that the "large spread in T_{max}" per campaign referred to in our manuscript is mostly due to the fact that we aggregate all compounds of all measured mass spectra at a certain location, and these compounds span orders of magnitude of volatilities and hence tens of degrees in T_{max} (Huang et al., 2019b; Lopez-Hilfiker et al., 2014, 2015). Lopez-Hilfiker et al. (2014) have shown that for individual compounds, thermograms and corresponding T_{max} are highly reproducible under stable conditions (within ~2 °C). Differences in instrumental settings between locations and campaigns affect average T_{max} to a lesser degree compared to the chemical composition of the bulk aerosol. Different FIGAERO geometry was speculated to not induce significant T_{max} changes (Ylisirniö et al., 2021). Doubling the ramp rates is expected to induce a T_{max} difference of maximum 5 ºC (Schobesberger et al., 2018;Ylisirniö et al., 2021;Thornton et al., 2020). Correction of the T_{max} values to a filter mass loading of 1 µg following our approach outlined earlier (Huang et al., 2018) only leads to a T_{max} change of <5 °C.

For clarification, we have added more discussion in Lines 420, 476, and 489 of the revised manuscript:

Line 420: "Sum thermogram shapes vary for different environments […] given the large spread in T_{max} […] over a whole campaign period using the same instrument and operating conditions (Thompson et al., 2017) (see an example of $C_6H_{10}O_5$, the molecular formula corresponding to levoglucosan, in Figure S7). However, T_{max} variation due to different instruments or operating conditions is generally smaller than that from the difference in monomers and dimers (Wu et al., 2021) and other factors like the presence of isomers (Thompson et al., 2017;Masoud and Ruiz, 2021) and particle-phase diffusivity, viscosity and matrix effects (Huang et al., 2018;Ren et al., 2022). Different FIGAERO geometry was speculated not to induce significant T_{max} changes (Ylisirniö et al., 2021). The ramp rates for all measurements shown in the present study varied between 6.7 and 13.3 ºC/min (see Table S2), inducing a T_{max} difference of maximum 5 ºC (Schobesberger et al., 2018;Ylisirniö et al., 2021;Thornton et al., 2020). Correction of the T_{max} values to a filter mass loading of 1 µg following our approach outlined earlier (Huang et al., 2018) only leads to a T_{max} change of <5 °C."

Line 476: "For the complex ambient particle matrix, other factors than the pure compounds' vapor pressures come into play, such as the presence of isomers with different vapor pressures (Thompson et al., 2017), thermal decomposition contributions of larger molecules (Lopez-Hilfiker et al., 2015), and matrix effects and viscosity (Huang et al., 2018;D'Ambro et al., 2017;Wang and Ruiz, 2018) even for same compounds in solutions mixed with different species (Ren et al., 2022)."

Line 489: "Such variation may be due to actual changes in effective volatilities of the observed OOA components, due to experimental factors, or both. However, as we discussed earlier, T_{max} variation due to different instruments or operating conditions is generally smaller compared to those due to changes in physico-chemical properties. Therefore, the relative variations in thermogram shapes and T_{max} we present and discuss here in our study are dominated by the presence of isomers (Thompson et al., 2017;Masoud and Ruiz, 2021) and particle-phase diffusivity, viscosity and matrix effects

(Huang et al., 2018;Ren et al., 2022). Due to unavailable calibrations of the relationship between T_{max} and C_{sat} (Wang et al., 2020; Ylisirniöet al., 2021) for most locations, the analysis and interpretation of OOA volatility based on FIGAERO-CIMS thermograms is challenging and, in the absence of additional constraints on OOA composition and thermal behavior, currently remains at the qualitative level (Graham et al., 2023;Voliotis et al., 2021), especially for complex field data."

6. Thermal decomposition: "the decomposition fraction is estimated to be 5.8–35.9%", and "The discrepancy could be due to thermal fragmentation of larger oligomeric molecules, which bias the Csat results towards higher volatilities and the sum thermogram shape to a lesser extent due to the dominance of monomer species". Then how does this affect the volatility calculation using the fragmented formulas? To what extent should we trust the calculated volatility? Need more discussion here.

As we stated in Line 554 of the manuscript: "There have been attempts to separate the thermal decomposition contribution for individual thermograms (Lutz et al., 2019;D'Ambro et al., 2018;Buchholz et al., 2020; Wu et al., 2021), but this poses the threat for introducing new uncertainties due to the difficulty in e.g. differentiating isomers from thermal decomposition products, and monomers from dimers in ambient samples with complex VOC precursors (Graham et al., 2023;Voliotis et al., 2021)." The decomposition estimation approach by Wu et al. (2021) we used in our study represents one option currently available to the best of our knowledge for controlled laboratory studies, but still it is a conservative approach for complex ambient particle matrix. As a sensitivity analysis, we have calculated the average mass-weighted $log_{10}C_{sat}$ (298 K) and $log_{10}C_{sat}$ (T), and $sumT_{max}$ values after removing the fraction of signal from potential thermal decomposition products (Table R1). As expected, the fragmentation effect on sum thermogram is small except for those multi-mode thermograms dominated by the second mode (e.g., MCC-d, RHT, and UDL; see Figure S6). The change in C_{sat} is roughly within +1 order of magnitude, which is within the uncertainties of the parametrization method (Isaacman-VanWertz and Aumont, 2021).

***Table R1.** Comparison of the campaign-average mass-weighted $log_{10}C_{sat}$ and $sumT_{max}$ values for different locations and seasons before and after removing the fraction of signal from potential thermal decomposition products.*

Name	$log_{10}C_{sat}$ (298 K) (μg m^{-3})		$log_{10}C_{sat}$ (T) (μg m^{-3})		$sumT_{max}$ (ºC)	
	Original	**Removed**	**Original**	**Removed**	**Original**	**Removed**
MCC-t	1.6	0.9	-0.2	-1.0	81.7	81.7
MCC-d	2.2	1.5	0.6	-0.3	107.7	99.2
REL	1.0	0.8	0.7	0.4	99.5	99.5
RAB	2.0	2.0	2.0	1.6	94.5	94.5
RHT	2.2	1.9	1.0	0.8	146.3	124
UST-s	1.6	1.5	1.6	1.4	80.5	80.5
UST-w	1.3	1.3	-0.4	-0.4	112.5	112.5
UKA-s	0.8	0.8	0.6	0.8	102	102
UKA-w	0.4	0.2	-0.5	-0.7	106.1	106.1
UDL	2.8	2.7	2.4	2.2	113	88

For clarification, we have added more discussion in Line 346 of the revised manuscript:

"This has an insignificant effect on the bulk molecular composition of OOA particles, and e.g. within the corresponding standard deviation range of nC, nO, and O:C ratios. If we remove the fraction of

signal from potential decomposition products (which is still not ideal), the change in C_{sat} is within the uncertainties of the parametrization method (Isaacman-VanWertz and Aumont, 2021). However, please note that the decomposition estimation approach we used in our study was initially used for controlled laboratory studies by Wu et al. (2021), and thus remains a conservative approach for ambient particle matrix with complex VOCs."

7. In my opinion, some of the conclusions are too strong and lack supporting information. For example:

7.1 "we achieve a comprehensive picture of the relationship between volatility and chemical composition of OOA particles", what is the exact relationship?

It is the aim of our study to investigate the relationship/interconnection between molecular composition-derived volatility and thermal-desorption-derived volatility for complex ambient particle matrix, since this is not always straightforward given the rather large uncertainties of both methods (Isaacman-VanWertz and Aumont, 2021;Voliotis et al., 2021;Masoud and Ruiz, 2021;Wu et al., 2021). For clarification, we have rephrased the sentences in Lines 559 and 576 of the revised manuscript:

Line 559: "Overall, however, for a limited number of our datasets from the exact same instrument, the lower apparent volatility (i.e., higher sumT_{max}) agrees qualitatively with the lower $log_{10}C_{sat}$ values, corroborating potential relationships and interconnections between volatility and chemical composition across different environments and systems despite the large uncertainties and artefacts of both methods."

Line 576: "[…] suggesting a potential relationship/interlink between the volatility and chemical composition for the different locations and systems.

Here, using FIGAERO-CIMS measurements of OOA particles from various locations, we achieve a comprehensive picture of the relationship/interconnection between volatility and chemical composition of OOA particles in different rural, urban, and mountain environments, which are characterized by different ambient meteorological parameters, trace gas levels, emission sources/chemistry, and resulting distinct OOA molecular composition and volatility."

7.2 "however, the effects on the bulk molecular composition and sum thermograms of all detected OOA compounds are small as these thermally-unstable oligomers do not dominate the OOA mass." I would suggest the authors reword it because 35.9% is not small.

Similar to previously reported thermal fragmentation contributions for nitrate SOA in a recent chamber study (1–27%; Graham et al., 2023), the thermal decomposition fractions for our study are 5.8–26.6%, except for one dataset for MCC-d (~35.9%), the sum thermogram of which is multi-modal and dominated by the second mode (see Figure S6). For more details about the thermal fragmentation effect on sum thermograms, please refer to the response to the Major Comment 6. We have also rephrased this sentence in Line 584 as following: "[…] however, the effects on the bulk molecular composition and sum thermograms of all detected OOA compounds for most sites studied here are not significant as these thermally-unstable oligomers do not dominate the OOA mass. For some locations with multi-mode thermograms dominated by the second mode (e.g., MCC-d, RHT, and UDL; see Figure S6), the effects would be larger."

7.3 "and that environmental conditions (e.g., ambient temperature) play a lesser, secondary role through their influence on sources and chemistry of a particular environment," I don't think any

strong conclusions can be drawn about source and chemistry, because there are no analysis of source apportionment and oxidative chemistry.

We agree with the reviewer that we cannot draw strong conclusions about sources and chemistry in our study. However, in previous studies source apportionment was performed for several locations we present here, such as the rural site in southeastern U.S. (RAB) by Massoli et al. (2018), the rural site in Hyytiälä Finland (RHT) by Lee et al.(2018), the urban site in Delhi India (UDL) by Kumar et al. (2022), and so on. These references are properly cited and added to support our discussion in this comparison study.

By comparing the volatility either derived from molecular composition or from thermograms with various environmental and measurement parameters (Figure S5 and S9), we conclude that compared to the chemical composition, the environmental conditions play a smaller role in the apparent volatility of OOA particles for the measurement locations we investigated in our study. However, the environmental conditions such as ambient temperature could affect the sources and chemistry of a particular environment, such as seasonal patterns of biogenic emissions and human behavior (e.g., residential heating), and thus the chemical composition.

7.4 "Our study thus provides new insights that will help guide choices of e.g. descriptions of OOA volatility in different model frameworks" The authors would need to explain more about this.

More explanations are added in Lines 50 and 601 of the revised manuscript:

Line 50: "Our study thus provides new insights that will help guide choices of e.g. descriptions of OOA volatility in different model frameworks such as air quality models and cloud parcel models."

Line 601: "Considering the major contribution of OA to total aerosol mass concentrations and implications for both human health and climate change (Jimenez et al., 2009;Nel, 2005;IPCC, 2021), our study provides new insights that will help guide choices of e.g. descriptions of OOA volatility in different model frameworks. For example, with a better constraint on the volatility of condensable vapors and the associated particles using e.g. the up-to-date CIMS measurements, the study could contribute to understanding the underlying oxidative chemistry and a better OA representation in air quality models. The potential contribution of co-condensation of organic vapors to aerosol forcing or to future cloud radiative effects could also be better accounted for in cloud parcel models (Heikkinen et al., 2023). A better understanding of […]".

Reviewer 2 ***(responses in italics)***

General comment

The authors present evaluations of a combination of aerosol field data taken in 5 different regions of the world (India, Germany, Bolivia, USA, Finland). The central instrumentation is FIGAERO-CIMS, a method often applied in field and laboratory studies. Some seasonal aspects are addressed for the Bolivian and German data sets.

The focus is on comparison of campaign averages for vapor pressures / volatility in relation to particle composition and some other atmospheric parameters. The data set the paper is based on represents a lot of work and effort and is quite impressive.

The manuscript is well written and well organized. The presented material is well chosen and suited to support the discussions and results presented in the manuscript. The manuscript is interesting to read in that presents some critical aspects of vapor pressure and volatility determinations.

The difficulty of the manuscript lies in selection of observations (sites). I believe that they are too singular in time and space to conclude something from the comparison with respect to particle properties in the atmosphere. (I understand that such observations are limited.) This prevents conclusions but very general ones. That is probably the reason why the authors focus more on the methodological aspects. However, whenever they found something interesting, which may be related to atmospheric processes, they step back and question the relations by referring to the experimental difficulties and operational aspects of FIGAERO measurements. The best indication is the statement on page 12 beginning in line 387 and ending in line 398.

And I am not sure if the results support the conclusion that just more efforts ("alternative approaches") are needed "for more quantitative estimations of volatility from FIGAERO-CIMS measurements" (line 534f). Overall, I would say the conclusions are bit weak regarding the atmospheric aspects.

I would still suggest to publishing the paper in ACP as it addresses important aspects and limits of FIGAERO approaches, which should be realized by a broader community. I suggest that authors should address the minor aspects below.

We sincerely thank the reviewer for the thoughtful evaluation and positive feedback of our manuscript. We are grateful for your recognition of the work and effort we put in this study. We appreciate your comments for further improving our manuscript. Below, we address your points in detail:

We agree with the reviewer's comments that the measurement locations presented in our study are limited in time and space. More (long-term) observation would be beneficial for drawing stronger conclusions related to atmospheric aspects for OOA particles in different environments and systems. Therefore, we have removed texts like "across the globe" or "global dataset" throughout the manuscript. However, we would like to stress here that the aim of this work is to investigate the relationship/interconnection between molecular composition-derived volatility and thermal-desorption-derived volatility for complex ambient particle matrix. Overall, for a limited number of our datasets from the exact same instrument, we do find the lower apparent volatility (i.e., higher $sumT_{max}$*) agrees qualitatively with the lower* $log_{10}C_{sat}$ *values, corroborating the potential relationships and interconnections between volatility and chemical composition across different environments and systems. Please refer the changes in the manuscript to the response to the Major Comment 7.1 by Reviewer 1.*

And as the reviewer pointed out, one interesting finding of our study is about the large T_{max} variation in different environments and systems in Section 3.2.2. We do agree with the reviewer that this could be related to atmospheric processes. The relative variations in thermogram shapes and T_{max} we present and discuss here in our study are dominated by the presence of isomers (Thompson et al., 2017;Masoud and Ruiz, 2021) and particle-phase diffusivity, viscosity and matrix effects (Huang et al., 2018). Please refer more details to the response to the Major Comment 5 by Reviewer 1. The changes in the manuscript can also be found there.

Minor comments

1. I would say that "volatility" of/in a mixture depends on the chemical composition, i.e. on the vapor pressure of the components, and the physical conditions, mainly the temperature. Translated to atmospheric situations this means that chemical composition depends on emissions and the atmospheric chemistry on the way to the observation point and the physical conditions depend on the let's say the (local) meteorology. Since you are looking at campaign averages ("bulk apparent volatility of OOA particles") you are looking at a kind of a systemic property of aerosol particles, but what you are searching for is still the physical aspects of vapor/pressure of an ensemble of compounds. However, in re-constructing the systemic volatility from the individual components, one is a priori limited by the mass spectrometric approach, which can give (here) chemical formulas at best, and the limits of vapor pressure information for the individual compounds or detected formulas. (On top the operational aspects of FIGAERO measurements.)

We agree with the reviewer that one important limitation of reconstructing systemic volatility from the individual compounds or detected formulae using FIGAERO measurements is the potential divergence from the sum of individual parametrized C_{sat} due to non-ideal intermolecular interactions (Compernolle et al., 2011;Isaacman-VanWertz and Aumont, 2021), as we also stated in Line 332 and 547 of the manuscript, in addition to the uncertainties related to the parametrization for e.g. nitrated organic compounds (Graham et al., 2023). We have added more discussion in Lines 84 and 547 of the revised manuscript:

Line 84: "This could induce uncertainties associated with volatility estimates particularly for the complex ambient particle matrix (O'Meara et al., 2014), in addition to the potential divergence from the sum of individual parametrized C_{sat} due to non-ideal intermolecular interactions (Compernolle et al., 2011;Isaacman-VanWertz and Aumont, 2021)."

Line 547: "[...] the bulk OOA volatility for the complex ambient particle matrix may also diverge from the sum of individual parametrized C_{sat} due to non-ideal intermolecular interactions (Compernolle et al., 2011;Isaacman-VanWertz and Aumont, 2021), in addition to the highly uncertain parametrization of C_{sat} for organonitrates with multiple nitrate groups (Graham et al., 2023)."

2. Could it be that what you tried in this manuscript is inherently an impossible task? A way out could be to drive everything empirically and relate the observations to classes of conditions. However, for that the presented data set is too particulate. Could you explain or justify explicitly your approach using campaign averages?

We agree with the reviewer that it would be too particulate to investigate the classes of conditions and atmospheric processes for each individual dataset. The reason why we use campaign average

values is that we would like to focus our analysis on the systemic bulk molecular composition and bulk volatility of OOA from different environments and systems (to avoid any extreme events or sudden plumes), in order to study whether there is any connection of chemical composition and volatility between molecular composition-derived volatility and thermal-desorption-derived volatility for complex ambient particle matrix.

3. Independently, I am asking myself when the use of campaign averages make sense. Naively, I would say if you had a bimodal distribution of conditions for example, then the campaign average cannot be observed by measurement. This would be different for a simple monomodal distribution of conditions where is a certain chance to indeed observe the campaign average. Can you comment on that?

We think that campaign averages including bimodal distributions still show characteristic features. Taking sumT_{max} values as an example, they are derived from campaign average sum thermograms, which are the summed signal evolution of all CHOX compounds as a function of desorption temperature. We can thus see the distribution of the mode of the sum thermograms over the range of the desorption temperature (single-mode vs. multi-mode) and robustness of using either mean or median sum thermograms (see Figure R2 and also Figure S6). As for $\log_{10}C_{sat}$ (T), it would be affected by both the composition and meteorological conditions such as ambient temperature (see also Figure S4). Therefore the standard deviations of $\log_{10}C_{sat}$ (298K) may indicate variations of the distribution. The standard deviations of $\log_{10}C_{sat}$ (298K) for different locations (Table R2) are within the uncertainties of the parametrization method (Isaacman-VanWertz and Aumont, 2021), and therefore suggests small variation of the $\log_{10}C_{sat}$ (298K) for the measurement locations investigated in our study.

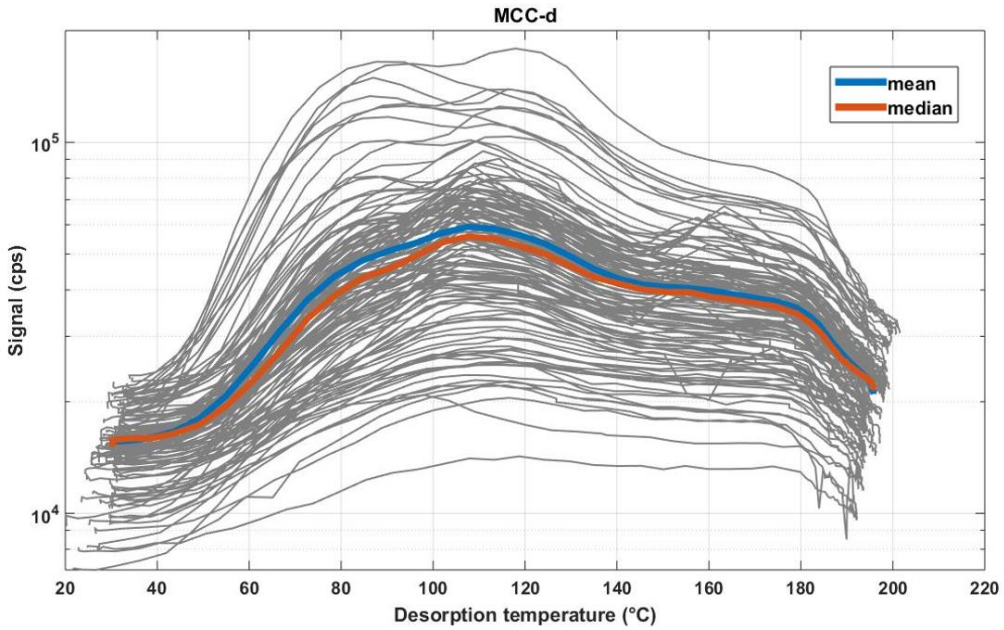

Figure R2. *An example of multi-mode sum thermograms of CHOX compounds for MCC-d. All campaign sum thermograms are in gray lines, mean one in blue and median in red.*

Table R2. *$log_{10}C_{sat}$ (298K) values (average ± 1 standard deviation) for the different locations.*

Name	*$log_{10}C_{sat}$ (298 K) (µg m^{-3})*
MCC-t	*1.6±0.3*
MCC-d	*2.2±0.4*
REL	*1.0±0.6*
RAB	*2.0±0.2*
RHT	*2.2±0.2*
UST-s	*1.6±0.2*
UST-w	*1.3±0.4*
UKA-s	*0.8±0.6*
UKA-w	*0.4±0.5*
UDL	*2.8±0.2*

4. line 385: Please can you shortly explain in the experimental sections what sum thermograms are, for non-FIGAERO users. What is exactly is summed in a sum thermogram?

More descriptions are added when first introducing sum thermograms in Line 418 as suggested: "Campaign-average sum thermograms of CHOX compounds (i.e., the sum of mass spectral signal evolution of all CHOX compounds as a function of desorption temperature) for the different locations […]".

5. line 399- 431: Shouldn't sumTmax tell us something about the persistency of the particles, when they are moving out of the source region?

The desorption temperature at which a compound exhibits maximum signal (T_{max}) correlates with the compound's enthalpy of sublimation and can be used to infer its saturation vapor pressure (Lopez-Hilfiker et al., 2015;Mohr et al., 2017), which in turn influences particulate mass and lifetime in the atmosphere. The sources and transformations of particles affect their role/fate in the atmosphere. After the particles are moving out of the source region, the processes/transformations would affect sumT_{max}, i.e., the bulk volatility and thus the physico-chemical nature of the particles (Thornton et al., 2020). Relative variations in thermogram shapes and sumT_{max} we present and discuss here in our study are dominated by the presence of isomers (Thompson et al., 2017;Masoud and Ruiz, 2021) and particle-phase diffusivity, viscosity and matrix effects (Huang et al., 2018). Please refer more details to the response to the Major Comment 5 by Reviewer 1. The changes in the manuscript can also be found there.

6. line 432-448: If I understand correctly, this questions the approach using Li et al. vapor pressure parametrization. If so, that should be mentioned.

In fact, the discussion here are mainly focused on the factors affecting the volatility derived from thermograms, instead of from the Li et al. parametrization method. The results in our study show some discrepancies between the two methods, and based on these results alone it is not possible to judge which method is more correct, which is also not the aim of our study.

7. line 456f: Here you show something interesting, but you discuss it away. If you don't trust the finding, why mentioning it?

We agree with the reviewer and have moved the corresponding text related to the correlation of sumT_{max} with SO_2 to the figure captions of Figure S9 in the Supplement to avoid confusion.

8. Figure 2: Please, take out the legend from the figure. It is hiding information. Could you tabulate the values of log10Csat in Table S1?

Revised Figure 2 and S4, and added the values of $log_{10}C_{sat}$ (298 K) and $log_{10}C_{sat}$ (T) in Table S1 as suggested.

9. Figures S4 and S8: It could be helpful to correlate log(Csat) and sumTmax also with the campaign averages of the OA mass concentrations. For ideal mixtures, those determine the critical threshold which "vapor pressures" are sufficient for a compound to remain in the condensed phase. And that should be related to the bulk apparent volatility of OOA particles. The data look like a correlation and if so, that should be mentioned in the main manuscript.

We agree with the reviewer that OA mass concentrations should be related to the bulk apparent volatility of OOA particles. And we did this correlation as well in Figure S5 and S9. However, the correlations of campaign-average mass weighted $log_{10}C_{sat}$ (T) values and sumT_{max} values vs. OA mass measured by AMS/ACSM are weak (0.3 and 0.1, respectively) and therefore we didn't discuss more in the main manuscript. Clarifications are added to the figure captions: "Org and $PM_{2.5}$ data were total non-refractory mass concentration from a high-resolution time-of-flight aerosol mass spectrometer (HR-ToF-AMS, Aerodyne Research Inc.) or an aerosol chemical speciation monitor (ACSM, Aerodyne Research Inc.)."

References:

Aliaga, D., Sinclair, V. A., Andrade, M., Artaxo, P., Carbone, S., Kadantsev, E., Laj, P., Wiedensohler, A., Krejci, R., and Bianchi, F.: Identifying source regions of air masses sampled at the tropical high-altitude site of Chacaltaya using WRF-FLEXPART and cluster analysis, Atmos Chem Phys, 21, 16453-16477, 10.5194/acp-21-16453-2021, 2021.

Bianchi, F., Sinclair, V. A., Aliaga, D., Zha, Q., Scholz, W., Wu, C., Heikkinen, L., Modini, R., Partoll, E., Velarde, F., Moreno, I., Gramlich, Y., Huang, W., Leiminger, M., Enroth, J., Peräkylä, O., Marinoni, A., Xuemeng, C., Blacutt, L., Forno, R., Gutierrez, R., Ginot, P., Uzu, G., Facchini, M. C., Gilardoni, S., Gysel-Beer, M., Cai, R., Petäjä, T., Rinaldi, M., Saathoff, H., Sellegri, K., Worsnop, D., Artaxo, P., Hansel, A., Kulmala, M., Wiedensohler, A., Laj, P., Krejci, R., Carbone, S., Andrade, M., and Mohr, C.: The SALTENA Experiment: Comprehensive Observations of Aerosol Sources, Formation, and Processes in the South American Andes, Bulletin of the American Meteorological Society, E212–E229, https://doi.org/10.1175/BAMS-D-20-0187.1, 2022.

Compernolle, S., Ceulemans, K., and Muller, J. F.: EVAPORATION: a new vapour pressure estimation methodfor organic molecules including non-additivity and intramolecular interactions, Atmos Chem Phys, 11, 9431-9450, 10.5194/acp-11-9431-2011, 2011.

Daumit, K. E., Kessler, S. H., and Kroll, J. H.: Average chemical properties and potential formation pathways of highly oxidized organic aerosol, Faraday Discuss, 165, 181-202, https://doi.org/10.1039/C3FD00045A, 2013.

Donahue, N. M., Epstein, S. A., Pandis, S. N., and Robinson, A. L.: A two-dimensional volatility basis set: 1. organic-aerosol mixing thermodynamics, Atmos Chem Phys, 11, 3303–3318, https://doi.org/10.5194/acp-11-3303-2011, 2011.

Graham, E. L., Wu, C., Bell, D. M., Bertrand, A., Haslett, S. L., Baltensperger, U., El Haddad, I., Krejci, R., Riipinen, I., and Mohr, C.: Volatility of aerosol particles from NO3 oxidation of various biogenic organic precursors, Atmos Chem Phys, 23, 7347-7362, https://doi.org/10.5194/acp-23-7347-2023, 2023.

Hu, K. S., Darer, A. I., and Elrod, M. J.: Thermodynamics and kinetics of the hydrolysis of atmospherically relevant organonitrates and organosulfates, Atmos Chem Phys, 11, 8307–8320, https://doi.org/10.5194/acp-11-8307-2011, 2011.

Huang, W., Saathoff, H., Pajunoja, A., Shen, X. L., Naumann, K.-H., Wagner, R., Virtanen, A., Leisner, T., and Mohr, C.: α-Pinene secondary organic aerosol at low temperature: chemical composition and implications for particle viscosity, Atmos Chem Phys, 18, 2883–2898, https://doi.org/10.5194/acp-18-2883-2018, 2018.

Huang, W., Saathoff, H., Shen, X., Ramisetty, R., Leisner, T., and Mohr, C.: Chemical characterization of highly functionalized organonitrates contributing to night-time organic aerosol mass loadings and particle growth, Environ Sci Technol, 53, 1165–1174, https://doi.org/10.1021/acs.est.8b05826, 2019a.

Huang, W., Saathoff, H., Shen, X. L., Ramisetty, R., Leisner, T., and Mohr, C.: Seasonal characteristics of organic aerosol chemical composition and volatility in Stuttgart, Germany, Atmos Chem Phys, 19, 11687–11700, https://doi.org/10.5194/acp-19-11687-2019, 2019b.

Isaacman-VanWertz, G., and Aumont, B.: Impact of organic molecular structure on the estimation of atmospherically relevant physicochemical parameters, Atmos Chem Phys, 21, 6541–6563, https://doi.org/10.5194/acp-21-6541-2021, 2021.

Kumar, V., Giannoukos, S., Haslett, S. L., Tong, Y. D., Singh, A., Bertrand, A., Lee, C. P., Wang, D. S., Bhattu, D., Stefenelli, G., Dave, J. S., Puthussery, J. V., Qi, L., Vats, P., Rai, P., Casotto, R., Satish, R., Mishra, S., Pospisilova, V., Mohr, C., Bell, D. M., Ganguly, D., Verma, V., Rastogi, N., Baltensperger, U., Tripathi, S. N., Prévôt, A. S. H., and Slowik, J. G.: Highly time-resolved chemical speciation and source apportionment of organic aerosol components in Delhi, India, using extractive electrospray ionization mass spectrometry, Atmos Chem Phys, 22, 7739-7761, https://doi.org/10.5194/acp-22-7739-2022, 2022.

Lee, B. H., Mohr, C., Lopez-Hilfiker, F. D., Lutz, A., Hallquist, M., Lee, L., Romer, P., Cohen, R. C., Iyer, S., Kurtén, T., Hu, W. W., Day, D. A., Campuzano-Jost, P., Jimenez, J. L., Xu, L., Ng, N. L., Guo, H. Y., Weber, R. J., Wild, R. J., Brown, S. S., Koss, A., de Gouw, J., Olson, K., Goldstein, A. H., Seco, R., Kim, S., McAvey, K., Shepson, P. B., Starn, T., Baumann, K., Edgerton, E. S., Liu, J. M., Shilling, J. E., Miller, D. O., Brune, W., Schobesberger, S., D'Ambro, E. L., and Thornton, J. A.: Highly functionalized organic nitrates in the southeast United States: Contribution to secondary organic aerosol and reactive nitrogen budgets, P Natl Acad Sci USA, 113, 1516–1521, https://doi.org/10.1073/pnas.1508108113, 2016.

Lee, B. H., Lopez-Hilfiker, F. D., D'Ambro, E. L., Zhou, P. T., Boy, M., Petäjä, T., Hao, L. Q., Virtanen, A., and Thornton, J. A.: Semi-volatile and highly oxygenated gaseous and particulate organic compounds observed above a boreal forest canopy, Atmos Chem Phys, 18, 11547–11562, https://doi.org/10.5194/acp-18-11547-2018, 2018.

Lee, B. H., D'Ambro, E. L., Lopez-Hilfiker, F. D., Schobesberger, S., Mohr, C., Zawadowicz, M. A., Liu, J., Shilling, J. E., Hu, W., Palm, B. B., Jimenez, J. L., Hao, L., Virtanen, A., Zhang, H., Goldstein, A. H., Pye, H. O. T., and Thornton, J. A.: Resolving ambient organic aerosol formation and aging pathways with simultaneous molecular composition and volatility observations, Acs Earth Space Chem, 4, 391-402, 10.1021/acsearthspacechem.9b00302, 2020.

Li, Y., Pöschl, U., and Shiraiwa, M.: Molecular corridors and parametrizations of volatility in the chemical evolution of organic aerosols, Atmos Chem Phys, 16, 3327–3344, https://doi.org/10.5194/acp-16-3327-2016, 2016.

Lopez-Hilfiker, F. D., Mohr, C., Ehn, M., Rubach, F., Kleist, E., Wildt, J., Mentel, T. F., Lutz, A., Hallquist, M., Worsnop, D., and Thornton, J. A.: A novel method for online analysis of gas and particle composition: description and evaluation of a Filter Inlet for Gases and AEROsols (FIGAERO), Atmos Meas Tech, 7, 983−1001, https://doi.org/10.5194/amt-7-983-2014, 2014.

Lopez-Hilfiker, F. D., Mohr, C., Ehn, M., Rubach, F., Kleist, E., Wildt, J., Mentel, T. F., Carrasquillo, A. J., Daumit, K. E., Hunter, J. F., Kroll, J. H., Worsnop, D. R., and Thornton, J. A.: Phase partitioning and volatility of secondary organic aerosol components formed from α-pinene ozonolysis and OH oxidation: the importance of accretion products and other low volatility compounds, Atmos Chem Phys, 15, 7765−7776, https://doi.org/10.5194/acp-15-7765-2015, 2015.

Masoud, C. G., and Ruiz, L. H.: Chlorine-Initiated Oxidation of α-Pinene: Formation of Secondary Organic Aerosol and Highly Oxygenated Organic Molecules, Acs Earth Space Chem, 5, 2307–2319, https://doi.org/10.1021/acsearthspacechem.1c00150, 2021.

Massoli, P., Stark, H., Canagaratna, M. R., Krechmer, J. E., Xu, L., Ng, N. L., Mauldin, R. L., Yan, C., Kimmel, J., Misztal, P. K., Jimenez, J. L., Jayne, J. T., and Worsnop, D. R.: Ambient measurements of highly oxidized gas-phase molecules during the Southern Oxidant and Aerosol Study (SOAS) 2013, Acs Earth Space Chem, 2, 653–672, https://doi.org/10.1021/acsearthspacechem.8b00028, 2018.

Mohr, C., Lopez-Hilfiker, F. D., Yli-Juuti, T., Heitto, A., Lutz, A., Hallquist, M., D'Ambro, E. L., Rissanen, M. P., Hao, L. Q., Schobesberger, S., Kulmala, M., Mauldin III, R. L., Makkonen, U., Sipilä, M., Petäjä, T., and Thornton, J. A.: Ambient observations of dimers from terpene oxidation in the gas phase: Implications for new particle formation and growth, Geophys Res Lett, 44, 2958−2966, https://doi.org/10.1002/2017gl072718, 2017.

Mohr, C., Thornton, J. A., Heitto, A., Lopez-Hilfiker, F. D., Lutz, A., Riipinen, I., Hong, J., Donahue, N. M., Hallquist, M., Petaja, T., Kulmala, M., and Yli-Juuti, T.: Molecular identification of organic vapors driving atmospheric nanoparticle growth, Nat Commun, 10, 4442, https://doi.org/10.1038/s41467-019-12473-2, 2019.

Nie, W., Yan, C., Huang, D. D., Wang, Z., Liu, Y. L., Qiao, X. H., Guo, Y. S., Tian, L. H., Zheng, P. G., Xu, Z. N., Li, Y. Y., Xu, Z., Qi, X. M., Sun, P., Wang, J. P., Zheng, F. X., Li, X. X., Yin, R. J., Dallenbach, K. R., Bianchi, F., Petäjä, T., Zhang, Y. J., Wang, M. Y., Schervish, M., Wang, S. N., Qiao, L. P., Wang, Q., Zhou, M., Wang, H. L., Yu, C. A., Yao, D. W., Guo, H., Ye, P. L., Lee, S. C., Li, Y. J., Liu, Y. C., Chi, X. G., Kerminen, V. M., Ehn, M., Donahue, N. M., Wang, T., Huang, C., Kulmala, M., Worsnop, D., Jiang, J. K., and Ding, A. J.: Secondary organic

aerosol formed by condensing anthropogenic vapours over China's megacities, Nat Geosci, 15, 255-+, 10.1038/s41561-022-00922-5, 2022.

Pye, H. O., Luecken, D. J., Xu, L., Boyd, C. M., Ng, N. L., Baker, K. R., Ayres, B. R., Bash, J. O., Baumann, K., Carter, W. P., Edgerton, E., Fry, J. L., Hutzell, W. T., Schwede, D. B., and Shepson, P. B.: Modeling the Current and Future Roles of Particulate Organic Nitrates in the Southeastern United States, Environ Sci Technol, 49, 14195-14203, 10.1021/acs.est.5b03738, 2015.

Schobesberger, S., D'Ambro, E. L., Lopez-Hilfiker, F. D., Mohr, C., and Thornton, J. A.: A model framework to retrieve thermodynamic and kinetic properties of organic aerosol from composition-resolved thermal desorption measurements, Atmos Chem Phys, 18, 14757−14785, https://doi.org/10.5194/acp-18-14757-2018, 2018.

Thompson, S. L., Yatavelli, R. L. N., Stark, H., Kimmel, J. R., Krechmer, J. E., Day, D. A., Hu, W. W., Isaacman-VanWertz, G., Yee, L., Goldstein, A. H., Khan, M. A. H., Holzinger, R., Kreisberg, N., Lopez-Hilfiker, F. D., Mohr, C., Thornton, J. A., Jayne, J. T., Canagaratna, M., Worsnop, D. R., and Jimenez, J. L.: Field intercomparison of the gas/particle partitioning of oxygenated organics during the Southern Oxidant and Aerosol Study (SOAS) in 2013, Aerosol Sci Tech, 51, 30–56, https://doi.org/10.1080/02786826.2016.1254719, 2017.

Thornton, J. A., Mohr, C., Schobesberger, S., D'Ambro, E. L., Lee, B. H., and Lopez-Hilfiker, F. D.: Evaluating Organic Aerosol Sources and Evolution with a Combined Molecular Composition and Volatility Framework Using the Filter Inlet for Gases and Aerosols (FIGAERO), Acc Chem Res, 53, 1415-1426, 10.1021/acs.accounts.0c00259, 2020.

Voliotis, A., Wang, Y., Shao, Y. Q., Du, M., Bannan, T. J., Percival, C. J., Pandis, S. N., Alfarra, M. R., and McFiggans, G.: Exploring the composition and volatility of secondary organic aerosols in mixed anthropogenic and biogenic precursor systems, Atmos Chem Phys, 21, 14251-14273, 10.5194/acp-21-14251-2021, 2021.

Wu, C., Bell, D., Graham, E. L., Haslett, S., Riipinen, I., Baltensperger, U., Bertrand, A., Giannoukos, S., Schoonbaert, J., El Haddad, I., Prevot, A. S. H., Huang, W., and Mohr, C.: Photolytically Induced Changes in Composition and Volatility of Biogenic Secondary Organic Aerosol from Nitrate Radical Oxidation during Night-to-day Transition, Atmos Chem Phys Discuss, 1-29, https://doi.org/10.5194/acp-2021-347, 2021.

Ylisirniö, A., Barreira, L. M. F., Pullinen, I., Buchholz, A., Jayne, J., Krechmer, J. E., Worsnop, D. R., Virtanen, A., and Schobesberger, S.: On the calibration of FIGAERO-ToF-CIMS: importance and impact of calibrant delivery for the particle-phase calibration, Atmos Meas Tech, 14, 355–367, https://doi.org/10.5194/amt-14-355-2021, 2021.

Zha, Q., Aliaga, D., Krejci, R., Sinclair, V. A., Wu, C., Ciarelli, G., Scholz, W., Heikkinen, L., Partoll, E., Gramlich, Y., Huang, W., Leiminger, M., Enroth, J., Peräkylä, O., Cai, R., Chen, X., Koenig, A. M., Velarde, F., Moreno, I., Petäjä, T., Artaxo, P., Laj, P., Hansel, A., Carbone, C., Kulmala, M., Andrade, M., Worsnop, D., Mohr, C., and Bianchi, F.: Oxidized organic molecules in the tropical free troposphere over Amazonia, National Science Review, nwad138, https://doi.org/10.1093/nsr/nwad138, 2023a.

Zha, Q. Z., Huang, W., Aliaga, D., Perakyla, O., Heikkinen, L., Koenig, A. M., Wu, C., Enroth, J., Gramlich, Y., Cai, J., Carbone, S., Hansel, A., Petaja, T., Kulmala, M., Worsnop, D., Sinclair, V., Krejci, R., Andrade, M., Mohr, C., and Bianchi, F.: Measurement report: Molecular-level investigation of atmospheric cluster ions at the tropical high-altitude research station Chacaltaya (5240 m a.s.l.) in the Bolivian Andes, Atmos Chem Phys, 23, 4559-4576, 10.5194/acp-23-4559-2023, 2023b.

Variation in chemical composition and volatility of oxygenated organic aerosol in different rural, urban, and ~~remote~~ mountain environments

Wei Huang[1], Cheng Wu[2,3], Linyu Gao[4], Yvette Gramlich[2,5], Sophie L. Haslett[2,5], Joel Thornton[6], Felipe D. Lopez-Hilfiker[7], Ben H. Lee[6], Junwei Song[4], Harald Saathoff[4], Xiaoli Shen[4,8], Ramakrishna Ramisetty[4,9], Sachchida N. Tripathi[10], Dilip Ganguly[11], Feng Jiang[4], Magdalena Vallon[4], Siegfried Schobesberger[12], Taina Yli-Juuti[12], Claudia Mohr[2,5,13,14,*]

[1]Institute for Atmospheric and Earth System Research / Physics, Faculty of Science, University of Helsinki, 00014, Helsinki, Finland

[2]Department of Environmental Science, Stockholm University, 11418, Stockholm, Sweden

[3]Now at: Department of Chemistry and Molecular Biology, University of Gothenburg, 41296, Gothenburg, Sweden

[4]Institute of Meteorology and Climate Research, Karlsruhe Institute of Technology, 76344, Eggenstein-Leopoldshafen, Germany

[5]Bolin Centre for Climate Research, Stockholm University, 11418, Stockholm, Sweden

[6]Department of Atmospheric Sciences, University of Washington Seattle, Washington 98195, United States

[7]Tofwerk AG, 3600 Thun, Switzerland

[8]Now at: Department of Earth, Atmospheric, and Planetary Sciences, Purdue University, West Lafayette, Indiana 47907, United States

[9]Now at: TSI Instruments India Private Limited, 560102, Bangalore, India

[10]Department of Civil Engineering, Indian Institute of Technology Kanpur, 208016, Kanpur, India

[11]Centre for Atmospheric Sciences, Indian Institute of Technology Delhi, 110016, New Delhi, India

[12]Department of Technical Physics, University of Eastern Finland, 70211, Kuopio, Finland

[13]Now at: Department of Environmental Systems Science, ETH Zürich, 8006 Zürich, Switzerland

[14]Now at: Laboratory of Atmospheric Chemistry, Paul Scherrer Institute, 5232 Villigen, Switzerland

**Correspondence to*: Claudia Mohr (claudia.mohr@psi.ch)

Abstract. The apparent volatility of atmospheric organic aerosol (OA) particles is determined by their chemical composition and environmental conditions (e.g., ambient temperature). A quantitative, experimental assessment of volatility and the respective importance of these two factors remains challenging, especially in ambient measurements. We present molecular composition and volatility of oxygenated OA (OOA) particles in different rural, urban, and ~~remote~~ mountain environments ~~across the globe~~ (including Chacaltaya, Bolivia; Alabama, U.S.; Hyytiälä, Finland; Stuttgart and Karlsruhe, Germany; and Delhi, India) based on deployments of a filter inlet for gases and aerosols coupled to a high-resolution time-of-flight chemical ionization mass spectrometer (FIGAERO-CIMS). We find on average larger carbon numbers (nC) and lower oxygen-to-carbon (O:C) ratios at the urban sites (nC: 9.8±0.7; O:C: 0.76±0.03; average ± 1 standard deviation), compared to the rural (nC: 8.8±0.6; O:C: 0.80±0.05) and ~~remote~~ mountain stations (nC: 8.1±0.8; O:C: 0.91±0.07), indicative of different emission sources and chemistry. Compounds containing only carbon, hydrogen, and oxygen atoms (CHO) contribute highest to the total OOA mass at the rural sites (79.9±5.2%), in accordance with their proximity to forested areas (66.2±5.5% at the mountain sites and 72.6±4.3% at the urban sites). The largest contribution of nitrogen-containing compounds (CHON) are found at the urban stations (27.1±4.3%), consistent with their higher NO_x levels. Besides, we parametrize OOA volatility (saturation mass concentrations, C_{sat}) using molecular composition information and compare it with the bulk apparent volatility derived from thermal desorption of the OOA particles within the FIGAERO. We find differences in C_{sat} values of up to ~3 orders of magnitude, and variation in thermal desorption profiles (thermograms) across different locations and systems. From our study, we draw the general conclusion that environmental conditions (e.g., ambient temperature) do not directly affect OOA apparent volatility, but rather indirectly by influencing the sources and chemistry of the environment and thus the chemical composition. The comprehensive ~~global~~ dataset provides results that show the complex thermodynamics and chemistry of OOA and their changes during its lifetime in the atmosphere, and that generally the chemical description of OOA suffices to predict its apparent volatility, at least qualitatively. Our study thus provides new insights that will help guide choices of e.g. descriptions of OOA volatility in different model frameworks ~~which has been previously simplified due to challenges to measure and represent it in models,~~ such as air quality models and cloud parcel models.

1 Introduction

Chemical composition and volatility of atmospheric organic aerosol (OA) particles are interconnected. Functionalization of organic molecules can modify their vapor pressure by several orders of magnitude (Pankow and Asher, 2008;Donahue et al., 2011;Graham et al., 2023;Isaacman-VanWertz and Aumont, 2021;Kroll and Seinfeld, 2008). Volatility determines whether a compound partitions into or evaporates from the particle phase and thus influences particulate mass and lifetime in the atmosphere. Accurate predictions of atmospheric organic particle mass thus require a quantitative understanding of the chemical nature and volatility of its components. This is of special importance for oxygenated organic aerosol (OOA), most of which is of secondary origin (i.e., SOA) (Jimenez et al., 2009) and involves phase transitions and chemical reactions in all phases. Further, the conditions of the atmosphere, e.g., temperature, play a critical role. A semi-volatile compound may be in the gas phase in the boundary layer at 25 °C but condense at an altitude of ~4.5 km where the ambient temperature is ~20 °C lower, and consequently its apparent volatility is lower by up to ~2 orders of magnitude (Bardakov et al., 2021;Donahue et al., 2011;Epstein et al., 2010;Stolzenburg et al., 2018). The complex thermodynamics and chemistry of OOA and their changes during its lifetime in the atmosphere are challenging to measure and represent

in modelling frameworks, resulting in simplified descriptions of volatility (Nozière et al., 2015;Hallquist et al., 2009).

The development of the filter inlet for gases and aerosols coupled to a time-of-flight chemical ionization mass spectrometer (FIGAERO-CIMS) has enabled the combined analysis of molecular composition and volatility of OOA particles in near-real time (Thornton et al., 2020;Lopez-Hilfiker et al., 2014). OOA volatility can be derived in two ways from the FIGAERO-CIMS:

1) The molecular information of OOA can be used to parametrize volatility via calculations of the effective saturation mass concentrations (C_{sat}) of different organic compounds (Donahue et al., 2011;Li et al., 2016;Mohr et al., 2019;Isaacman-VanWertz and Aumont, 2021;Graham et al., 2023). There are various parametrization methods to calculate C_{sat}, based on different assumptions, training datasets, or structure-based estimation methods (Isaacman-VanWertz and Aumont, 2021). However, calculated C_{sat} from different parametrizations may vary among each other: while modified Li method (Li et al., 2016;Isaacman-VanWertz and Aumont, 2021) tends to estimate higher vapor pressures than expected for low-volatility species, Daumit method (Daumit et al., 2013) and Donahue method (Donahue et al., 2011) (also the updated Mohr method (Mohr et al., 2019)) are found to estimate lower vapor pressures (Isaacman-VanWertz and Aumont, 2021). The discrepancy in C_{sat} among different parametrizations can span several orders of magnitude and become even larger for compounds with increasing nitrogen numbers, especially for organonitrates with multiple nitrate groups (Wu et al., 2021;Isaacman-VanWertz and Aumont, 2021;Graham et al., 2023). This could induce uncertainties associated with volatility estimates particularly for the complex ambient particle matrix (O'Meara et al., 2014), in addition to the potential divergence from the sum of individual parametrized C_{sat} due to non-ideal intermolecular interactions (Compernolle et al., 2011;Isaacman-VanWertz and Aumont, 2021).

2) While the particles are thermally desorbed within the FIGAERO for molecular composition analysis with CIMS, the instrument also yields a qualitative measure of particle volatility through the signal evolution as a function of desorption temperature (i.e., thermograms) (Lopez-Hilfiker et al., 2014;Lopez-Hilfiker et al., 2015). A model framework has also been developed to reproduce the shape of thermograms (Schobesberger et al., 2018). The desorption temperature at which a compound exhibits maximum signal (T_{max}) correlates with the compound's enthalpy of sublimation and can be used to infer its saturation vapor pressure (Lopez-Hilfiker et al., 2015;Mohr et al., 2017). Evaporative behavior, and hence thermogram shape, T_{max} and inferred volatility of a particle-bound compound are subject to artefacts from thermal decomposition (Lopez-Hilfiker et al., 2015;Yang et al., 2021), heating rate (Yang et al., 2021;Ylisirniö et al., 2021;Thornton et al., 2020;Schobesberger et al., 2018), FIGAERO geometry (Ylisirniö et al., 2021), the presence of isomers (Thompson et al., 2017;Masoud and Ruiz, 2021), and particle-phase diffusivity and viscosity (Yli-Juuti et al., 2017;Huang et al., 2018). As a consequence, thermogram shape and T_{max} for an individual compound can vary among different chamber studies (D'Ambro et al., 2017;Huang et al., 2018;Wang and Ruiz, 2018) and field measurements (Thompson et al., 2017;Huang et al., 2019b;Gaston et al., 2016), which could also induce uncertainties associated with volatility estimates, similar to parametrization methods.

Overall, the relationship between molecular composition-derived volatility and thermal-desorption-derived volatility is not always straight forward given the rather large uncertainties of both methods (Isaacman-VanWertz and Aumont, 2021;Voliotis et al., 2021;Masoud and Ruiz, 2021;Wu et al., 2021). Huang et al. (2019b) found consistent results of bulk volatility for OOA particles measured in Stuttgart, Germany, when using volatility parametrizations and thermograms, indicative of the connection between chemical composition and volatility. Wu

et al. (2021) found a qualitative agreement between T_{max} and C_{sat} for individual compounds of SOA particles in their chamber studies, but varying results for the bulk volatility when using different parametrizations and thermograms. Further comprehensive investigations of the relationship between volatility and chemical composition of OOA particles are warranted, particularly for ambient measurements.

In this study, we present an overview of the chemical composition of OOA and OOA volatility derived from both molecular composition measurements and thermogram analyses for a number of ambient FIGAERO-CIMS datasets ~~across the globe~~ (Chacaltaya, Bolivia; Alabama, U.S.; Hyytiälä, Finland; Stuttgart and Karlsruhe, Germany; Delhi, India). We assess how different environments (e.g., emission sources and meteorological parameters) influence the particle chemical composition and volatility derived from these two methods, discuss the reasons for differences and similarities, and the relationship between volatility and chemical composition for the different locations.

2 Methodology

2.1 Measurement sites

The measurement sites of this study are listed in Table 1. The list includes one ~~remote~~ mountain site (MCC, 16°21'00.0" S, 68°07'48.0" W), located at the GAW (Global Atmosphere Watch) high altitude research station Chacaltaya (~5240 m a.s.l.), ~25 km northeast of La Paz city (~3640 m a.s.l.), Bolivia (Bianchi et al., 2022); three rural sites, the first one located in the Rhine river valley near Eggenstein-Leopoldshafen, ~12 km north of the city of Karlsruhe, Germany (REL, 49°6′10.54″ N, 8°24′26.07″ E) (Huang et al., 2019a), the second one in the boreal forest of Hyytiälä, Finland (RHT, 61°50'47.2" N, 24°17'43.3" E) (Mohr et al., 2017;Mohr et al., 2019), and the third one located near Centreville, Alabama, United States (RAB, 33°10'48.0" N, 86°46'48.0" W) (Lopez-Hilfiker et al., 2016); and three urban sites, the first one located in a park in the city of Stuttgart, Germany (UST, 48°47′55.1" N, 9°12′13.5" E) (Huang et al., 2019b); the second one right next to a road crossing the city center of Karlsruhe, Germany (UKA, 49°00'35.0" N, 8°25'02.8" E), and the third one on a university campus in the city of Delhi, India (UDL, 28°32'48.8" N, 77°011'26.8" E). For MCC, UST, and UKA, measurements from different seasons were included to investigate the influence of seasonal variation in emission sources and/or chemistry on OOA composition and volatility. The campaign-average values for co-located measurements of meteorological parameters (temperature (*T*) and relative humidity (RH)), trace gases (O_3, NO_2, and SO_2), equivalent black carbon (eBC), and total non-refractory particulate mass are listed in Table S1.

Table 1. Overview of the measurement sites included in this study, their locations, and the measurement periods.

Abbreviation	Location	Measurement period	Description
MCC	Chacaltaya, Bolivia	April 9-26, 2018 (transition season); May 7-June 2, 2018 (dry season)	Mountain site
REL	near Eggenstein-Leopoldshafen, Germany	August 18-Sept. 1, 2016	Rural site
RAB	near Centreville, Alabama, U.S.	June 4-July 16, 2013	Rural site
RHT	Hyytiälä, Finland	April 11-June 3, 2014	Rural site
UST	Stuttgart, Germany	July 5-August 17, 2017 (summer); February 5-March 5, 2018 (winter)	Urban background site
UKA	Karlsruhe, Germany	June 28-July 29, 2019 (summer); February 22-March 30, 2020 (winter)	Urban curb site
UDL	Delhi, India	January 11-February 5, 2019	Urban background site

2.2 Measurements and volatility determination of OOA particles

2.2.1 Measurements of OOA particles

Particulate oxygenated organic compounds were measured with a FIGAERO-CIMS (Aerodyne Research Inc. or from the University of Washington (Lopez-Hilfiker et al., 2014)) using iodide (I^-) as the reagent ion. Iodide-CIMS is sensitive to more polar oxygenated organic compounds with three to eight oxygen atoms (Lee et al., 2014;Riva et al., 2019;Huang et al., 2019a). Inlet flow and residence time, particle deposition time, mass loadings on the filter, and instrumental parameters for the different campaigns are summarized in Table S2. Differences in instrumental parameters such as IMR (ion molecule reaction chamber) pressure, ion source, the ratio of sample and ionizer flow, and the voltage settings of the mass spectrometer can affect the sensitivities of organic compounds and therefore their measured distribution. Here we simply use mass fractions of compounds calculated using sensitivities assumed or assessed for the individual campaigns/instruments, since the focus of this study is not to report and compare absolute mass concentrations of OOA at different locations. An in-depth analysis of the differences in instrumental parameters among different campaigns, and how they affect the measured OOA composition, is beyond the scope of this paper. Data were analyzed with the software packages "tofTools" (developed by Junninen et al. (Junninen et al., 2010)) or "Tofware" (provided by Tofwerk Ltd.).

For REL, RHT, RAB, MCC, and UDL, aerosol particles were measured in-situ with the FIGAERO-CIMS (Huang et al., 2018;Mohr et al., 2019;Lopez-Hilfiker et al., 2016;Bianchi et al., 2022). Particle-phase backgrounds were assessed in regular intervals by placing an additional Teflon (Polytetrafluoroethylene, PTFE) filter upstream of the normal filter and using the same deposition procedure as for the ambient measurements. These data were then used for background subtraction.

For UST and UKA, aerosol particles were deposited on Teflon filters and analyzed later in the laboratory with FIGAERO-CIMS ("offline mode"; see Table S2) (Huang et al., 2019b;Cai et al., 2023). Filters were kept frozen until analysis. Deposition times were varied (see Table S2) based on ambient organic mass concentrations measured by a concurrent high-resolution time-of-flight aerosol mass spectrometer (HR-ToF-AMS, Aerodyne

Research Inc.) in order to achieve similar organic mass loadings on the filter and to avoid mass loading effects (Huang et al., 2018;Wang and Ruiz, 2018). A total of 21 (10) and 29 (23) filter samples were collected in summer (winter) at UST and UKA, respectively. Particle-phase backgrounds were assessed by placing prebaked clean filters in the filter holder at the measurement sites with the deposition flow switched off. These field blank samples were also analyzed by FIGAERO-CIMS in the laboratory like the samples and used for background subtraction.

2.2.2 Volatility determination of OOA particles

OOA volatility was determined for all sites based on FIGAERO-CIMS thermograms and C_{sat} parametrizations. Different temperature ramp rates affect T_{max} (Schobesberger et al., 2018;Yang et al., 2021;Ylisirniö et al., 2021;Thornton et al., 2020). The ramp rates for all measurements shown here varied between 6.7 and 13.3 ºC/min (see Table S2), inducing a T_{max} difference of up to 5 ºC (Schobesberger et al., 2018;Ylisirniö et al., 2021;Thornton et al., 2020). Since for most locations no calibrations of the relationship between T_{max} and C_{sat} are available (Wang et al., 2020;Ylisirniö et al., 2021), we present and discuss here only relative variations in thermogram shapes and T_{max}, including the variations caused by different ramp rates, and compare them qualitatively to the variation in C_{sat} determined from parametrization.

C_{sat} (298 K) was calculated ~~for all sites~~ using the approach by Li et al. (2016) as in equation (1) for all sites in order to not introduce more bias:

$$\log_{10} C_{sat}\,(298\ \mathrm{K}) = (n_C^0 - n_C) \times b_C - n_O \times b_O - 2 \times \frac{n_C \times n_O}{(n_C + n_O)} \times b_{CO} - n_N \times b_N - n_S \times b_S \quad (1)$$

where n_C, n_O, n_N, and n_S are the number of carbon, oxygen, nitrogen, and sulfur atoms in the organic compound, respectively; n_C^0 is the reference carbon number; b_C, b_O, b_N, and b_S are the contribution of each atom to $\log_{10}C_{sat}$, respectively; b_{CO} is the carbon–oxygen nonideality (Donahue et al., 2011). Since the empirical approach by Li et al. (2016) was derived with very few organonitrates, we modified the C_{sat} (298 K) of CHON compounds by treating all NO_3 groups like OH groups following the approach by Daumit et al. (Daumit et al., 2013;Isaacman-VanWertz and Aumont, 2021). A recent study however found that the parametrization of C_{sat} for nitrate groups is highly uncertain (Graham et al., 2023). Even for different biogenic terpene+NO_3 systems, none of the four parametrizations Graham et al. (2023) investigated performed perfectly for all systems, as parametrizations which are developed based on different datasets comprising different compounds with different functionalities can yield different results for the same dataset (e.g., Graham et al., 2023). For example, the Mohr et al. (2019) parametrization method, which was tuned for -OOH functional groups, was found to work better for α-pinene+O_3 system and thus it was speculated that the α-pinene+O_3 system has more -OOH functional groups. The Daumit et al. (2013) parametrization method, which assumes all oxygen atoms except those from -NO_3 are from -OH and =O functional groups, was found to work better for α-pinene+NO_3 system and thus the α-pinene+NO_3 system is speculated to have more -OH and =O groups (Graham et al., 2023). These results underline again the complexity (and with that also the limitations) of assessments of the volatility (especially at the quantitative level) through parametrizations using the molecular composition as input, as already shown for laboratory measurements (Graham et al., 2023), and even more so for complex ambient data from different locations and periods.

We also adjusted the C_{sat} (298 K) to the measured ambient temperature, C_{sat} (T), using the approach by Donahue et al. (2011) and Epstein et al. (2010) as in equations (2) and (3):

$$\log_{10} C_{\text{sat}}(T) = \log_{10} C_{\text{sat}}(298\ \text{K}) + \frac{\Delta H_{\text{vap}}}{R\ln(10)} \times \left(\frac{1}{298} - \frac{1}{T}\right), \quad (2)$$

$$\Delta H_{\text{vap}}(\text{kJ mol}^{-1}) = -11 \times \log_{10} C_{\text{sat}}(298\ \text{K}) + 129 \quad (3)$$

where T is the temperature in Kelvin; C_{sat} (298 K) is the saturation mass concentration at 298 K; ΔH_{vap} is the vaporization enthalpy; and R is the gas constant (8.3143 J K^{-1} mol^{-1}). We have added a comparison of the results from using the parametrization by Donahue et al. (2011) (Figure S1a) if making a simple assumption about predominant aliphatic/aromatic OOA at urban sites in winter (i.e., UST-w, UKA-w, and UDL) and predominant isoprene OOA in MCC-t and RAB (Nie et al., 2022). The $\log_{10}C_{\text{sat}}$ (T) shows a similar trend for both parametrizations; however, the C_{sat} (T) using the Donahue et al. (2011) parametrization is on average 4 to 8 orders of magnitude lower, with the largest difference for UKA-w and smallest for UDL (Figure S1b). The discrepancies seem to be correlated with the average number of oxygen atoms (nO) in the bulk aerosol of the different environments (Pearson's R: 0.85; Figure S1b), confirming the influence of different functional groups on parametrization results. Our discussion of volatility results in this study is therefore mostly qualitative.

3 Results and discussion

3.1 Bulk molecular composition of OOA particles

3.1.1 Average number of carbon and oxygen atoms and oxygen-to-carbon ratios

We focus our analysis of the bulk molecular composition of OOA from the different locations here on the average number of carbon (nC) and oxygen atoms (nO) as they affect the parametrized C_{sat}, and ~~also could be used to indicate~~give an indication of potential precursor sources (Huang et al., 2019a) and oxidation processes, respectively. Figure 1a shows the average mass-weighted nO vs. nC for all compounds with the molecular formula $C_{x\geq1}H_{y\geq1}O_{z\geq1}X_{0-n}$ (CHOX; X are different atoms such as N, S, Cl, or a combination thereof) measured by FIGAERO-CIMS for each campaign. The markers are color-coded by the average mass-weighted oxygen-to-carbon (O:C) ratios. The observed average nC and nO range from 7.7 to 11.2 and from 4.9 to 7.1, respectively. There is an overall trend of increasing nO with increasing nC (Figure 1a), with the spring-time OOA at the rural station Hyytiälä, Finland (RHT), and the wintertime OOA at the urban station Delhi, India (UDL) deviating from that general trend (see discussions below). The overall trend shows the effect of the length of carbon backbone on the number of potential oxygen atoms that can be added to the carbon chain (Huang et al., 2019a).

Generally, at the urban sites, OOA particles exhibit on average larger nC (9.8±0.7; average ± 1 standard deviation) compared to the rural (8.8±0.6) and mountain stations (8.1±0.8), indicative of different emission sources and OOA precursors (Huang et al., 2019b).

At the ~~remote~~ mountain site Chacaltaya, Bolivia, OOA has a relatively longer carbon backbone (nC: 8.4±0.8) in the transition season (MCC-t) than in the dry season (MCC-d, nC: 7.7±0.7). The air masses arriving at Chacaltaya present a diverse mixture from various sources, which vary significantly between the transition and the dry seasons (Aliaga et al. 2021). While air masses arriving at Chacaltaya during the dry season are more affected by volcanic SO_2 emissions as well as ~~the~~ anthropogenic ~~sources~~ compounds such as toluene (also seen in the slightly higher contributions of C_7 compounds in Figure S2) (Bianchi et al., 2022;Zha et al., 2023b), air masses

reaching Chacaltaya during the transition season have more influence from e.g. the Amazon Basin (Aliaga et al., 2021;Zha et al., 2023b)~~,~~; ~~and~~ hence, a higher contribution of monoterpene ($C_{10}H_{16}$) and especially isoprene (C_5H_8) oxidation products ~~are~~ is expected (also reflected in the clear peak of C_5 compounds and the second hump of C_{8-10} compounds in Figure ~~S1~~S2) (Zha et al., 2023a).

Rural Alabama in U.S. (RAB) and rural Hyytiälä in Finland (RHT), which are both forested stations albeit in different biomes, show respective OOA composition with nC of 8.0±0.4 at RAB and 9.1±0.6 at RHT. This is likely due to the different distributions of terpene emissions with more isoprene at RAB (Lopez-Hilfiker et al., 2016;Lee et al., 2016) and mostly monoterpenes at RHT (Li et al., 2020;Huang et al., 2021). It is also seen in the higher contributions of C_{8-10} compounds for RHT, and comparable contributions of C_5 and C_{8-10} compounds for RAB (Zhang et al., 2018;Massoli et al., 2018) (Figure ~~S1~~S2). The third rural site, REL, which is situated at a location with substantial anthropogenic as well as biogenic influence dominated by monoterpene emissions (Huang et al., 2019a), has a comparable nC (9.2±0.8) to RHT and again shows a relatively higher contributions of C_{8-10} compounds (Figure ~~S1~~S2).

For the urban sites, the curb site in Karlsruhe, Germany (UKA) has a larger nC (summer: 10.7±0.8; winter: 11.2±0.8) compared to the urban background site in the nearby city of Stuttgart (UST, summer: 8.8±0.4; winter: 8.7±0.9). The nC for wintertime Delhi in India (UDL, 9.4±0.4) is between that of UKA and UST. Such differences are likely due to the UKA and UDL measurement locations being more directly impacted by traffic emissions (Kumar et al., 2022) with higher contributions of larger aromatic compounds (Zheng et al., 2017;Lim et al., 1999). This is substantiated by the observed elevated contributions of C_{11-18} compounds (Figure ~~S1~~S2) and higher DBE (double bond equivalent) values (Table S1). In addition, all three urban sites, despite their very different locations, show a similar seasonal pattern, with higher contributions of C_{8-10} compounds in summer from biogenic emissions, and higher contributions of C_6 compounds (e.g., levoglucosan, $C_6H_{10}O_5$) in winter due to biomass burning emissions (Figure ~~S1~~S2) (Huang et al., 2019b;Kumar et al., 2022).

Whereas the nC values may give some indication of OOA precursor emission sources, the average nO and O:C ratios are linked to different aging processes and/or varying distance from the sources (Jimenez et al., 2009). The urban stations exhibit on average the lowest O:C ratios (0.76±0.03), compared to the rural (0.80±0.05) and ~~remote~~ mountain stations (0.91±0.07).

OOA particles during the transition season at the mountain site Chacaltaya, Bolivia (MCC-t), have relatively larger nO (6.2±0.3), but slightly lower O:C ratio (0.89±0.08) compared to the dry season (MCC-d; nO: 5.8±0.3; O:C: 0.94±0.05). For two of the rural stations (RAB in the southeastern U.S. and RHT in Finland), nO is comparable (RAB: 5.7±0.2; RHT: 5.7±0.3), but O:C is slightly higher at RAB (0.81±0.04; RHT: 0.77±0.05). This may again be due to the difference in dominating terpene sources (isoprene for RAB (Lopez-Hilfiker et al., 2016) and monoterpenes for RHT (Li et al., 2020); also reflected in Figure ~~S1~~S2). The third rural site, REL in Germany (during summertime with substantial anthropogenic and biogenic influence) (Huang et al., 2019a), has higher nO (6.6±0.5) and O:C (0.83±0.06) compared to RAB and RHT, despite the fairly large nC (9.2±0.8). This could be related to more intense photochemistry/oxidation with higher temperature and/or solar radiation at this site (Table S1). Lower temperature and solar radiation could also be the reason for RHT deviating from the general trend of nO and nC in Figure 1a.

The urban sites in Germany (Karlsruhe, UKA, and Stuttgart, UST) have similar nO in summer and in winter (UKA: summer: 7.0±0.4; winter: 7.1±0.4; UST: summer: 6.4±0.2; winter: 6.7±0.2). In comparison, nO for the winter Delhi site (UDL) is 4.9±0.1 due to the dominance of primary OA (Kumar et al., 2022), resulting in its

deviation from the general trend of nO and nC (Figure 1a). Besides, O:C ratios are lower for UKA (summer: 0.73±0.02; winter: 0.73±0.04) and UDL (0.66±0.02) compared to UST (summer: 0.82±0.02; winter: 0.89±0.06), which relates back to its larger nC (see Figure 1a) as a result of its high proximity to traffic emissions (Kumar et al., 2022) with more larger aromatic compounds (Lim et al., 1999;Zheng et al., 2017) (see discussions above and Figure ~~S1~~S2). Despite the influence of different OOA sources in summer and winter (biogenic emissions vs. biomass burning contributions) for both German urban sites UKA and UST (Huang et al., 2019b), only UST exhibits higher O:C ratios in winter than summer. This could be due to the complex topography of the city of Stuttgart, resulting in stronger surface temperature inversions and consequently longer aging time of air masses (Huang et al., 2019b;Baumbach and Vogt, 2003).

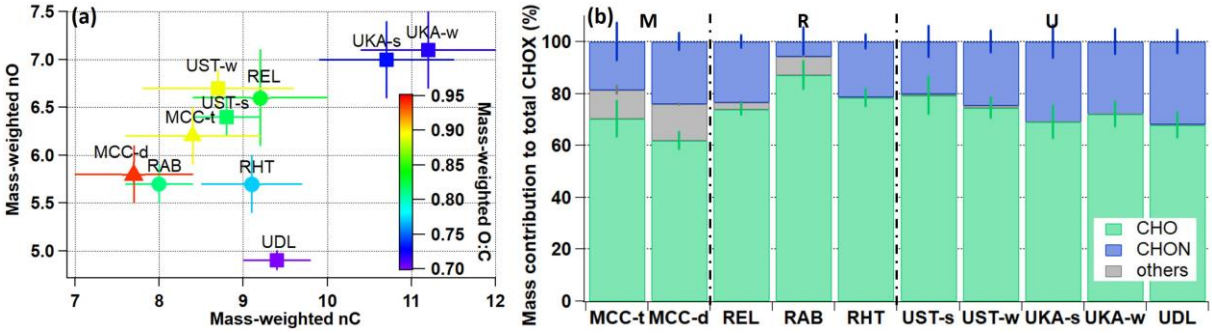

Figure 1. (a) Campaign-average mass-weighted number of oxygen atoms (nO) vs. number of carbon atoms (nC) at the different locations and seasons (Mountain sites in triangles, Rural sites in circles, and Urban sites in squares; for a list of nC and nO values see Table S1), with the markers colored by the corresponding campaign-average mass-weighted oxygen-to-carbon (O:C) ratios; **(b)** Campaign-average mass contributions of organic compounds (separated into CHO, CHON, and other compounds) for the different campaigns (M = mountain sites, R = rural sites, U = urban sites) and seasons (s = summer, w = winter, t = transition, d = dry).

3.1.2 Mass contribution of organonitrates

The presence of NO_x during the oxidation of volatile organic compounds (VOC) can lead to the formation of organonitrates, either via reactions with peroxy radicals or formation of NO_3 radicals acting as VOC oxidants, and influence SOA yields and properties of OOA (D'Ambro et al., 2017;Ng et al., 2007;Faxon et al., 2018;Wu et al., 2021). Organonitrates have been found to make up an important fraction of total OA particle mass globally (Kiendler-Scharr et al., 2016;Huang et al., 2019a;Lee et al., 2018). Due to their connection to emissions from fossil fuel burning, they can be indicators of the anthropogenic influence of a particular location. To a lesser extent, also lightning is a source of atmospheric NO_x (Murray, 2016). Here we simply group all organic compounds containing at least one nitrogen atom (CHON) and loosely define them as organonitrates (Lee et al., 2016;Huang et al., 2019a). Compounds containing only carbon, hydrogen, and oxygen atoms are grouped as CHO.

Average mass contributions of CHO and CHON for the different locations are shown in Figure 1b. Overall, CHO compounds clearly dominate the OOA mass at all locations (62.0–87.1%). CHO contributions are on average higher at the rural sites (79.9±5.2%) compared to the mountain (66.2±5.5%) and urban sites (72.6±4.3%), in accordance with their proximity to forested areas. The nitrogen-containing compounds (CHON) contribute 18.7–31.8% to the total OOA mass, except ~~. A low CHON fraction is observed~~ at the rural station in southeastern U.S. (RAB; 5.6±2.6%). This low contribution could be ~~possibly~~ due to the less efficient production rates of CHON

and/or their faster loss rates caused by hydrolysis under the high RH conditions there (83.1±15.2%; Table S1) (Lee et al., 2020;Hu et al., 2011;Lee et al., 2016;Pye et al., 2015). At the mountain site Chacaltaya, Bolivia, CHON contributes more (23.9±4.1%) in the dry season (MCC-d) than in the transition season (MCC-t, 18.7±5.9%), as a result of enhanced transport of anthropogenic pollutants from the nearby La Paz–El Alto metropolitan area during the daytime in the dry season (Bianchi et al., 2022;Aliaga et al., 2021;Zha et al., 2023b). As expected, the largest contributions of CHON compounds are found at the urban stations (27.1±4.3%), coinciding with their higher NO_x levels (15.8±8.7 ppbv; Table S1), but overall, differences between stations and seasons are small.

The compounds labelled as "others" in Figure 1b are mostly identified as CHOS or CHONS compounds, making up 0.1–14.1% of the total OOA mass. Sulfur-containing compounds exhibit non-negligible contributions for MCC, REL, and RAB. This is likely due to varying sources for these locations: The mountain site in Bolivia (MCC) was influenced by volcanic emissions during the campaign (Bianchi et al., 2022), the rural sites in central Europe (REL) and southeastern U.S. (RAB) by nearby refineries and/or power plants (Huang et al., 2019a;Fry et al., 2018).

3.2 Volatility of OOA particles

3.2.1 Volatility derived from molecular composition

For each campaign we calculated C_{sat} (T) for each compound based on its molecular composition (see more details in section 2.2.2) (Donahue et al., 2011;Isaacman-VanWertz and Aumont, 2021;Li et al., 2016;Mohr et al., 2019) and grouped all compounds into a 25-bin VBS (volatility basis set; Figure ~~S2~~S3) (Donahue et al., 2011;Donahue et al., 2012). The 25 volatility bins were then further aggregated into extremely low-volatile organic compounds (ELVOC, C_{sat} (T) lower than $10^{-4.5}$ µg m^{-3}), low-volatile organic compounds (LVOC, C_{sat} (T) between $10^{-4.5}$ and $10^{-0.5}$ µg m^{-3}), semi-volatile organic compounds (SVOC, C_{sat} (T) between $10^{-0.5}$ and $10^{2.5}$ µg m^{-3}), and intermediate-volatility organic compounds (IVOC, C_{sat} (T) between $10^{2.5}$ and $10^{6.5}$ µg m^{-3}) (Donahue et al., 2009). The average contributions of different volatility groups to total OOA are shown in Figure 2, together with the average mass-weighted $\log_{10}C_{sat}$ (T). Note that the bulk apparent volatility of OOA particles, i.e., average mass-weighted $\log_{10}C_{sat}$ (T), which represents the overall observed $\log_{10}C_{sat}$ (T) of the OOA as a whole (D'Ambro et al., 2018), is different from the $\log_{10}C_{sat}$ (T) and volatility of the (pure) compounds detected.

We find that the more volatile species with C_{sat} (T) between 10^0 and 10^4 µg m^{-3} make up the biggest mass contributions at all locations (47.7–83.8%); LVOC and ELVOC contribute substantially (13.4–42.1%; Figure 2 and ~~S2~~S3). In general, the VBS distribution pattern does not seem to have huge differences across different systems and environments, despite that a large (though not all) fraction of OOA can be detected by iodide-CIMS (Riva et al., 2019;Huang et al., 2021). Whereas LVOC and ELVOC may be important for the early stages of atmospheric new particle formation, they certainly do not dominate the OOA mass. Note that thermal decomposition of larger organic compounds during particle desorption with the FIGAERO could contribute, in particular, to the IVOC fraction (Huang et al., 2019b;Lopez-Hilfiker et al., 2016). Resolving and subtracting the thermal decomposition compounds using multi-peak fitting methods (Lutz et al., 2019) or with the help of positive matrix factorization (Buchholz et al., 2020) may, however, introduce uncertainties due to some ambiguity during the implementation and interpretation (Graham et al., 2023;Voliotis et al., 2021). Using the thermal decomposition estimation approach by Wu et al. (2021) the decomposition fraction is estimated to be 5.8–35.9% (see more discussions below), which is close to the reported thermal fragmentation contributions (1–27%) for nitrate SOA in a recent chamber study

(Graham et al., 2023). This has ~~however~~ an insignificant effect on the bulk molecular composition of OOA particles, ~~which is~~and e.g. within the corresponding standard deviation range of nC, nO, and O:C ratios. If we remove the fraction of signal from potential decomposition products (which is still not ideal), the change in C_{sat} is within the uncertainties of the parametrization method (Isaacman-VanWertz and Aumont, 2021). However, please note that the decomposition estimation approach we used in our study was initially used for controlled laboratory studies by Wu et al. (2021), and thus remains a conservative approach for ambient particle matrix with complex VOCs.

The mountain site in Bolivia exhibits slightly higher contributions from the more volatile species (i.e., IVOC) in the dry season (MCC-d, 31.2±3.9%) compared to the transition season (MCC-t, 20.0±5.0%). Consistently, also the average mass-weighted $\log_{10}C_{sat}$ (T) value is higher for MCC-d (0.58±0.35 μg m^{-3}) than MCC-t (-0.18±0.43 μg m^{-3}). In addition to the higher thermal decomposition contribution for MCC-d (~34.3%) compared to MCC-t (~26.3%), higher contributions of CHON and sulfur-containing organic compounds during the dry season (see also Figure 1b) could also play a role (Peräkylä et al., 2020). Even though the addition of a NO_3 functional group is assumed to decrease a compound's vapor pressure by up to several orders of magnitude (Donahue et al., 2011;Graham et al., 2023;Pankow and Asher, 2008), CHON compounds with the same nC and nO as a CHO compound (e.g., $C_{10}H_{15}NO_7$ vs. $C_{10}H_{16}O_7$), are expected to have a higher vapor pressure (Donahue et al., 2011;Lee et al., 2018;Pankow and Asher, 2008). Different origin of air masses and hence atmospheric processing time and chemistry may be another reason for the slight differences in OOA volatility between the seasons (Aliaga et al., 2021;Bianchi et al., 2022).

Among the rural sites in Germany (REL), Finland (RHT), and southeastern U.S. (RAB), RAB shows the highest volatility (IVOC: 49.2±4.9%; ELVOC: 2.4±1.3%; $\log_{10}C_{sat}$ (T): 2.0±0.4 μg m^{-3}) compared to REL (IVOC: 38.8±6.3%; ELVOC: 12.5±5.4%; $\log_{10}C_{sat}$ (T): 0.67±0.67 μg m^{-3}) and RHT (IVOC: 32.7±6.1%; ELVOC: 5.5±2.1%; $\log_{10}C_{sat}$ (T): 1.0±0.5 μg m^{-3}). RAB is the southernmost station of all rural sites, with the highest RH (also temperature; Table S1) and high emissions of isoprene, and thus the reactive uptake of IEPOX (isoprene-epoxydiol) in aqueous aerosol is likely a more important SOA pathway compared to REL and RHT. This result again shows that the interpretation of OOA volatility derived from molecular composition is complex, and warrants careful consideration of various parameters (Graham et al., 2023;Voliotis et al., 2021).

The urban site in Delhi, India (UDL) exhibits the lowest LVOC and lowest ELVOC mass fractions (13.4% in total), highest IVOC mass fractions (54.5±3.4%) and mass-weighted $\log_{10}C_{sat}$ (T) values (2.3±0.3 μg m^{-3}; also consistent with its lowest O:C ratios, see Figure 1a), compared to the two urban sites in Germany (UKA: LVOC+ELVOC: 18.4–42.1%; IVOC: 20.5–42.8%; $\log_{10}C_{sat}$ (T): -0.37–1.6 μg m^{-3}; UST: LVOC+ELVOC: 27.9–41.9%; IVOC: 23.8–32.5%; $\log_{10}C_{sat}$ (T): -0.50–0.63 μg m^{-3}). The relatively higher volatility of OOA in Delhi compared to that in the German cities may be likely related to the dominance of primary OA with very high biomass burning (also reflected in the large peak of C_6 compounds in Figure ~~S1~~S2) and traffic emissions (Kumar et al., 2022). The biomass burning vapors have been found to be responsible for the nighttime particle growth at UDL (Mishra et al., 2023). As for UKA and UST, higher LVOC and ELVOC mass fractions (41.9–42.1%) and lower mass-weighted $\log_{10}C_{sat}$ (T) values (-0.50–-0.37 μg m^{-3}) are observed in winter compared to summer (18.4–27.9% and 0.63–1.6 μg m^{-3}, respectively), indicating that the bulk winter OOA is less volatile. Similar results were also observed in Zurich, Switzerland based on AMS data (Canonaco et al., 2015). Higher O:C ratios (Figure 1a) could be part of the reason for the less volatile OOA in winter in Stuttgart (UST) compared to summer (Huang et al., 2019b). For the Karlsruhe curb site (UKA), the O:C ratios are quite similar for winter and summer (Figure 1a) and therefore other factors, such as the relatively higher contributions of larger molecules (nC >16; Figure ~~S1~~S2)

as well as the reduced volatility of OOA from biomass burning due to aging processes (Keller and Burtscher, 2017) (see also the higher O:C ratios in Figure 1a compared to UDL with more primary emissions (Kumar et al., 2022)), might play a role.

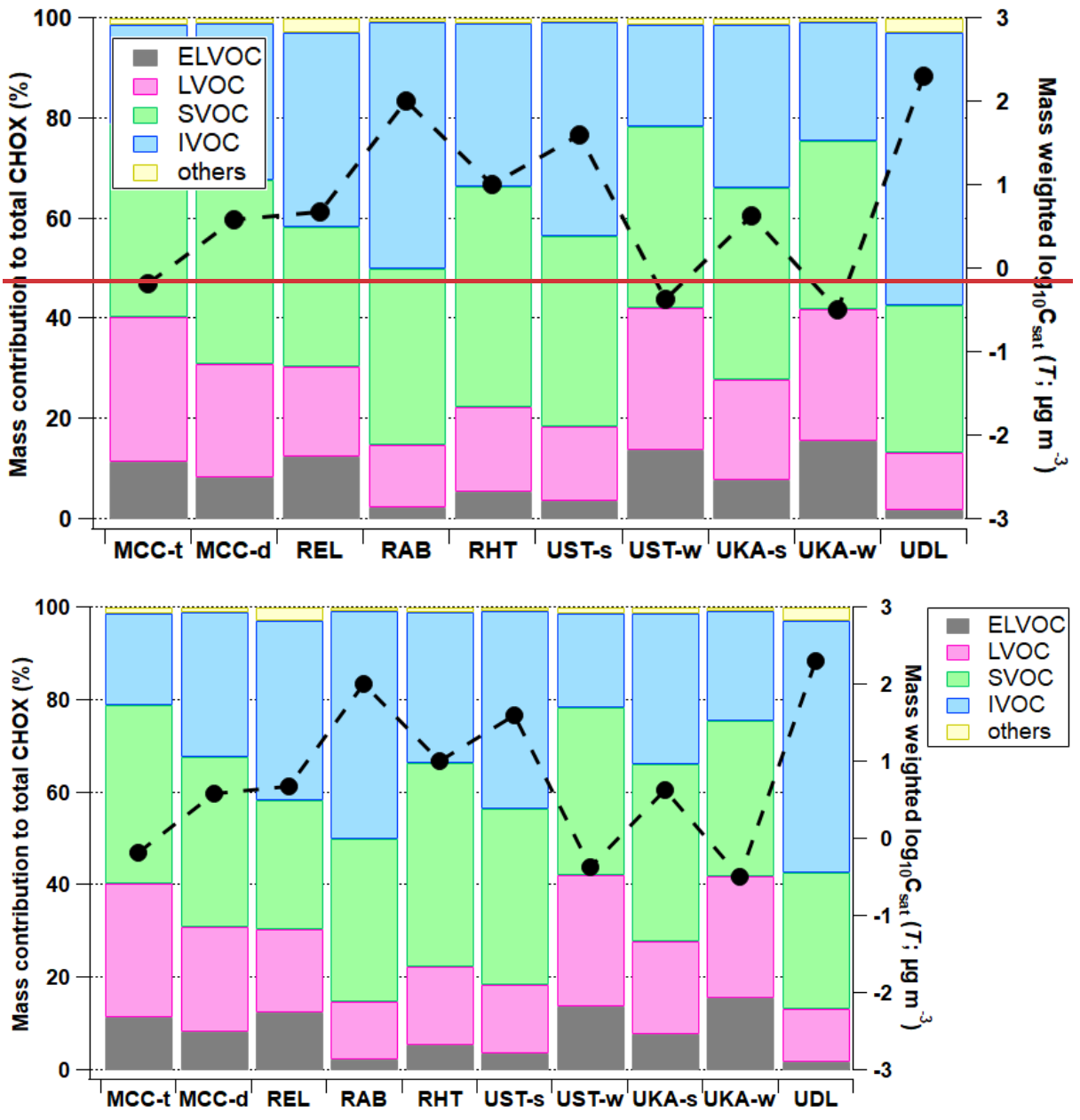

Figure 2. Campaign-average contribution (%) to total organics of different volatility groups resulting from VBS calculations (colored in bars) and campaign-average mass-weighted $\log_{10}C_{sat}$ (T) values (in black markers) for different campaigns with the modified Li et al. (2016) parametrization method (Daumit et al., 2013;Isaacman-VanWertz and Aumont, 2021). Compounds more volatile than IVOC with C_{sat} (T) higher than $10^{6.5}$ μg m^{-3} (labelled as "others") contributed negligibly (0.8−2.9%).

The mass-weighted $\log_{10}C_{sat}$ (T) shows a qualitatively similar distribution as the ambient temperature (Pearson's R: 0.58; Figure ~~S3~~ S4 and ~~S4~~S5). This makes sense insofar as on the one hand the $\log_{10}C_{sat}$ (T) calculated using molecular composition is shifted based on ambient temperature (compare Eq. 2) - the same compound exhibits a higher apparent volatility under warmer conditions and vice versa; on the other hand, a higher apparent

volatility is also expected at higher ambient temperatures due to higher local emissions of biogenic precursors. In addition, we find a positive correlation between $\log_{10}C_{sat}$ (T) and humidity (Pearson's R for RH and absolute humidity: 0.57 and 0.68, respectively; Figure ~~S4~~S5), indicating potential hydrolysis effects on OOA particles (forming smaller and more volatile compounds) caused by potentially high aerosol liquid water content at higher humidity levels (Lee et al., 2020;Hu et al., 2011;Hinks et al., 2018). Negative correlations are found between $\log_{10}C_{sat}$ (T) vs. nO (Pearson's R: -0.72) and the average mass-weighted molecular weight (MW) of CHOX compounds (Pearson's R: -0.56), following the parametrization assumption of the oxidation effect on volatility and of lower volatility for larger and complex molecules (Donahue et al., 2011).

3.2.2 Volatility derived from thermograms

We further investigate the volatility derived from FIGAERO thermograms qualitatively for the different sites and compare it to the volatility derived from the molecular composition measurements. It is important to note that, similar to D'Ambro et al. (2018), the term "volatility" we discuss here refers to the effective volatility of bulk OOA particles, which combines the impacts of diffusion limitations and thermal decomposition of lower-volatility species. We focus the bulk OOA volatility analysis here on the shape and distribution of sum thermograms, which are found to give representative qualitative volatility estimations as they take into account the whole signal distribution and reduce potential artefacts from thermal decomposition of individual compounds (Voliotis et al., 2021).

Campaign-average sum thermograms of CHOX compounds (i.e., the sum of mass spectral signal evolution of all CHOX compounds as a function of desorption temperature) for the different locations are shown in Figure 3, normalized to their maximum values. Sum ~~T~~thermogram shapes vary for different environments, and they exhibit maximum signal at temperatures (sumT_{max}) ranging from 80.5 to 146.3 °C (see also Figure ~~S5~~S6). Such differences of sumT_{max} of >60 °C across different systems and environments are hardly surprising, given the large spread in T_{max} for all compounds in one single mass spectrum (Huang et al., 2019b;Wang and Ruiz, 2018), in T_{max} calibrations with different instrumental settings, experimental procedures or calibrants (Wang et al., 2020;Ylisirniö et al., 2021), as well as for one compound with the same molecular formula between day vs. night (Thompson et al., 2017;Gaston et al., 2016), field vs. laboratory (Thompson et al., 2017), or over a whole campaign period using the same instrument and operating conditions (Thompson et al., 2017) (see an example of $C_6H_{10}O_5$, the molecular formula corresponding to levoglucosan, in Figure ~~S6~~S7). However, T_{max} variation due to different instruments or operating conditions is generally smaller than that from the difference in monomers and dimers (Wu et al., 2021) and other factors like the presence of isomers (Thompson et al., 2017;Masoud and Ruiz, 2021) and particle-phase diffusivity, viscosity and matrix effects (Huang et al., 2018;Ren et al., 2022). Different FIGAERO geometry was speculated to not induce significant T_{max} changes (Ylisirniö et al., 2021). The ramp rates for all measurements shown in the present study varied between 6.7 and 13.3 ºC/min (see Table S2), inducing a T_{max} difference of maximum 5 ºC (Schobesberger et al., 2018;Ylisirniö et al., 2021;Thornton et al., 2020). Correction of the T_{max} values to a filter mass loading of 1 µg following our approach outlined earlier (Huang et al., 2018) only leads to a T_{max} change of <5 °C. It is also worth noting that thermal decomposition of larger organic compounds during particle desorption with the FIGAERO could form products with lower masses and lower T_{max} values, and hence higher effective volatility. Although the calculated decomposition fraction has a minor effect on the molecular composition of OOA particles (see more details in section 3.2.1), the contribution of fragments to their parent compounds and the impact on the "original" volatility should not be ignored.

The mountain site in Bolivia in the transition season (MCC-t) exhibits some of the lowest $sumT_{max}$ values of all stations (81.7 °C), indicating relatively higher bulk volatility. In contrast, during the dry season, the bulk OOA appears less volatile (MCC-d $sumT_{max}$: 107.7 °C). This trend is in disagreement with $\log_{10}C_{sat}$ (T), which is higher for MCC-d (i.e. higher volatility) than MCC-t. The discrepancy could be due to thermal fragmentation of larger oligomeric molecules, which bias the C_{sat} results towards higher volatilities and the sum thermogram shape to a lesser extent due to the dominance of monomer species (i.e., ending up with a "tail"). Compared to MCC-t (~26.6%), MCC-d exhibits a higher contribution of thermal fragmentation (~35.9%; also reflected in the higher IVOC fractions in Figure 2a), with multi-mode thermograms showing elevated signals at high desorption temperatures (~150 °C), i.e., with long "tails" (see also Figure S~~5~~6a–b).

The rural sites in Germany (REL) and southeastern U.S. (RAB) have similar $sumT_{max}$ values of ~100°C. Both also show contributions (up to 21%) from thermal fragmentation through multi-mode thermograms or long tails at high desorption temperatures (~150 °C; see also Figure S~~5~~6c–d; similar to the dry season for the mountain site MCC-d). The lowest $sumT_{max}$ value (94.5 °C) at RAB is consistent with its highest average $\log_{10}C_{sat}$ (T) value (2.0±0.4 μg m^{-3}) among the rural stations. The rural site in Finland (RHT) exhibits a high $sumT_{max}$ value of 146.3 °C with a thermogram shape reaching a plateau after 120 °C and the signal only starting to decrease at a desorption temperature >180 °C (see also Figure S~~5~~6e). This might be related to an older age (D'Ambro et al., 2018) and/or a more viscous phase state of the OOA particles at RHT caused by its lowest temperature and RH of all rural stations (Table S1) (Shiraiwa et al., 2011), affecting the evaporative behavior and inferred volatility of the particle-bound compounds (Yli-Juuti et al., 2017;Huang et al., 2018).

The urban sites in Germany (UKA and UST) exhibit similar trends in $sumT_{max}$, with relatively higher values in winter (106.1–112.5 °C) compared to summer (80.5–102.0 °C). Such a seasonal trend is mirrored in their average $\log_{10}C_{sat}$ (T) values. Differences in $sumT_{max}$ between summer and winter are found to be larger for Stuttgart (UST; ~32 °C) than for Karlsruhe (UKA; ~4 °C). This could be due to the differences in measurement environments and topography. The topography at UST prevents dispersion (Huang et al., 2019b;Baumbach and Vogt, 2003), and thus the formation of more oxygenated molecules in winter at UST can be expected due to longer residence time of the air masses (Buchholz et al., 2019) (also reflected in the higher O:C ratios; see Figure 1a). The UKA site is a curb site with more influence from direct traffic emissions (Kumar et al., 2022) including larger aromatic compounds (Lim et al., 1999;Zheng et al., 2017) (see above-mentioned discussions and Figure ~~S1~~S2), and smaller differences for summer vs. winter are therefore expected. The winter Delhi site in India (UDL) exhibits a similar $sumT_{max}$ value (113.0 °C) as UST and UKA in winter (106.1–112.5 °C). All three urban locations show indication of substantial contribution (up to 14%) of thermal fragmentation in their thermograms (see also Figure S~~5~~6f–j), which might also be the reason for the highest $sumT_{max}$ value not corresponding to the lowest $\log_{10}C_{sat}$ (T) value, similar to MCC.

As shown in earlier publications (Huang et al., 2018;Ylisirniö et al., 2021), the connection between T_{max} and volatility is complex, and direct relationships between T_{max} and vapor pressures can only be established for solutions of pure or few compound(s) (Wang et al., 2020;Ylisirniö et al., 2021;Ren et al., 2022). For the complex ambient particle matrix, other factors than the pure compounds' vapor pressures come into play, such as the presence of isomers with different vapor pressures (Thompson et al., 2017), thermal decomposition contributions of larger molecules (Lopez-Hilfiker et al., 2015), and matrix effects and viscosity (Huang et al., 2018;D'Ambro et al., 2017;Wang and Ruiz, 2018) even for same compounds in solutions mixed with different species (Ren et al., 2022). This is exemplified here showing varying T_{max} values for compounds with the same molecular formula

across different campaigns (with an average T_{max} difference of 55.0±24.3 °C), such as $C_5H_{12}O_4$ (molecular formula corresponding to 2-methyltetrol, a tracer of isoprene oxidation products (D'Ambro et al., 2019)), $C_6H_{10}O_5$ (molecular formula corresponding to levoglucosan, a tracer for biomass burning (Saarnio et al., 2010)), $C_8H_{10}O_5$ (identified in the laboratory as a monoterpene oxidation product (Hammes et al., 2019)), $C_8H_{12}O_5$ (molecular formula corresponding to 2-hydroxyterpenylic acid identified in α-pinene SOA (Claeys et al., 2009)), $C_{10}H_{15}NO_7$ (identified in the laboratory as a monoterpene oxidation product (Boyd et al., 2015;Faxon et al., 2018)), and $C_{17}H_{24}O_6$ (identified in the laboratory as a monoterpene oxidation product (Kenseth et al., 2020); Figure ~~S7~~S8). Such variation~~s~~ may be due to actual changes in effective volatilities of the observed OOA components, due to experimental factors, or both. ~~For example, correction of the T_{max} values to a filter mass loading of 1 µg following our approach outlined earlier (Huang et al., 2018) only leads to a T_{max} change of <5 °C, which is not enough to explain the T_{max} differences alone.~~ However, as we discussed earlier, T_{max} variation due to different instruments or operating conditions is generally smaller compared to those due to changes in physico-chemical properties. Therefore, the relative variations in thermogram shapes and T_{max} we present and discuss here in our study are dominated by the presence of isomers (Thompson et al., 2017;Masoud and Ruiz, 2021) and particle-phase diffusivity, viscosity and matrix effects (Huang et al., 2018;Ren et al., 2022). Due to unavailable calibrations of the relationship between T_{max} and C_{sat} (Wang et al., 2020; Ylisirniöet al., 2021) for most locations, ~~We conclude that~~ the analysis and interpretation of OOA volatility based on FIGAERO-CIMS thermograms is challenging and, in the absence of additional constraints on OOA composition and thermal behavior, currently remains at the qualitative level (Graham et al., 2023;Voliotis et al., 2021), especially for complex field data.

Similar to $\log_{10}C_{sat}$ (T), we also compare the sumT_{max} with various environmental and measurement parameters (Figure ~~S8~~S9). Correlations of sumT_{max} values with other parameters (e.g., meteorology, trace gases) are weak (Pearson's R within ±0.3)~~, except for SO_2 (Pearson's R: -0.67). However, this could be artificial as SO_2 would not react/condense directly onto aerosol particles and also too few SO_2 data points were available for this correlation (see also Table S1). Levels of sulfur containing organics (CHOS and CHONS) and non-refractory particulate sulfate show no correlations with sumT_{max} values as well~~. These results further show the complexity in assessing the effective volatility derived from thermogram behavior and T_{max}, especially for a diverse set of field data. Contributing to the lack of clear correlations in this analysis may be potential effects of experimental parameters on the FIGAERO thermograms (Table S2) (Thornton et al., 2020), as well as open questions in their interpretation, as noted above.

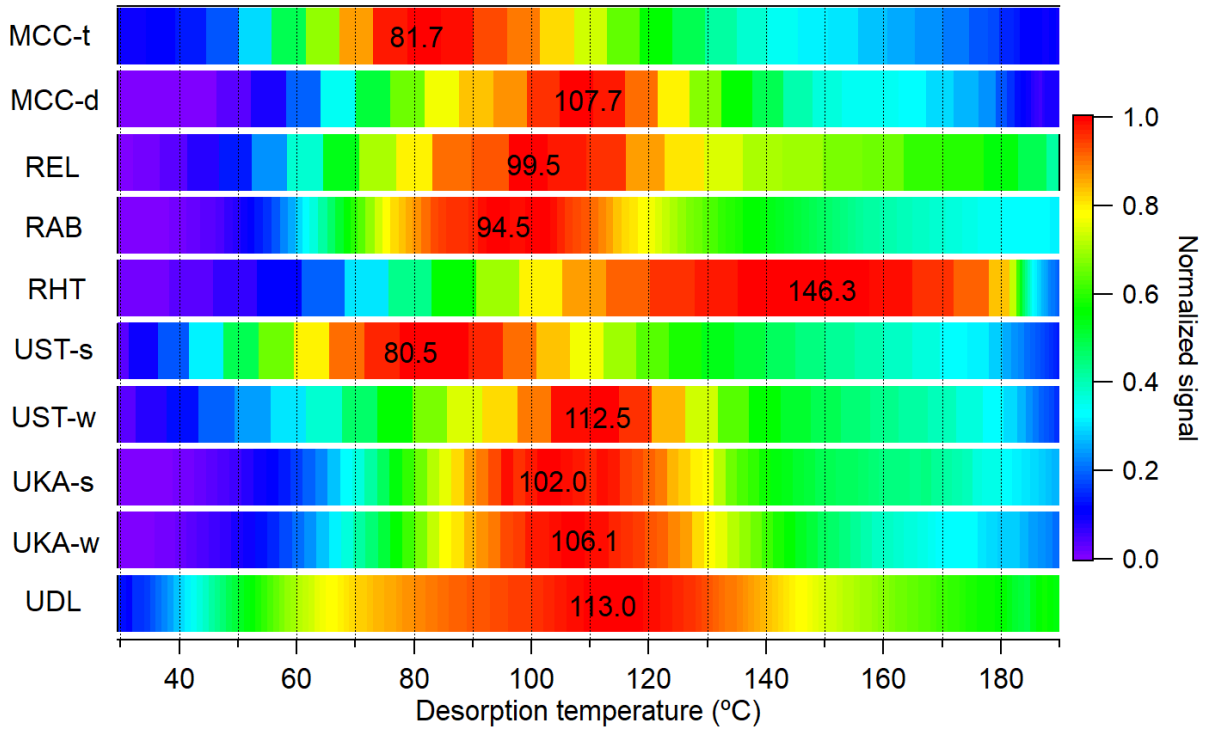

Figure 3. Campaign-average sum thermograms of CHOX compounds (normalized to their maximum values) for all campaigns with corresponding sumT_{max} values labeled on the plot.

3.3 Relationship between thermal desorption-derived volatility and molecular composition-derived volatility

In order to investigate whether there is consistency in the bulk OOA volatility derived from molecular composition and thermograms, we compare the average $\log_{10}C_{sat}$ (i.e, molecular composition-derived volatility) with the sumT_{max} (i.e., thermal desorption-derived volatility) in Figure 4 and Figure ~~S9~~S10. The gray area covers the previously reported calibration fit curves of $\log_{10}C_{sat}$ (298 K) vs. calibrant T_{max} values in colored dashed lines. The As we can see from Figure 4, overall the $\log_{10}C_{sat}$ (298 K) values from different locations are close to the range given by the calibration curves. However, it is important to note that this does not suggest T_{max} calibrations are not needed for field measurements (unavailable for our datasets). Although we cannot find a correlation between $\log_{10}C_{sat}$ (298 K) and sumT_{max} with all data points included, that correlation might be to some extent improved with laboratory T_{max} calibrations. This underlines again the complexity of assessments of the volatility through either method, as already shown for laboratory measurements (Graham et al., 2023), but even more so for comparisons of complex ambient data from different locations and periods, and different instrument versions (see Table S2).

If we only focus on the datasets collected with the same FIGAERO setup (REL, UST-s, UST-w, UKA-s, and UKA-w) assuming similar calibration factors, a negative correlation (Pearson's R: -0.54) is observed between $\log_{10}C_{sat}$ (298 K) and sumT_{max}. And the correlation still holds between ambient temperature-corrected $\log_{10}C_{sat}$ and sumT_{max} (Pearson's R: -0.92). Although C_{sat} values can be biased by orders of magnitude using other parametrization methods (Graham et al., 2023), the general slope and trend is similar to the calibration curves or to that using other parametrization methods such as Donahue et al. (2011) method (Figure S1). The results hence provide an overall broad qualitative agreement between bulk volatility derived from thermograms and composition.

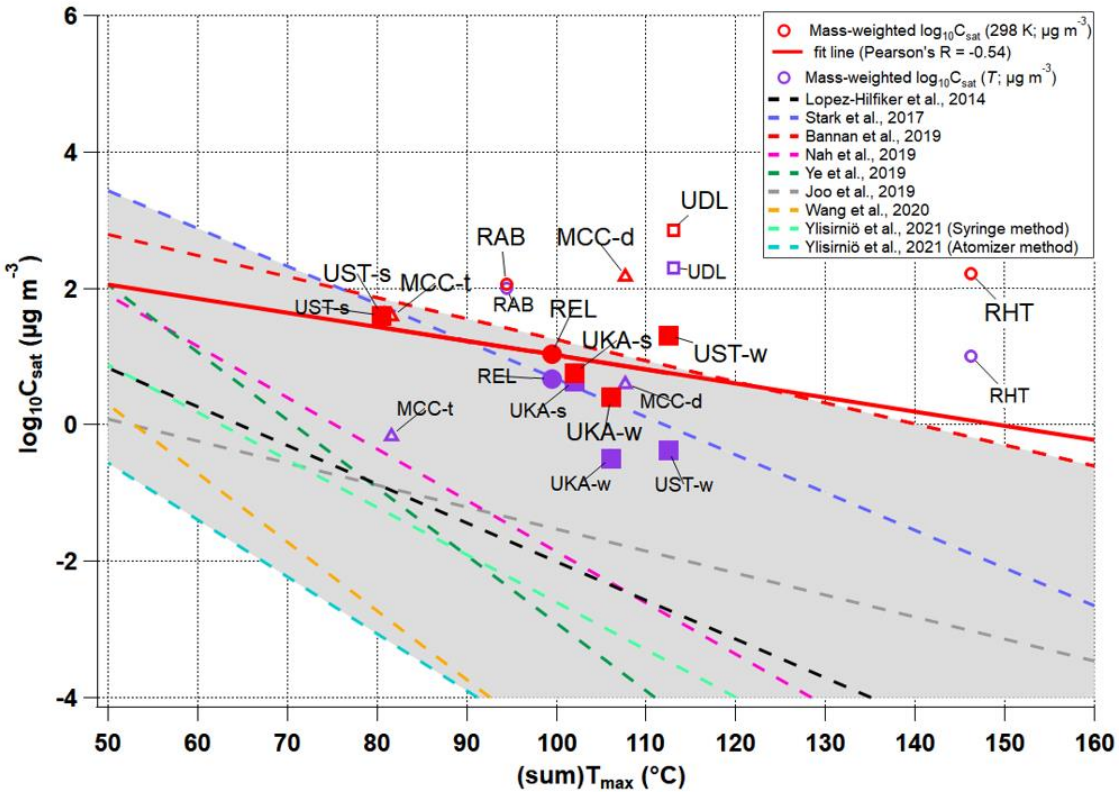

Figure 4. Comparison of the campaign-average mass-weighted $\log_{10}C_{sat}$ and $sumT_{max}$ values for different locations and seasons (Mountain sites in triangles, Rural sites in circles, and Urban sites in squares), with mass-weighted $\log_{10}C_{sat}$ (298 K) in red and mass-weighted $\log_{10}C_{sat}$ (T) in purple. The red solid line is the fit line for the red solid markers only, the data of which are from the same FIGAERO setup. The gray area covers the previously reported calibrations of $\log_{10}C_{sat}$ (298 K) vs. calibrant T_{max} values in colored dashed lines. The wide spread of these calibration lines is believed to result from variations in instrument designs, experimental procedures, and the ranges of used calibration compounds (Ylisirniö et al., 2021).

Other than the effects of different FIGAERO geometries (Ylisirniö et al., 2021), parameters affecting the correlation between $\log_{10}C_{sat}$ and $sumT_{max}$ are manifold and the correlation is subject to uncertainties and artefacts for both methods. On the one hand, molecular composition-derived volatility is limited by its incapability in differentiating isomers with different vapor pressures since it is solely based on molecular formula (Graham et al., 2023), and the bulk OOA volatility for the complex ambient particle matrix may also diverge from the sum of individual parametrized C_{sat} due to non-ideal intermolecular interactions (Compernolle et al., 2011;Isaacman-VanWertz and Aumont, 2021), in addition to the highly uncertain parametrization of C_{sat} for organonitrates with multiple nitrate groups (Graham et al., 2023). On the other hand, thermal desorption-derived volatility can suffer from artefacts from oligomer content, viscosity, and possible mutual interactions between them (i.e., oligomer content vs. viscosity) (Huang et al., 2018;D'Ambro et al., 2017;Wang and Ruiz, 2018). Thermal decomposition of larger oligomeric molecules can bias the C_{sat} towards higher volatilities and the sum thermogram shape and $sumT_{max}$ to a lesser extent due to the dominance of monomer species (i.e., ending up with a longer tail). There have been attempts to separate the thermal decomposition contribution for individual thermograms (Lutz et al., 2019;D'Ambro et al., 2018;Buchholz et al., 2020;Wu et al., 2021), but this poses the threat for introducing new uncertainties due to the difficulty in e.g. differentiating isomers from thermal decomposition products, and monomers from dimers in ambient samples with complex VOC precursors (Graham et al., 2023;Voliotis et al.,

2021). Overall, however, for a limited number of our datasets from the exact same instrument, the lower apparent volatility (i.e., higher sumT_{max}) agrees qualitatively with the lower $\log_{10}C_{sat}$ values, corroborating potential relationships and interconnections between volatility and chemical composition across different environments and systems despite the large uncertainties and artefacts of both methods.

4 Conclusions and atmospheric implications

In this paper, the molecular composition and volatility of OOA particles at different rural, urban, and ~~remote~~ mountain environments ~~across the globe~~ were investigated with the deployments of FIGAERO-CIMS. We find distinct molecular composition for different environments: OOA particles exhibit on average larger nC and lower O:C ratios at the urban sites (nC: 9.8±0.7; O:C: 0.76±0.03), followed by the rural (nC: 8.8±0.6; O:C: 0.80±0.05) and ~~remote~~ mountain stations (nC: 8.1±0.8; O:C: 0.91±0.07), indicative of different emission sources and chemistry. While the CHO contributions are on average higher (79.9±5.2%) compared to the mountain (66.2±5.5%) and urban sites (72.6±4.3%), in accordance with their proximity to forested areas, the largest contributions of CHON compounds are found at the urban stations (27.1±4.3%), consistent with their higher NO_x levels.

Besides, the bulk OOA volatility differences are found in C_{sat} values by up to ~3 orders of magnitude, and in thermogram shapes with average sumT_{max} values by up to 60 °C across different locations and systems. Despite of the uncertainties/limitations for volatility derived from both sumT_{max} and molecular formula as well as the translated uncertainties in the relationship between them, sumT_{max} are found to exhibit an overall negative correlation with molecular formula based C_{sat}, suggesting a potential relationship/interlink between the volatility and chemical composition for the different locations and systems.

Here, using FIGAERO-CIMS measurements of OOA particles from various locations ~~across the globe~~, we achieve a comprehensive picture of the relationship/interconnection between volatility and chemical composition of OOA particles in different rural, urban, and mountain~~remote~~ environments, which are characterized by different ambient meteorological parameters, trace gas levels, emission sources/chemistry, and resulting distinct OOA molecular composition and volatility. Our study shows a connection between chemical composition and thermal desorption behavior, but also the limitations of using measurements of either for the assessment of volatility. Thermal decomposition has been a well-known issue for FIGAERO-CIMS measurements, however, the effects on the bulk molecular composition and sum thermograms of all detected OOA compounds for most sites studied here are ~~small~~ not significant as these thermally-unstable oligomers do not dominate the OOA mass. For some locations with multi-mode thermograms dominated by the second mode (e.g., MCC-d, RHT, and UDL; see Figure S6), the effects would be larger. Still, alternative approaches need to be developed for more quantitative estimations of volatility from FIGAERO-CIMS measurements.

Overall we find that it is clearly the chemical composition of OOA that determines its apparent volatility, and that environmental conditions (e.g., ambient temperature) play a lesser, secondary role through their influence on sources and chemistry of a particular environment, such as seasonal patterns of biogenic emissions and human behavior (e.g., residential heating). For example, summer OOA particles tend to be more volatile than the winter OOA particles due to higher ambient temperatures in summer and consequently higher local emissions of biogenic precursors and higher reaction rates. In winter, OOA particles are subject to higher biomass burning emissions and/or traffic emissions from human activities. Therefore, the importance of chemical composition and environmental conditions (e.g., ambient temperature) on the apparent volatility of OOA particles is different, with

the chemical composition (i.e., sources and chemistry) being a more direct and important factor than the environmental conditions. The comprehensive ~~global~~ dataset from our results shows the complex thermodynamics and chemistry of OOA and their changes during its lifetime in the atmosphere, and that the chemical description of OOA generally suffices to predict its apparent volatility, at least qualitatively. Considering the major contribution of OA to total aerosol mass concentrations and implications for both human health and climate change (Jimenez et al., 2009;Nel, 2005;IPCC, 2021), ~~O~~our study ~~thus~~ provides new insights that will help guide choices of e.g. descriptions of OOA volatility in different model frameworks~~, which has been previously simplified due to challenges to measure and represent it in models~~. For example, with a better constraint on the volatility of condensable vapors and the associated particles using e.g. the up-to-date CIMS measurements, the study could contribute to understanding the underlying oxidative chemistry and a better OA representation in air quality models. The potential contribution of co-condensation of organic vapors to aerosol forcing or to future cloud radiative effects could also be better accounted for in cloud parcel models (Heikkinen et al., 2023). A better understanding of the chemical nature and volatility of OA components can thus ultimately improve predictions of atmospheric organic particle mass and climate effects of atmospheric OA.

Data availability

The data that are involved in the figures can be found at https://doi.org/10.5281/zenodo.7983797 (Huang, 2023).

Author contributions

JT, HS, DG, and CM designed the research; WH, CW, LG, YG, SLH, FDL, BHL, JS, XS, RR, SNT, DG, FJ, MV, and CM conducted field measurements; WH, CW, LG, SLH, FDL, BHL, JS, HS, XS, SNT, DG, and CM analysed the data; CW, LG, YG, SLH, JT, SS, TY, JS, HS, XS, MV, and CM provided suggestions for the data analysis, interpretation, and discussion; WH and CM wrote the paper with contributions of all authors. All authors have given approval to the final text.

Competing interests

At least one of the (co-)authors is a member of the editorial board of Atmospheric Chemistry and Physics.

Acknowledgements

Technical support by the staff at IMK-AAF is gratefully acknowledged. Support by Deutsche Bahn AG, University of Stuttgart, and partners of the project “Three-Dimensional Observation of Atmospheric Processes in Cities (3DO)” (uc2-3do.org/) during the UST campaigns is gratefully acknowledged. Support by University of Helsinki, Innsbruck University, Stockholm University, and Universidad Mayor de San Andres during the MCC campaign is gratefully acknowledged.

Financial support

We acknowledge the financial support from the H2020 European Research Council (CHAPAs, grant no. 850614), Academy of Finland (grant no. 337550 and 346371), the Knut and Alice Wallenberg (KAW) foundation (WAF project CLOUDFORM, grant no. 2017.0165) and GRACE (Graduate School for Climate and Environment Center of Karlsruhe Institute of Technology). We also thank the financial support from the Central Pollution Control Board (CPCB) and Government of India (grant no. AQM/Source apportionment_EPC Project/2017) as well as the financial support under Centre of Excellence Advanced Technologies for Monitoring Air-quality iNdicators (ATMAN) approved by PSA office, Government of India and supported by a group of philanthropic funders including the Bloomberg Philanthropies, the Children's Investment Fund Foundation (CIFF), the Open Philanthropy, and the Clean Air Fund, during the campaign at UDL site. Linyu Gao, Junwei Song, and Feng Jiang are thankful for the financial support from China Scholarship Council (CSC).

References

Aliaga, D., Sinclair, V. A., Andrade, M., Artaxo, P., Carbone, S., Kadantsev, E., Laj, P., Wiedensohler, A., Krejci, R., and Bianchi, F.: Identifying source regions of air masses sampled at the tropical high-altitude site of Chacaltaya using WRF-FLEXPART and cluster analysis, Atmos Chem Phys, 21, 16453-16477, 10.5194/acp-21-16453-2021, 2021.

Bardakov, R., Thornton, J. A., Riipinen, I., Krejci, R., and Ekman, A. M. L.: Transport and chemistry of isoprene and its oxidation products in deep convective clouds, Tellus B, 73, 1979856, https://doi.org/10.1080/16000889.2021.1979856, 2021.

Baumbach, G., and Vogt, U.: Influence of inversion layers on the distribution of air pollutants in urban areas, Water, Air, & Soil Pollution: Focus, 3, 67–78, https://doi.org/10.1023/A:1026098305581, 2003.

Bianchi, F., Sinclair, V. A., Aliaga, D., Zha, Q., Scholz, W., Wu, C., Heikkinen, L., Modini, R., Partoll, E., Velarde, F., Moreno, I., Gramlich, Y., Huang, W., Leiminger, M., Enroth, J., Peräkylä, O., Marinoni, A., Xuemeng, C., Blacutt, L., Forno, R., Gutierrez, R., Ginot, P., Uzu, G., Facchini, M. C., Gilardoni, S., Gysel-Beer, M., Cai, R., Petäjä, T., Rinaldi, M., Saathoff, H., Sellegri, K., Worsnop, D., Artaxo, P., Hansel, A., Kulmala, M., Wiedensohler, A., Laj, P., Krejci, R., Carbone, S., Andrade, M., and Mohr, C.: The SALTENA Experiment: Comprehensive Observations of Aerosol Sources, Formation, and Processes in the South American Andes, Bulletin of the American Meteorological Society, E212–E229, https://doi.org/10.1175/BAMS-D-20-0187.1, 2022.

Boyd, C. M., Sanchez, J., Xu, L., Eugene, A. J., Nah, T., Tuet, W. Y., Guzman, M. I., and Ng, N. L.: Secondary organic aerosol formation from the beta-pinene+NO3 system: effect of humidity and peroxy radical fate, Atmos Chem Phys, 15, 7497–7522, https://doi.org/10.5194/acp-15-7497-2015, 2015.

Buchholz, A., Lambe, A. T., Ylisirniö, A., Li, Z., Tikkanen, O.-P., Faiola, C., Kari, E., Hao, L. Q., Luoma, O., Huang, W., Mohr, C., Worsnop, D. R., Nizkorodov, S. A., Yli-Juuti, T., Schobesberger, S., and Virtanen, A.: Insights into the O:C-dependent mechanisms controlling the evaporation of α-pinene secondary organic aerosol particles, Atmos Chem Phys, 19, 4061–4073, https://doi.org/10.5194/acp-19-4061-2019, 2019.

Buchholz, A., Ylisirnio, A., Huang, W., Mohr, C., Canagaratna, M., Worsnop, D., Schobesberger, S., and Virtanen, A.: Deconvolution of FIGAERO-CIMS thermal desorption profiles using positive matrix factorisation to identify chemical and physical processes during particle evaporation, Atmos Chem Phys, 20, 7693-7716, 10.5194/acp-20-7693-2020, 2020.

Cai, J., Daellenbach, K. R., Wu, C., Zheng, Y., Zheng, F. X., Du, W., Haslett, S. L., Chen, Q., Kulmala, M., and Mohr, C.: Characterization of offline analysis of particulate matter with FIGAERO-CIMS, Atmos Meas Tech, 16, 1147-1165, 10.5194/amt-16-1147-2023, 2023.

Canonaco, F., Slowik, J. G., Baltensperger, U., and Prévôt, A. S. H.: Seasonal differences in oxygenated organic aerosol composition: implications for emissions sources and factor analysis, Atmos Chem Phys, 15, 6993–7002, https://doi.org/10.5194/acp-15-6993-2015, 2015.

Claeys, M., Iinuma, Y., Szmigielski, R., Surratt, J. D., Blockhuys, F., Van Alsenoy, C., Böge, O., Sierau, B., Gómez-González, Y., Vermeylen, R., Van der Veken, P., Shahgholi, M., Chan, A. W. H., Herrmann, H., Seinfeld, J. H., and Maenhaut, W.: Terpenylic acid and related compounds from the oxidation of α-pinene: Implications for new particle formation and growth above forests, Environ Sci Technol, 43, 6976–6982, https://doi.org/10.1021/es9007596, 2009.

Compernolle, S., Ceulemans, K., and Muller, J. F.: EVAPORATION: a new vapour pressure estimation methodfor organic molecules including non-additivity and intramolecular interactions, Atmos Chem Phys, 11, 9431-9450, 10.5194/acp-11-9431-2011, 2011.

D'Ambro, E. L., Lee, B. H., Liu, J. M., Shilling, J. E., Gaston, C. J., Lopez-Hilfiker, F. D., Schobesberger, S., Zaveri, R. A., Mohr, C., Lutz, A., Zhang, Z. F., Gold, A., Surratt, J. D., Rivera-Rios, J. C., Keutsch, F. N., and Thornton, J. A.: Molecular composition and volatility of isoprene photochemical oxidation secondary organic aerosol under low- and high-NOx conditions, Atmos Chem Phys, 17, 159–174, https://doi.org/10.5194/acp-17-159-2017, 2017.

D'Ambro, E. L., Schobesberger, S., Zaveri, R. A., Shilling, J. E., Lee, B. H., Lopez-Hilfiker, F. D., Mohr, C., and Thornton, J. A.: Isothermal Evaporation of alpha-Pinene Ozonolysis SOA: Volatility, Phase State, and Oligomeric Composition, Acs Earth Space Chem, 2, 1058-1067, 10.1021/acsearthspacechem.8b00084, 2018.

D'Ambro, E. L., Schobesberger, S., Gaston, C. J., Lopez-Hilfiker, F. D., Lee, B. H., Liu, J., Zelenyuk, A., Bell, D., Cappa, C. D., Helgestad, T., Li, Z., Guenther, A., Wang, J., Wise, M., Caylor, R., Surratt, J. D., Riedel, T., Hyttinen, N., Salo, V.-T., Hasan, G., Kurtén, T., Shilling, J. E., and Thornton, J. A.: Chamber-based insights into the factors controlling epoxydiol (IEPOX) secondary organic aerosol (SOA) yield, composition, and volatility, Atmos Chem Phys, 19, 11253–11265, https://doi.org/10.5194/acp-19-11253-2019, 2019.

Daumit, K. E., Kessler, S. H., and Kroll, J. H.: Average chemical properties and potential formation pathways of highly oxidized organic aerosol, Faraday Discuss, 165, 181-202, https://doi.org/10.1039/C3FD00045A, 2013.

Donahue, N. M., Robinson, A. L., and Pandis, S. N.: Atmospheric organic particulate matter: from smoke to secondary organic aerosol, Atmos Environ, 43, 94–106, https://doi.org/10.1016/j.atmosenv.2008.09.055, 2009.

Donahue, N. M., Epstein, S. A., Pandis, S. N., and Robinson, A. L.: A two-dimensional volatility basis set: 1. organic-aerosol mixing thermodynamics, Atmos Chem Phys, 11, 3303–3318, https://doi.org/10.5194/acp-11-3303-2011, 2011.

Donahue, N. M., Kroll, J. H., Pandis, S. N., and Robinson, A. L.: A two-dimensional volatility basis set – Part 2: diagnostics of organic-aerosol evolution, Atmos Chem Phys, 12, 615–634, https://doi.org/10.5194/acp-12-615-2012, 2012.

Epstein, S. A., Riipinen, I., and Donahue, N. M.: A semiempirical correlation between enthalpy of vaporization and saturation concentration for organic aerosol, Environ Sci Technol, 44, 743–748, https://doi.org/10.1021/es902497z, 2010.

Faxon, C., Hammes, J., Le Breton, M., Pathak, R. K., and Hallquist, M.: Characterization of organic nitrate constituents of secondary organic aerosol (SOA) from nitrate-radical-initiated oxidation of limonene using high-resolution chemical ionization mass spectrometry, Atmos Chem Phys, 18, 5467–5481, https://doi.org/10.5194/acp-18-5467-2018, 2018.

Fry, J. L., Brown, S. S., Middlebrook, A. M., Edwards, P. M., Campuzano-Jost, P., Day, D. A., Jimenez, J. L., Allen, H. M., Ryerson, T. B., Pollack, I., Graus, M., Warneke, C., de Gouw, J. A., Brock, C. A., Gilman, J., Lerner, B. M., Dube, W. P., Liao, J., and Welti, A.: Secondary organic aerosol (SOA) yields from NO3 radical + isoprene based on nighttime aircraft power plant plume transects, Atmos Chem Phys, 18, 11663-11682, 10.5194/acp-18-11663-2018, 2018.

Gaston, C. J., Lopez-Hilfiker, F. D., Whybrew, L. E., Hadley, O., McNair, F., Gao, H. L., Jaffe, D. A., and Thornton, J. A.: Online molecular characterization of fine particulate matter in Port Angeles, WA: Evidence for a major impact from residential wood smoke, Atmos Environ, 138, 99–107, https://doi.org/10.1016/j.atmosenv.2016.05.013, 2016.

Graham, E. L., Wu, C., Bell, D. M., Bertrand, A., Haslett, S. L., Baltensperger, U., El Haddad, I., Krejci, R., Riipinen, I., and Mohr, C.: Volatility of aerosol particles from NO3 oxidation of various biogenic organic precursors, Atmos Chem Phys, 23, 7347-7362, https://doi.org/10.5194/acp-23-7347-2023, 2023.

Hallquist, M., Wenger, J. C., Baltensperger, U., Rudich, Y., Simpson, D., Claeys, M., Dommen, J., Donahue, N. M., George, C., Goldstein, A. H., Hamilton, J. F., Herrmann, H., Hoffmann, T., Iinuma, Y., Jang, M., Jenkin, M. E., Jimenez, J. L., Kiendler-Scharr, A., Maenhaut, W., McFiggans, G., Mentel, T. F., Monod, A., Prévôt, A. S. H., Seinfeld, J. H., Surratt, J. D., Szmigielski, R., and Wildt, J.: The formation, properties and impact of secondary organic aerosol: current and emerging issues, Atmos Chem Phys, 9, 5155–5236, https://doi.org/10.5194/acp-9-5155-2009, 2009.

Hammes, J., Lutz, A., Mentel, T., Faxon, C., and Hallquist, M.: Carboxylic acids from limonene oxidation by ozone and hydroxyl radicals: insights into mechanisms derived using a FIGAERO-CIMS, Atmos Chem Phys, 19, 13037–13052, https://doi.org/10.5194/acp-19-13037-2019, 2019.

Heikkinen, L., Partridge, D. G., Huang, W., Blichner, S., Ranjan, R., Tovazzi, E., Petäjä, T., Mohr, C., and Riipinen, I.: Cloud response to co-condensation of water and organic vapors over the boreal forest, EGUsphere, [preprint], https://doi.org/10.5194/egusphere-2023-164, 2023.

Hinks, M. L., Montoya-Aguilera, J., Ellison, L., Lin, P., Laskin, A., Laskin, J., Shiraiwa, M., Dabdub, D., and Nizkorodov, S. A.: Effect of relative humidity on the composition of secondary organic aerosol from the oxidation of toluene, Atmos Chem Phys, 18, 1643-1652, 10.5194/acp-18-1643-2018, 2018.

Hu, K. S., Darer, A. I., and Elrod, M. J.: Thermodynamics and kinetics of the hydrolysis of atmospherically relevant organonitrates and organosulfates, Atmos Chem Phys, 11, 8307–8320, https://doi.org/10.5194/acp-11-8307-2011, 2011.

Huang, W., Saathoff, H., Pajunoja, A., Shen, X. L., Naumann, K.-H., Wagner, R., Virtanen, A., Leisner, T., and Mohr, C.: α-Pinene secondary organic aerosol at low temperature: chemical composition and implications for particle viscosity, Atmos Chem Phys, 18, 2883–2898, https://doi.org/10.5194/acp-18-2883-2018, 2018.

Huang, W., Saathoff, H., Shen, X., Ramisetty, R., Leisner, T., and Mohr, C.: Chemical characterization of highly functionalized organonitrates contributing to night-time organic aerosol mass loadings and particle growth, Environ Sci Technol, 53, 1165–1174, https://doi.org/10.1021/acs.est.8b05826, 2019a.

Huang, W., Saathoff, H., Shen, X. L., Ramisetty, R., Leisner, T., and Mohr, C.: Seasonal characteristics of organic aerosol chemical composition and volatility in Stuttgart, Germany, Atmos Chem Phys, 19, 11687–11700, https://doi.org/10.5194/acp-19-11687-2019, 2019b.

Huang, W., Li, H. Y., Sarnela, N., Heikkinen, L., Tham, Y. J., Mikkila, J., Thomas, S. J., Donahue, N. M., Kulmala, M., and Bianchi, F.: Measurement report: Molecular composition and volatility of gaseous organic compounds in a boreal forest - from volatile organic compounds to highly oxygenated organic molecules, Atmos Chem Phys, 21, 8961–8977, https://doi.org/10.5194/acp-21-8961-2021, 2021.

IPCC: Climate change 2021: the physical scientific basis, in, Cambridge University Press, Cambridge, United Kingdom and New York, NY, USA, 33−144, 2021.

Isaacman-VanWertz, G., and Aumont, B.: Impact of organic molecular structure on the estimation of atmospherically relevant physicochemical parameters, Atmos Chem Phys, 21, 6541–6563, https://doi.org/10.5194/acp-21-6541-2021, 2021.

Jimenez, J. L., Canagaratna, M. R., Donahue, N. M., Prevot, A. S. H., Zhang, Q., Kroll, J. H., DeCarlo, P. F., Allan, J. D., Coe, H., Ng, N. L., Aiken, A. C., Docherty, K. S., Ulbrich, I. M., Grieshop, A. P., Robinson, A. L., Duplissy, J., Smith, J. D., Wilson, K. R., Lanz, V. A., Hueglin, C., Sun, Y. L., Tian, J., Laaksonen, A., Raatikainen, T., Rautiainen, J., Vaattovaara, P., Ehn, M., Kulmala, M., Tomlinson, J. M., Collins, D. R., Cubison, M. J., Dunlea, E. J., Huffman, J. A., Onasch, T. B., Alfarra, M. R., Williams, P. I., Bower, K., Kondo, Y., Schneider, J., Drewnick, F., Borrmann, S., Weimer, S., Demerjian, K., Salcedo, D., Cottrell, L., Griffin, R., Takami, A., Miyoshi, T., Hatakeyama, S., Shimono, A., Sun, J. Y., Zhang, Y. M., Dzepina, K., Kimmel, J. R., Sueper, D., Jayne, J. T., Herndon, S. C., Trimborn, A. M., Williams, L. R., Wood, E. C., Middlebrook, A. M., Kolb, C. E., Baltensperger, U., and Worsnop, D. R.: Evolution of organic aerosols in the atmosphere, Science, 326, 1525–1529, https://doi.org/10.1126/science.1180353 2009.

Junninen, H., Ehn, M., Petäjä, T., Luosujärvi, L., Kotiaho, T., Kostiainen, R., Rohner, U., Gonin, M., Fuhrer, K., Kulmala, M., and Worsnop, D. R.: A high-resolution mass spectrometer to measure atmospheric ion composition, Atmos Meas Tech, 3, 1039–1053, https://doi.org/10.5194/amt-3-1039-2010, 2010.

Keller, A., and Burtscher, H.: Characterizing particulate emissions from wood burning appliances including secondary organic aerosol formation potential, J Aerosol Sci, 114, 21–30, https://doi.org/10.1016/j.jaerosci.2017.08.014, 2017.

Kenseth, C. M., Hafeman, N. J., Huang, Y., Dalleska, N. F., Stoltz, B. M., and Seinfeld, J. H.: Synthesis of Carboxylic Acid and Dimer Ester Surrogates to Constrain the Abundance and Distribution of Molecular Products in alpha-Pinene and beta-Pinene Secondary Organic Aerosol, Environ Sci Technol, 54, 12829-12839, 10.1021/acs.est.0c01566, 2020.

Kiendler-Scharr, A., Mensah, A. A., Friese, E., Topping, D., Nemitz, E., Prevot, A. S. H., Äijälä, M., Allan, J., Canonaco, F., Canagaratna, M., Carbone, S., Crippa, M., Dall Osto, M., Day, D. A., De Carlo, P., Di Marco, C. F., Elbern, H., Eriksson, A., Freney, E., Hao, L., Herrmann, H., Hildebrandt, L., Hillamo, R., Jimenez, J. L., Laaksonen, A., McFiggans, G., Mohr, C., O'Dowd, C., Otjes, R., Ovadnevaite, J., Pandis, S. N., Poulain, L., Schlag, P., Sellegri, K., Swietlicki, E., Tiitta, P., Vermeulen, A., Wahner, A., Worsnop, D., and Wu, H.-C.: Ubiquity of organic nitrates from nighttime chemistry in the European submicron aerosol, Geophys Res Lett, 43, 7735–7744, https://doi.org/10.1002/2016GL069239, 2016.

Kroll, J. H., and Seinfeld, J. H.: Chemistry of secondary organic aerosol: Formation and evolution of low-volatility organics in the atmosphere, Atmos Environ, 42, 3593–3624, https://doi.org/10.1016/j.atmosenv.2008.01.003, 2008.

Kumar, V., Giannoukos, S., Haslett, S. L., Tong, Y. D., Singh, A., Bertrand, A., Lee, C. P., Wang, D. S., Bhattu, D., Stefenelli, G., Dave, J. S., Puthussery, J. V., Qi, L., Vats, P., Rai, P., Casotto, R., Satish, R., Mishra, S., Pospisilova, V., Mohr, C., Bell, D. M., Ganguly, D., Verma, V., Rastogi, N., Baltensperger, U., Tripathi, S. N., Prévôt, A. S. H., and Slowik, J. G.: Highly time-resolved chemical speciation and source apportionment of organic aerosol components in Delhi, India, using extractive electrospray ionization mass spectrometry, Atmos Chem Phys, 22, 7739-7761, https://doi.org/10.5194/acp-22-7739-2022, 2022.

Lee, B. H., Lopez-Hilfiker, F. D., Mohr, C., Kurtén, T., Worsnop, D. R., and Thornton, J. A.: An iodide-adduct high-resolution time-of-flight chemical-ionization mass spectrometer: Application to atmospheric inorganic and organic compounds, Environ Sci Technol, 48, 6309−6317, https://doi.org/10.1021/es500362a, 2014.

Lee, B. H., Mohr, C., Lopez-Hilfiker, F. D., Lutz, A., Hallquist, M., Lee, L., Romer, P., Cohen, R. C., Iyer, S., Kurtén, T., Hu, W. W., Day, D. A., Campuzano-Jost, P., Jimenez, J. L., Xu, L., Ng, N. L., Guo, H. Y., Weber, R. J., Wild, R. J., Brown, S. S., Koss, A., de Gouw, J., Olson, K., Goldstein, A. H., Seco, R., Kim, S., McAvey, K., Shepson, P. B., Starn, T., Baumann, K., Edgerton, E. S., Liu, J. M., Shilling, J. E., Miller, D. O., Brune, W., Schobesberger, S., D'Ambro, E. L., and Thornton, J. A.: Highly functionalized organic nitrates in the southeast

United States: Contribution to secondary organic aerosol and reactive nitrogen budgets, P Natl Acad Sci USA, 113, 1516–1521, https://doi.org/10.1073/pnas.1508108113, 2016.

Lee, B. H., Lopez-Hilfiker, F. D., D'Ambro, E. L., Zhou, P. T., Boy, M., Petäjä, T., Hao, L. Q., Virtanen, A., and Thornton, J. A.: Semi-volatile and highly oxygenated gaseous and particulate organic compounds observed above a boreal forest canopy, Atmos Chem Phys, 18, 11547–11562, https://doi.org/10.5194/acp-18-11547-2018, 2018.

Lee, B. H., D'Ambro, E. L., Lopez-Hilfiker, F. D., Schobesberger, S., Mohr, C., Zawadowicz, M. A., Liu, J., Shilling, J. E., Hu, W., Palm, B. B., Jimenez, J. L., Hao, L., Virtanen, A., Zhang, H., Goldstein, A. H., Pye, H. O. T., and Thornton, J. A.: Resolving ambient organic aerosol formation and aging pathways with simultaneous molecular composition and volatility observations, Acs Earth Space Chem, 4, 391-402, 10.1021/acsearthspacechem.9b00302, 2020.

Li, H. Y., Riva, M., Rantala, P., Heikkinen, L., Daellenbach, K., Krechmer, J. E., Flaud, P. M., Worsnop, D., Kulmala, M., Villenave, E., Perraudin, E., Ehn, M., and Bianchi, F.: Terpenes and their oxidation products in the French Landes forest: insights from Vocus PTR-TOF measurements, Atmos Chem Phys, 20, 1941–1959, https://doi.org/10.5194/acp-20-1941-2020, 2020.

Li, Y., Pöschl, U., and Shiraiwa, M.: Molecular corridors and parameterizations of volatility in the chemical evolution of organic aerosols, Atmos Chem Phys, 16, 3327–3344, https://doi.org/10.5194/acp-16-3327-2016, 2016.

Lim, L. H., Harrison, R. M., and Harrad, S.: The Contribution of Traffic to Atmospheric Concentrations of Polycyclic Aromatic Hydrocarbons, Environ Sci Technol, 33, 3538–3542, https://doi.org/10.1021/es990392d, 1999.

Lopez-Hilfiker, F. D., Mohr, C., Ehn, M., Rubach, F., Kleist, E., Wildt, J., Mentel, T. F., Lutz, A., Hallquist, M., Worsnop, D., and Thornton, J. A.: A novel method for online analysis of gas and particle composition: description and evaluation of a Filter Inlet for Gases and AEROsols (FIGAERO), Atmos Meas Tech, 7, 983−1001, https://doi.org/10.5194/amt-7-983-2014, 2014.

Lopez-Hilfiker, F. D., Mohr, C., Ehn, M., Rubach, F., Kleist, E., Wildt, J., Mentel, T. F., Carrasquillo, A. J., Daumit, K. E., Hunter, J. F., Kroll, J. H., Worsnop, D. R., and Thornton, J. A.: Phase partitioning and volatility of secondary organic aerosol components formed from α-pinene ozonolysis and OH oxidation: the importance of accretion products and other low volatility compounds, Atmos Chem Phys, 15, 7765−7776, https://doi.org/10.5194/acp-15-7765-2015, 2015.

Lopez-Hilfiker, F. D., Mohr, C., D'Ambro, E. L., Lutz, A., Riedel, T. P., Gaston, C. J., Iyer, S., Zhang, Z., Gold, A., Surratt, J. D., Lee, B. H., Kurten, T., Hu, W. W., Jimenez, J., Hallquist, M., and Thornton, J. A.: Molecular composition and volatility of organic aerosol in the Southeastern U.S.: Implications for IEPOX derived SOA, Environ Sci Technol, 50, 2200–2209, https://doi.org/10.1021/acs.est.5b04769, 2016.

Lutz, A., Mohr, C., Le Breton, M., Lopez-Hilfiker, F. D., Priestley, M., Thornton, J. A., and Hallquist, M.: Gas to Particle Partitioning of Organic Acids in the Boreal Atmosphere, Acs Earth Space Chem, 3, 1279-1287, 10.1021/acsearthspacechem.9b00041, 2019.

Masoud, C. G., and Ruiz, L. H.: Chlorine-Initiated Oxidation of α-Pinene: Formation of Secondary Organic Aerosol and Highly Oxygenated Organic Molecules, Acs Earth Space Chem, 5, 2307–2319, https://doi.org/10.1021/acsearthspacechem.1c00150, 2021.

Massoli, P., Stark, H., Canagaratna, M. R., Krechmer, J. E., Xu, L., Ng, N. L., Mauldin, R. L., Yan, C., Kimmel, J., Misztal, P. K., Jimenez, J. L., Jayne, J. T., and Worsnop, D. R.: Ambient measurements of highly oxidized gas-phase molecules during the Southern Oxidant and Aerosol Study (SOAS) 2013, Acs Earth Space Chem, 2, 653–672, https://doi.org/10.1021/acsearthspacechem.8b00028, 2018.

Mishra, S., Tripathi, S. N., Kanawade, V. P., Haslett, S. L., Dada, L., Ciarelli, G., Kumar, V., Singh, A., Bhattu, D., Rastogi, N., Daellenbach, K. R., Ganguly, D., Gargava, P., Slowik, J. G., Kulmala, M., Mohr, C., El-Haddad, I., and Prevot, A. S. H.: Rapid night-time nanoparticle growth in Delhi driven by biomass-burning emissions, Nat Geosci, 16, 224-+, 10.1038/s41561-023-01138-x, 2023.

Mohr, C., Lopez-Hilfiker, F. D., Yli-Juuti, T., Heitto, A., Lutz, A., Hallquist, M., D'Ambro, E. L., Rissanen, M. P., Hao, L. Q., Schobesberger, S., Kulmala, M., Mauldin III, R. L., Makkonen, U., Sipilä, M., Petäjä, T., and Thornton, J. A.: Ambient observations of dimers from terpene oxidation in the gas phase: Implications for new particle formation and growth, Geophys Res Lett, 44, 2958−2966, https://doi.org/10.1002/2017gl072718, 2017.

Mohr, C., Thornton, J. A., Heitto, A., Lopez-Hilfiker, F. D., Lutz, A., Riipinen, I., Hong, J., Donahue, N. M., Hallquist, M., Petaja, T., Kulmala, M., and Yli-Juuti, T.: Molecular identification of organic vapors driving atmospheric nanoparticle growth, Nat Commun, 10, 4442, https://doi.org/10.1038/s41467-019-12473-2, 2019.

Murray, L. T.: Lightning NOx and Impacts on Air Quality, Curr Pollut Rep, 2, 115–133, 10.1007/s40726-016-0038-0, 2016.

Nel, A.: Air pollution-related illness: effects of particles, Science, 308, 804−806, https://doi.org/10.1126/science.1108752 2005.

Ng, N. L., Chhabra, P. S., Chan, A. W. H., Surratt, J. D., Kroll, J. H., Kwan, A. J., McCabe, D. C., Wennberg, P. O., Sorooshian, A., Murphy, S. M., Dalleska, N. F., Flagan, R. C., and Seinfeld, J. H.: Effect of NOx level on secondary organic aerosol (SOA) formation from the photooxidation of terpenes, Atmos Chem Phys, 7, 5159–5174, DOI 10.5194/acp-7-5159-2007, 2007.

Nie, W., Yan, C., Huang, D. D., Wang, Z., Liu, Y. L., Qiao, X. H., Guo, Y. S., Tian, L. H., Zheng, P. G., Xu, Z. N., Li, Y. Y., Xu, Z., Qi, X. M., Sun, P., Wang, J. P., Zheng, F. X., Li, X. X., Yin, R. J., Dallenbach, K. R., Bianchi, F., Petäjä, T., Zhang, Y. J., Wang, M. Y., Schervish, M., Wang, S. N., Qiao, L. P., Wang, Q., Zhou, M., Wang, H. L., Yu, C. A., Yao, D. W., Guo, H., Ye, P. L., Lee, S. C., Li, Y. J., Liu, Y. C., Chi, X. G., Kerminen, V. M., Ehn, M., Donahue, N. M., Wang, T., Huang, C., Kulmala, M., Worsnop, D., Jiang, J. K., and Ding, A. J.: Secondary organic aerosol formed by condensing anthropogenic vapours over China's megacities, Nat Geosci, 15, 255-+, 10.1038/s41561-022-00922-5, 2022.

Nozière, B., Kaberer, M., Claeys, M., Allan, J., D'Anna, B., Decesari, S., Finessi, E., Glasius, M., Grgić, I., Hamilton, J. F., Hoffmann, T., Iinuma, Y., Jaoui, M., Kahno, A., Kampf, C. J., Kourtchev, I., Maenhaut, W., Marsden, N., Saarikoski, S., Schnelle-Kreis, J., Surratt, J. D., Szidat, S., Szmigielski, R., and Wisthaler, A.: The molecular identification of organic compounds in the atmosphere: State of the art and challenges, Chem Rev, 115, 3919−3983, https://doi.org/10.1021/cr5003485, 2015.

O'Meara, S., Booth, A. M., Barley, M. H., Topping, D., and McFiggans, G.: An assessment of vapour pressure estimation methods, Phys Chem Chem Phys, 16, 19453-19469, 10.1039/c4cp00857j, 2014.

Pankow, J. F., and Asher, W. E.: SIMPOL.1: a simple group contribution method for predicting vapor pressures and enthalpies of vaporization of multifunctional organic compounds, Atmos Chem Phys, 8, 2773–2796, https://doi.org/10.5194/acp-8-2773-2008, 2008.

Peräkylä, O., Riva, M., Heikkinen, L., Quelever, L., Roldin, P., and Ehn, M.: Experimental investigation into the volatilities of highly oxygenated organic molecules (HOMs), Atmos Chem Phys, 20, 649-669, 10.5194/acp-20-649-2020, 2020.

Pye, H. O., Luecken, D. J., Xu, L., Boyd, C. M., Ng, N. L., Baker, K. R., Ayres, B. R., Bash, J. O., Baumann, K., Carter, W. P., Edgerton, E., Fry, J. L., Hutzell, W. T., Schwede, D. B., and Shepson, P. B.: Modeling the Current and Future Roles of Particulate Organic Nitrates in the Southeastern United States, Environ Sci Technol, 49, 14195-14203, 10.1021/acs.est.5b03738, 2015.

Ren, S. M., Yao, L., Wang, Y. W., Yang, G., Liu, Y. L., Li, Y. Y., Lu, Y. Q., Wang, L. H., and Wang, L.: Volatility parameterization of ambient organic aerosols a a rural site of the North China Plain, Atmos Chem Phys, 22, 9283-9297, 10.5194/acp-22-9283-2022, 2022.

Riva, M., Rantala, P., Krechmer, J. E., Perakyla, O., Zhang, Y. J., Heikkinen, L., Garmash, O., Yan, C., Kulmala, M., Worsnop, D., and Ehn, M.: Evaluating the performance of five different chemical ionization techniques for detecting gaseous oxygenated organic species, Atmos Meas Tech, 12, 2403–2421, https://doi.org/10.5194/amt-12-2403-2019, 2019.

Saarnio, K., Aurela, M., Timonen, H., Saarikoski, S., Teinila, K., Makela, T., Sofiev, M., Koskinen, J., Aalto, P. P., Kulmala, M., Kukkonen, J., and Hillamo, R.: Chemical composition of fine particles in fresh smoke plumes from boreal wild-land fires in Europe, Sci Total Environ, 408, 2527-2542, 10.1016/j.scitotenv.2010.03.010, 2010.

Schobesberger, S., D'Ambro, E. L., Lopez-Hilfiker, F. D., Mohr, C., and Thornton, J. A.: A model framework to retrieve thermodynamic and kinetic properties of organic aerosol from composition-resolved thermal desorption measurements, Atmos Chem Phys, 18, 14757−14785, https://doi.org/10.5194/acp-18-14757-2018, 2018.

Shiraiwa, M., Ammann, M., Koop, T., and Pöschl, U.: Gas uptake and chemical aging of semisolid organic aerosol particles, P Natl Acad Sci USA, 108, 11003−11008, https://doi.org/10.1073/pnas.1103045108, 2011.

Stolzenburg, D., Fischer, L., Vogel, A. L., Heinritzi, M., Schervish, M., Simon, M., Wagner, A. C., Dada, L., Ahonen, L. R., Amorim, A., Baccarini, A., Bauer, P. S., Baumgartner, B., Bergen, A., Bianchi, F., Breitenlechner, M., Brilke, S., Mazon, S. B., Chen, D. X., Dias, A., Draper, D. C., Duplissy, J., Haddad, I., Finkenzeller, H., Frege, C., Fuchs, C., Garmash, O., Gordon, H., He, X., Helm, J., Hofbauer, V., Hoyle, C. R., Kim, C., Kirkby, J., Kontkanen, J., Kürten, A., Lampilahti, J., Lawler, M., Lehtipalo, K., Leiminger, M., Mai, H., Mathot, S., Mentler, B., Molteni, U., Nie, W., Nieminen, T., Nowak, J. B., Ojdanic, A., Onnela, A., Passananti, M., Petäjä, T., Quéléver, L. L. J., Rissanen, M. P., Sarnela, N., Schallhart, S., Tauber, C., Tomé, A., Wagner, R., Wang, M., Weitz, L., Wimmer, D., Xiao, M., Yan, C., Ye, P., Zha, Q., Baltensperger, U., Curtius, J., Dommen, J., Flagan, R. C., Kulmala, M., Smith, J. N., Worsnop, D. R., Hansel, A., Donahue, N. M., and Winkler, P. M.: Rapid growth of organic aerosol nanoparticles over a wide tropospheric temperature range, P Natl Acad Sci USA, 115, 9122–9127, https://doi.org/10.1073/pnas.1807604115, 2018.

Thompson, S. L., Yatavelli, R. L. N., Stark, H., Kimmel, J. R., Krechmer, J. E., Day, D. A., Hu, W. W., Isaacman-VanWertz, G., Yee, L., Goldstein, A. H., Khan, M. A. H., Holzinger, R., Kreisberg, N., Lopez-Hilfiker, F. D., Mohr, C., Thornton, J. A., Jayne, J. T., Canagaratna, M., Worsnop, D. R., and Jimenez, J. L.: Field intercomparison of the gas/particle partitioning of oxygenated organics during the Southern Oxidant and Aerosol Study (SOAS) in 2013, Aerosol Sci Tech, 51, 30–56, https://doi.org/10.1080/02786826.2016.1254719, 2017.

Thornton, J. A., Mohr, C., Schobesberger, S., D'Ambro, E. L., Lee, B. H., and Lopez-Hilfiker, F. D.: Evaluating Organic Aerosol Sources and Evolution with a Combined Molecular Composition and Volatility Framework Using the Filter Inlet for Gases and Aerosols (FIGAERO), Acc Chem Res, 53, 1415-1426, 10.1021/acs.accounts.0c00259, 2020.

Voliotis, A., Wang, Y., Shao, Y. Q., Du, M., Bannan, T. J., Percival, C. J., Pandis, S. N., Alfarra, M. R., and McFiggans, G.: Exploring the composition and volatility of secondary organic aerosols in mixed anthropogenic and biogenic precursor systems, Atmos Chem Phys, 21, 14251-14273, 10.5194/acp-21-14251-2021, 2021.

Wang, D. S., and Ruiz, L. H.: Chlorine-initiated oxidation of n-alkanes under high-NOx conditions: insights into secondary organic aerosol composition and volatility using a FIGAERO-CIMS, Atmos Chem Phys, 18, 15535−15553, https://doi.org/10.5194/acp-18-15535-2018, 2018.

Wang, M. Y., Chen, D. X., Xiao, M., Ye, Q., Stolzenburg, D., Hofbauer, V., Ye, P. L., Vogel, A. L., Mauldin III, R. L., Amorim, A., Baccarini, A., Baumgartner, B., Brilke, S., Dada, L., Dias, A., Duplissy, J., Finkenzeller, H., Garmash, O., He, X. C., Hoyle, C. R., Kim, C., Kvashnin, A., Lehtipalo, K., Fischer, L., Molteni, U., Petäjä, T., Pospisilova, V., Quéléver, L. L. J., Rissanen, M., Simon, M., Tauber, C., Tomé, A., Wagner, A. C., Weitz, L., Volkamer, R., Winkler, P. M., Kirkby, J., Worsnop, D. R., Kulmala, M., Baltensperger, U., Dommen, J., El-Haddad, I., and Donahue, N. M.: Photo-oxidation of aromatic hydrocarbons produces low-volatility organic compounds, Environ Sci Technol, 54, 7911–7921, https://doi.org/10.1021/acs.est.0c02100, 2020.

Wu, C., Bell, D., Graham, E. L., Haslett, S., Riipinen, I., Baltensperger, U., Bertrand, A., Giannoukos, S., Schoonbaert, J., El Haddad, I., Prevot, A. S. H., Huang, W., and Mohr, C.: Photolytically Induced Changes in Composition and Volatility of Biogenic Secondary Organic Aerosol from Nitrate Radical Oxidation during Night-to-day Transition, Atmos Chem Phys Discuss, 1-29, https://doi.org/10.5194/acp-2021-347, 2021.

Yang, L. H., Takeuchi, M., Chen, Y. L., and Ng, N. L.: Characterization of thermal decomposition of oxygenated organic compounds in FIGAERO-CIMS, Aerosol Sci Tech, 55, 1321-1342, 10.1080/02786826.2021.1945529, 2021.

Yli-Juuti, T., Pajunoja, A., Tikkanen, O.-P., Buchholz, A., Faiola, C., Väisänen, O., Hao, L., Kari, E., Peräkylä, O., Garmash, O., Shiraiwa, M., Ehn, M., Lehtinen, K., and Virtanen, A.: Factors controlling the evaporation of secondary organic aerosol from α-pinene ozonolysis, Geophys Res Lett, 44, 2562−2570, https://doi.org/10.1002/2016GL072364, 2017.

Ylisirniö, A., Barreira, L. M. F., Pullinen, I., Buchholz, A., Jayne, J., Krechmer, J. E., Worsnop, D. R., Virtanen, A., and Schobesberger, S.: On the calibration of FIGAERO-ToF-CIMS: importance and impact of calibrant delivery for the particle-phase calibration, Atmos Meas Tech, 14, 355–367, https://doi.org/10.5194/amt-14-355-2021, 2021.

Zha, Q., Aliaga, D., Krejci, R., Sinclair, V. A., Wu, C., Ciarelli, G., Scholz, W., Heikkinen, L., Partoll, E., Gramlich, Y., Huang, W., Leiminger, M., Enroth, J., Peräkylä, O., Cai, R., Chen, X., Koenig, A. M., Velarde, F., Moreno, I., Petäjä, T., Artaxo, P., Laj, P., Hansel, A., Carbone, C., Kulmala, M., Andrade, M., Worsnop, D., Mohr, C., and Bianchi, F.: Oxidized organic molecules in the tropical free troposphere over Amazonia, National Science Review, nwad138, https://doi.org/10.1093/nsr/nwad138, 2023a.

Zha, Q. Z., Huang, W., Aliaga, D., Perakyla, O., Heikkinen, L., Koenig, A. M., Wu, C., Enroth, J., Gramlich, Y., Cai, J., Carbone, S., Hansel, A., Petaja, T., Kulmala, M., Worsnop, D., Sinclair, V., Krejci, R., Andrade, M., Mohr, C., and Bianchi, F.: Measurement report: Molecular-level investigation of atmospheric cluster ions at the tropical high-altitude research station Chacaltaya (5240 m a.s.l.) in the Bolivian Andes, Atmos Chem Phys, 23, 4559-4576, 10.5194/acp-23-4559-2023, 2023b.

Zhang, H. F., Yee, L. D., Lee, B. H., Curtis, M. P., Worton, D. R., Isaacman-VanWertz, G., Offenberg, J. H., Lewandowski, M., Kleindienst, T. E., Beaver, M. R., Holder, A. L., Lonneman, W. A., Docherty, K. S., Jaoui, M., Pye, H. O. T., Hu, W. W., Day, D. A., Campuzano-Jost, P., Jimenez, J. L., Guo, H. Y., Weber, R. J., de Gouw, J., Koss, A. R., Edgerton, E. S., Brune, W., Mohr, C., Lopez-Hilfiker, F. D., Lutz, A., Kreisberg, N. M., Spielman, S. R., Hering, S. V., Wilson, K. R., Thornton, J. A., and Goldstein, A. H.: Monoterpenes are the largest source of summertime organic aerosol in the southeastern United States, P Natl Acad Sci USA, 115, 2038–2043, https://doi.org/10.1073/pnas.1717513115, 2018.

Zheng, X., Wu, Y., Zhang, S., Hu, J., Zhang, K. M., Li, Z., He, L., and Hao, J.: Characterizing particulate polycyclic aromatic hydrocarbon emissions from diesel vehicles using a portable emissions measurement system, Sci Rep-Uk, 7, 10058, https://doi.org/10.1038/s41598-017-09822-w, 2017.

Supplement for:

Variation in chemical composition and volatility of oxygenated organic aerosol in different rural, urban, and ~~remote~~ mountain environments

Wei Huang[1], Cheng Wu[2,3], Linyu Gao[4], Yvette Gramlich[2,5], Sophie L. Haslett[2,5], Joel Thornton[6], Felipe D. Lopez-Hilfiker[7], Ben H. Lee[6], Junwei Song[4], Harald Saathoff[4], Xiaoli Shen[4,8], Ramakrishna Ramisetty[4,9], Sachchida N. Tripathi[10], Dilip Ganguly[11], Feng Jiang[4], Magdalena Vallon[4], Siegfried Schobesberger[12], Taina Yli-Juuti[12], Claudia Mohr[2,5,13,14,*]

[1]Institute for Atmospheric and Earth System Research / Physics, Faculty of Science, University of Helsinki, 00014, Helsinki, Finland

[2]Department of Environmental Science, Stockholm University, 11418, Stockholm, Sweden

[3]Now at: Department of Chemistry and Molecular Biology, University of Gothenburg, 41296, Gothenburg, Sweden

[4]Institute of Meteorology and Climate Research, Karlsruhe Institute of Technology, 76344, Eggenstein-Leopoldshafen, Germany

[5]Bolin Centre for Climate Research, Stockholm University, 11418, Stockholm, Sweden

[6]Department of Atmospheric Sciences, University of Washington Seattle, Washington 98195, United States

[7]Tofwerk AG, 3600 Thun, Switzerland

[8]Now at: Department of Earth, Atmospheric, and Planetary Sciences, Purdue University, West Lafayette, Indiana 47907, United States

[9]Now at: TSI Instruments India Private Limited, 560102, Bangalore, India

[10]Department of Civil Engineering, Indian Institute of Technology Kanpur, 208016, Kanpur, India

[11]Centre for Atmospheric Sciences, Indian Institute of Technology Delhi, 110016, New Delhi, India

[12]Department of Technical Physics, University of Eastern Finland, 70211, Kuopio, Finland

[13]Now at: Department of Environmental Systems Science, ETH Zürich, 8006 Zürich, Switzerland

[14]Now at: Laboratory of Atmospheric Chemistry, Paul Scherrer Institute, 5232 Villigen, Switzerland

**Correspondence to*: Claudia Mohr (claudia.mohr@psi.ch)

Table S1. Campaign-average (average ± 1 standard deviation) parameters for meteorology, trace gases, equivalent black carbon (eBC), total organics and total $PM_{2.5}$, double bond equivalent (DBE) values, and number of carbon atoms (nC) and oxygen atoms (nO) at different locations and different seasons.

Name	*T* (°C)	RH (%)	O_3 (ppbv)	NO_2 (ppbv)	SO_2 (ppbv)	eBC (μg m^{-3})	Org[a] (μg m^{-3})	$PM_{2.5}$[a] (μg m^{-3})	DBE	nC	nO	$\log_{10}C_{sat}$ (*298K*) (μg m^{-3})	$\log_{10}C_{sat}$ (*T*) (μg m^{-3})
MCC-t	0.3±2.1	53.0±22.4	/	/	/	0.2±0.4	0.3±0.5	1.0±1.8	3.1±0.2	8.4±0.8	6.2±0.3	1.6±0.3	-0.2±0.4
MCC-d	-0.4±1.9	52.2±18.8	/	/	/	0.3±0.4	0.5±0.5	1.6±1.4	3.2±0.1	7.7±0.7	5.8±0.3	2.2±0.4	0.6±0.3
REL	19.9±3.9	76.1±15.2	22.7±12.4	11.3±5.2	1.4±1.0	0.7±0.4	3.7±2.1	6.6±4.2	3.1±0.1	9.2±0.8	6.6±0.5	1.0±0.6	0.7±0.7
RAB	24.2±3.2	83.1±15.2	25.0±12.5	0.6±0.6	0.2±0.4	/	4.1±2.5	6.0±3.2	2.9±0.1	8.0±0.4	5.7±0.2	2.0±0.2	2.0±0.3
RHT	8.1±6.1	66.0±23.7	36.1±10.1	0.4±0.6	0.2±0.2	0.1±0.2	1.6±2.0	2.3±2.3	3.1±0.1	9.1±0.6	5.7±0.3	2.2±0.2	1.0±0.4
UST-s	24.6±4.0	55.1±12.8	29.6±7.5	9.7±4.1	3.9±2.8	1.0±0.3	5.1±3.2	7.1±3.3	3.4±0.1	8.8±0.4	6.4±0.2	1.6±0.2	1.6±0.3
UST-w	2.0±3.7	61.4±10.1	17.1±8.7	15.8±3.9	1.4±0.8	1.2±0.1	8.4±5.6	27.0±11.9	3.4±0.1	8.7±0.9	6.7±0.2	1.3±0.4	-0.4±0.4
UKA-s	25.9±6.6	49.8±21.0	37.4±19.8	9.6±6.4	/	0.7±0.4	3.9±2.4	5.9±2.8	3.6±0.2	10.7±0.8	7.0±0.4	0.8±0.6	0.6±0.8
UKA-w	13.2±3.3	56.4±13.4	27.8±10.0	9.2±7.1	0.6±1.0	0.5±0.5	1.9±1.6	3.9±3.6	3.5±0.1	11.2±0.8	7.1±0.4	0.4±0.5	-0.5±0.7
UDL	16.8±4.1	73.3±16.7	11.1±13.3	34.6±22.0	/	16.1±13.3	86.4±66.7	172.7±103.8	4.0±0.2	9.4±0.4	4.9±0.1	2.8±0.2	2.4±0.2

[a]Data were total non-refractory mass concentration from a high-resolution time-of-flight aerosol mass spectrometer (HR-ToF-AMS, Aerodyne Research Inc.) or an aerosol chemical speciation monitor (ACSM, Aerodyne Research Inc.).

Table S2. Deposition parameters and instrumental parameters at different locations and different seasons.

Name	Total inlet flow (L/min)/ Residence time (s)	Deposition time (min)	Mass loading (μg)[c]	FIGAERO type/ Sample mode	IMR body T (°C)	IMR pressure (mbar)	Ion source	Ratio of sample flow : ionizer flow	Ramp rate (°C/min)
MCC-t	7.0/1.4	120	0.3±0.3	Aerodyne/online	45	100	Corona discharge	2:1.3	13.3
MCC-d	7.0/1.4	120	0.4±0.4	Aerodyne/online	45	480	X-ray	2:1.3	13.3
REL	8.6/1.2	30	1.0±0.7	Aerodyne/online	45	100	Po-210	2:2	13.3
RAB	22/3.6	20	1.8±1.3	UW/online[d]	25	100	Po-210	2:2	10.0
RHT	11/4.2	30	0.5±0.8	UW/online[d]	25	100	Po-210	2:2	10.0
UST-s	8.7/0.8	112±43[b]	3.5±1.4	Aerodyne/offline	45	100	Po-210	2:2	13.3
UST-w	10.0/0.7	86±70[b]	4.0±1.0	Aerodyne/offline	45	100	Po-210	2:2	13.3
UKA-s	6.4/0.8	128±99[b]	3.2±2.1	Aerodyne/offline	45	100	Po-210	2:2	13.3
UKA-w	6.4/0.8	245±124[b]	3.0±1.5	Aerodyne/offline	45	100	Po-210	2:2	13.3
UDL	2.4[a]/2.8	3±1	0.6±0.5	Aerodyne/online	25	250	X-ray	2:1.5	6.7

[a]Average inlet flow of 3.5 L/min for the 1st week and 2 L/min for the next 2.5 weeks.

[b]Deposition time was average ± 1 standard deviation from offline filters.

[c]Mass loadings were calculated based on concurrent HR-ToF-AMS or ACSM measurements.

[d]FIGAERO inlet from the University of Washington, U.S., designed by Lopez-Hilfiker et al. (2014).

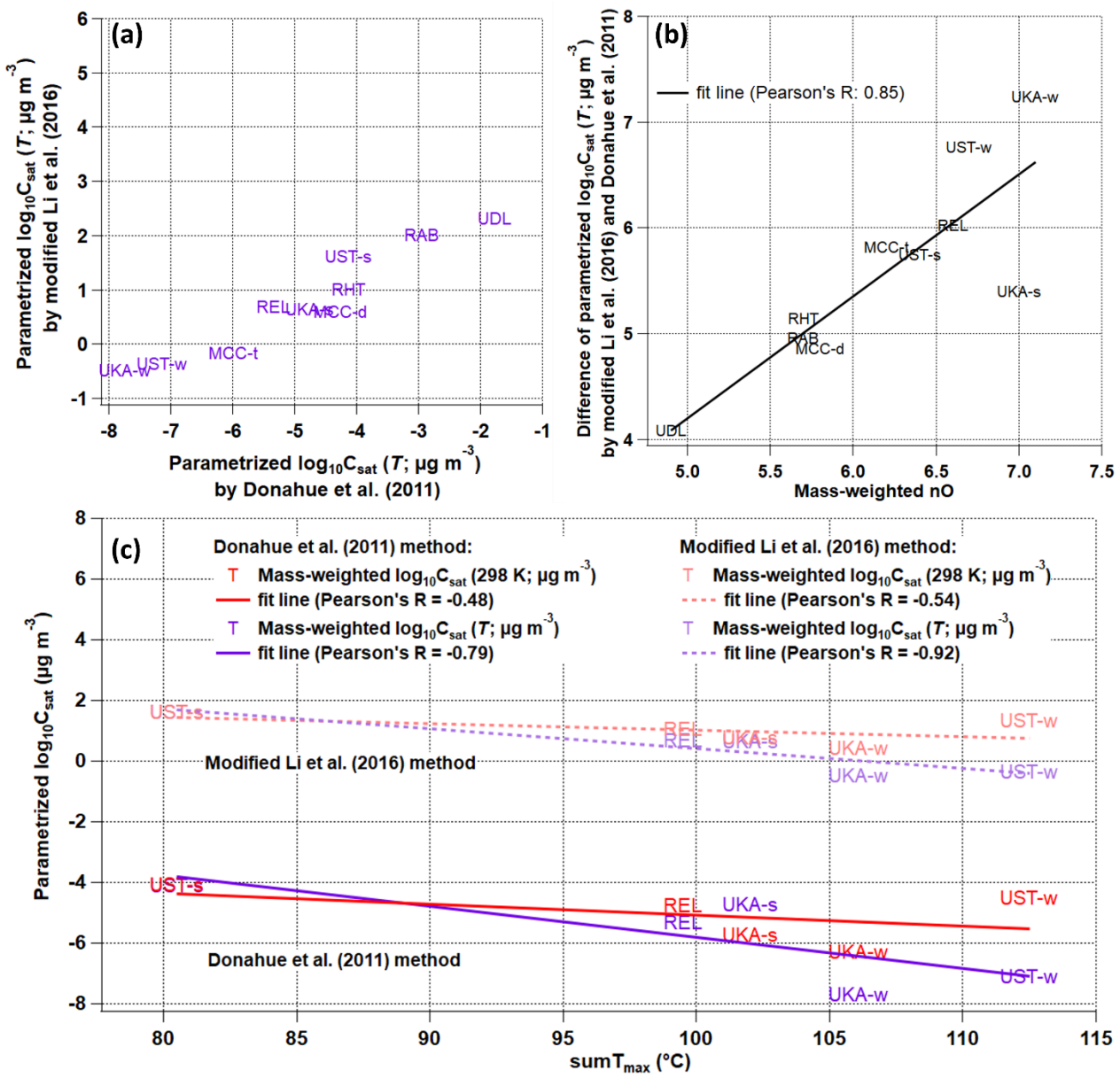

Figure S1. (a) Comparison of the campaign-average mass-weighted $\log_{10}C_{sat}$ (T) values using the modified Li et al. (2016) parametrization method (Daumit et al., 2013;Isaacman-VanWertz and Aumont, 2021) and the Donahue et al. (2011) method. **(b)** Comparison of the difference of campaign-average mass-weighted $\log_{10}C_{sat}$ (T) values using the modified Li et al. (2016) parametrization method (Daumit et al., 2013;Isaacman-VanWertz and Aumont, 2021) and the Donahue et al. (2011) method with the mass-weighted number of oxygen atoms (nO). **(c)** Comparison of the campaign-average mass-weighted $\log_{10}C_{sat}$ values and $sumT_{max}$ values for different locations and seasons (only datasets where the exact same FIGAERO setup was used), with mass-weighted $\log_{10}C_{sat}$ (298 K) in red and mass-weighted $\log_{10}C_{sat}$ (T) in purple; the colored lines are the fit lines for the corresponding markers.

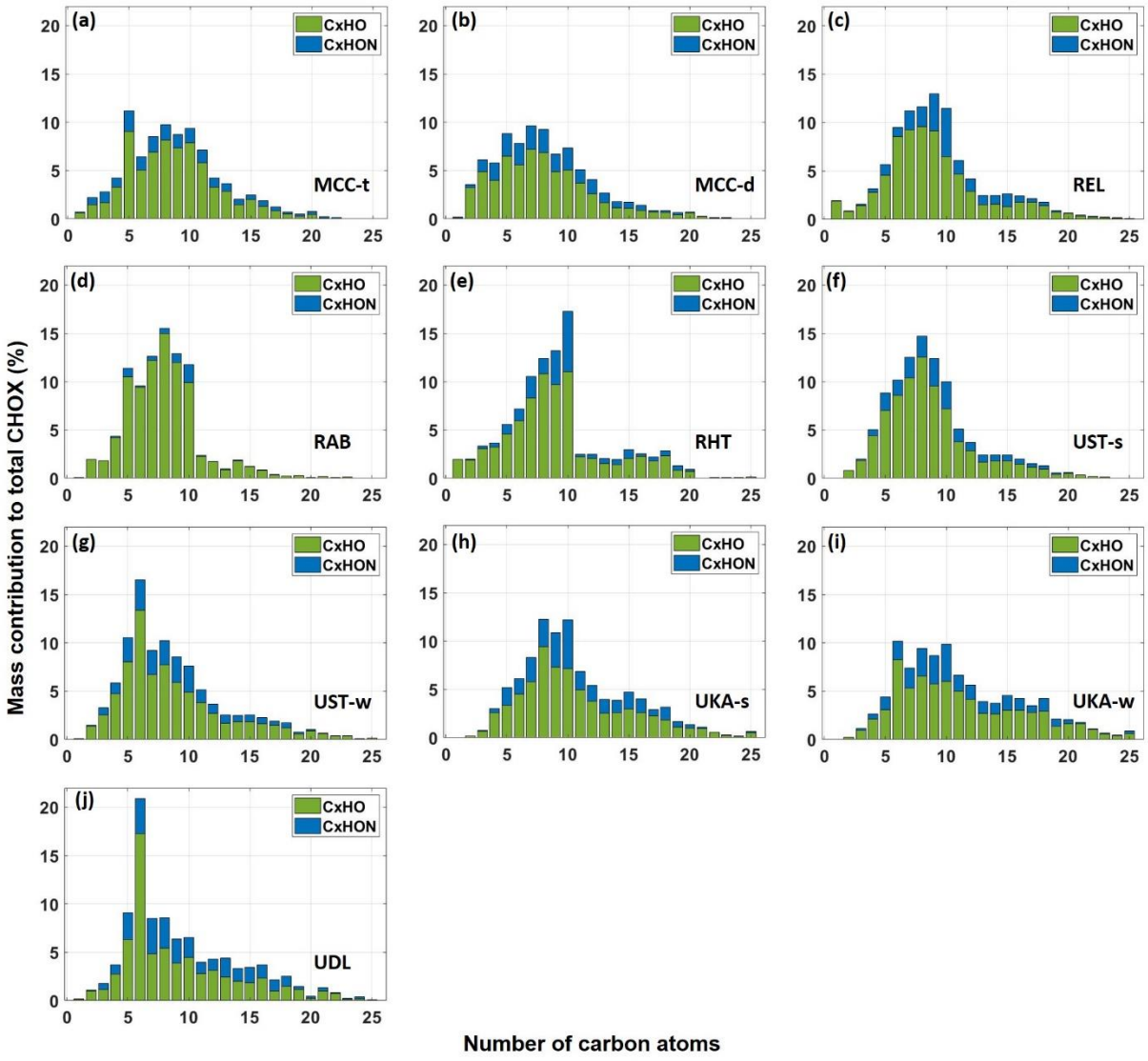

Figure ~~S1~~S2. Mass contributions of CHO and CHON compounds to total CHOX compounds as a function of the number of carbon atoms for MCC-t (a), MCC-d (b), REL (c), RAB (d), RHT (e), UST-s (f), UST-w (g), UKA-s (h), UKA-w (i), and UDL (j).

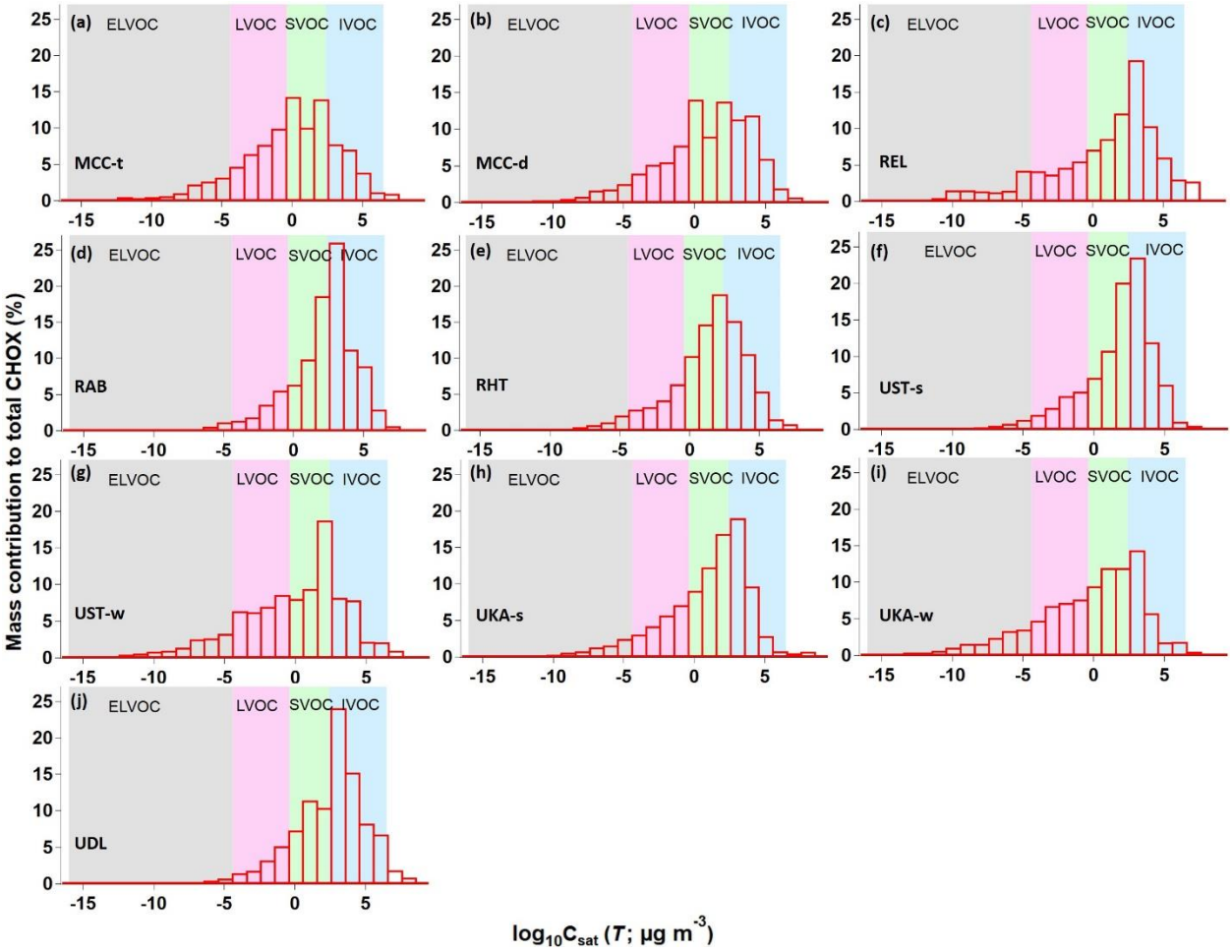

Figure ~~S2~~S3. Volatility distribution for MCC-t (a), MCC-d (b), REL (c), RAB (d), RHT (e), UST-s (f), UST-w (g), UKA-s (h), UKA-w (i), and UDL (j) with the modified Li et al. (2016) parameterization method (Daumit et al., 2013;Isaacman-VanWertz and Aumont, 2021).

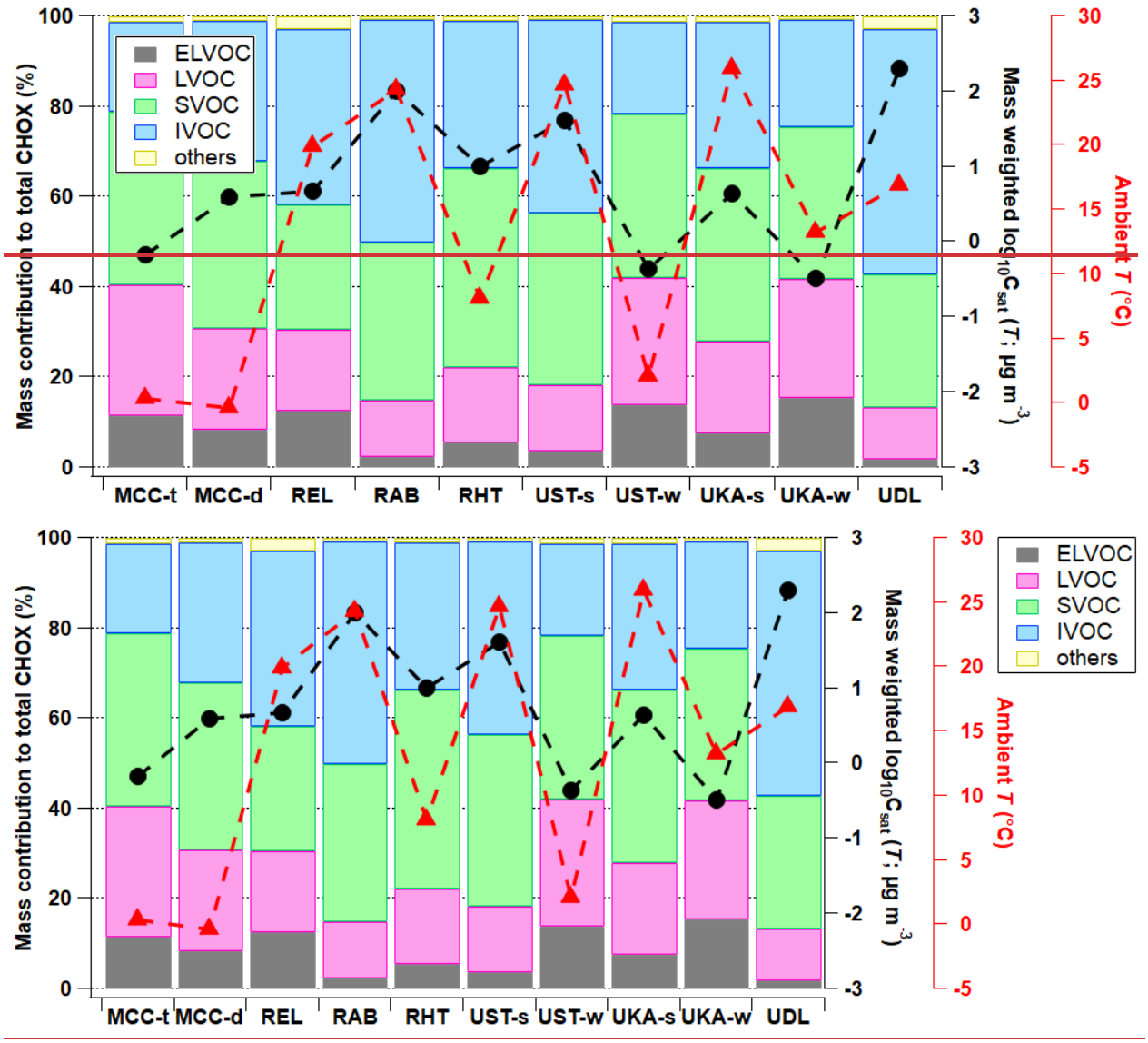

Figure S3S4. Comparison between ambient temperature (T) and campaign-average contribution (%) of different volatility groups resulting from VBS calculations to total organics (colored in bars) and campaign-average mass weighted $\log_{10}C_{sat}$ (T) values (in black markers) for different campaigns with the modified Li et al. (2016) parameterization method (Daumit et al., 2013;Isaacman-VanWertz and Aumont, 2021) (same as Figure 2). Compounds more volatile than IVOC with C_{sat} higher than $10^{6.5}$ μg m^{-3} (labelled as "others") contributed negligibly (0.8−2.9 %).

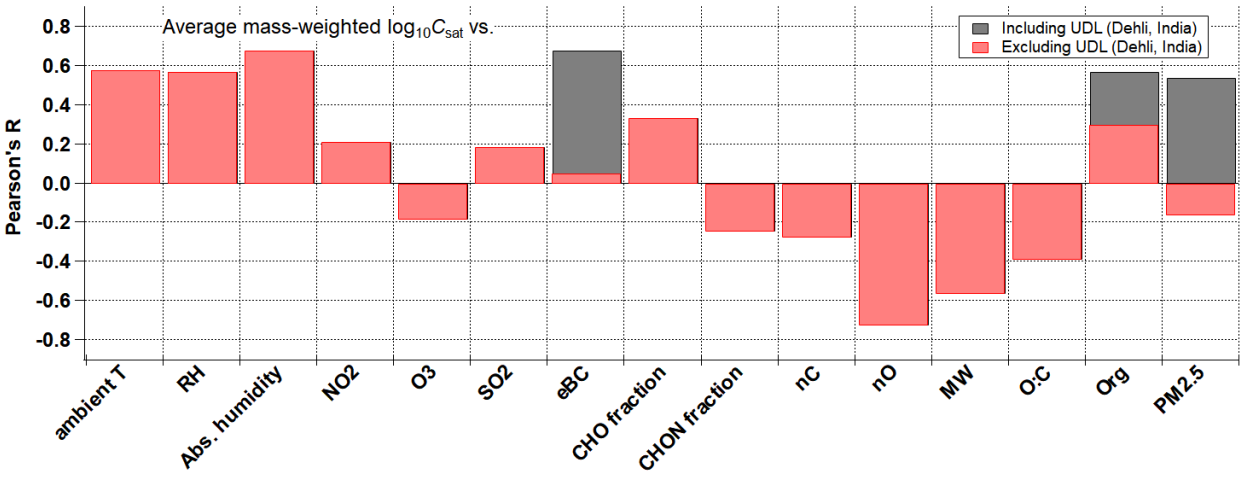

Figure ~~S4~~S5. Correlations of campaign-average mass weighted $\log_{10}C_{sat}$ values vs. other parameters. Pearson's R values including and excluding UDL (Dehli, India) data point for eBC, Org, and $PM_{2.5}$ are in gray bars and red bars, respectively, due to their extremely high levels at UDL (see Table S1). Org and $PM_{2.5}$ data were total non-refractory mass concentration from a high-resolution time-of-flight aerosol mass spectrometer (HR-ToF-AMS, Aerodyne Research Inc.) or an aerosol chemical speciation monitor (ACSM, Aerodyne Research Inc.).

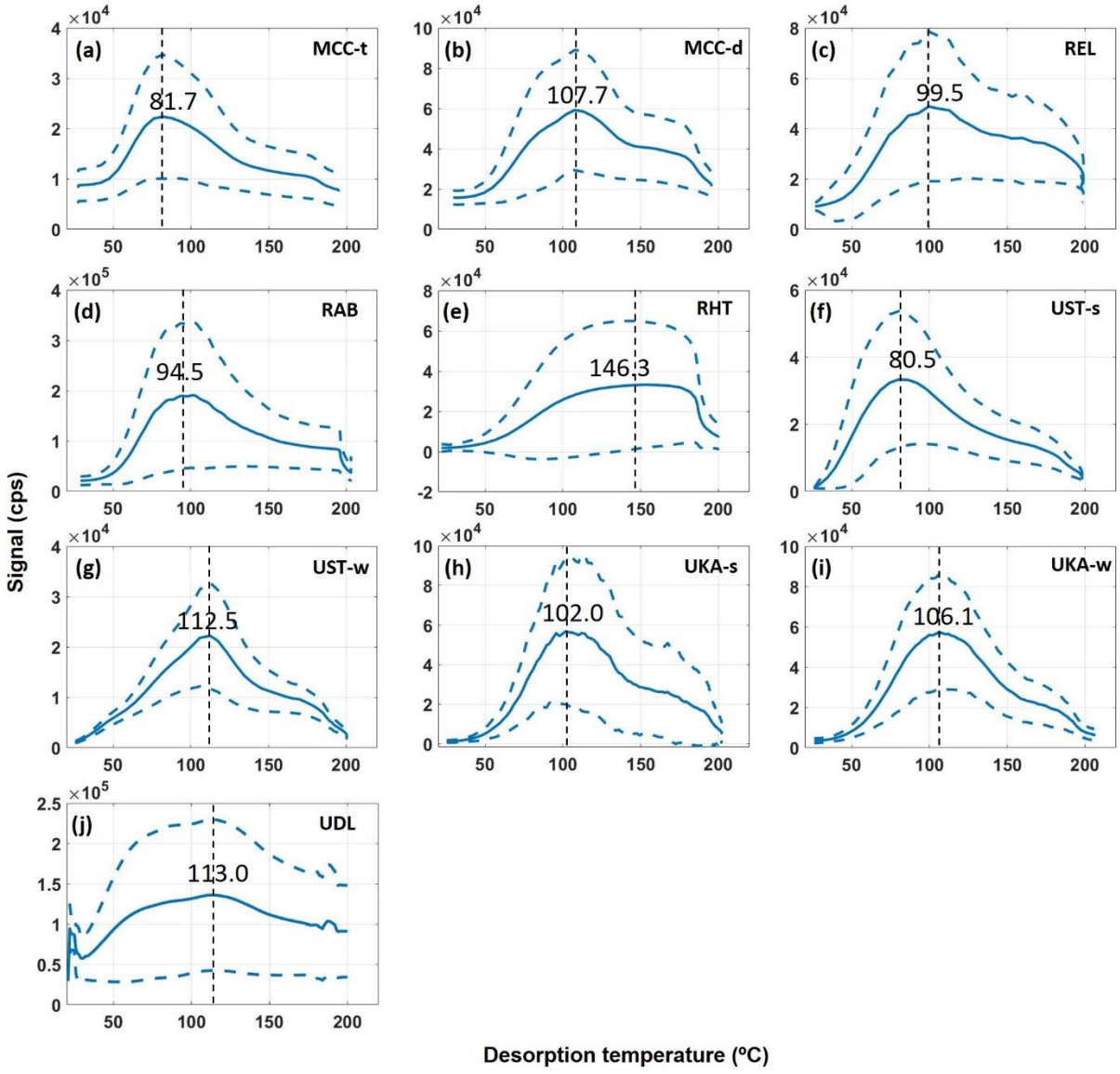

60 **Figure ~~S5~~S6.** Campaign-average sum thermograms of CHOX compounds for MCC-t (a), MCC-d (b), REL (c), RAB (d), RHT (e), UST-s (f), UST-w (g), UKA-s (h), UKA-w (i), and UDL (j). Dashed blue lines represent ±1 standard deviation and dashed black lines indicate the sumT_{max} values.

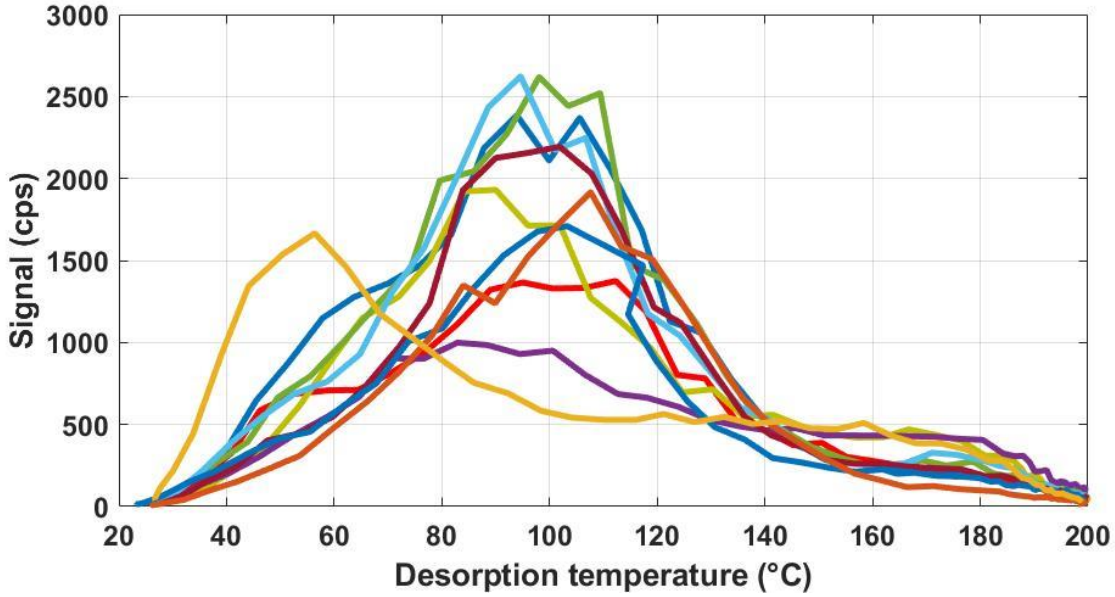

Figure ~~S6~~S7. Thermograms of $C_6H_{10}O_5$ compound during the whole campaign in winter Stuttgart (UST-w).

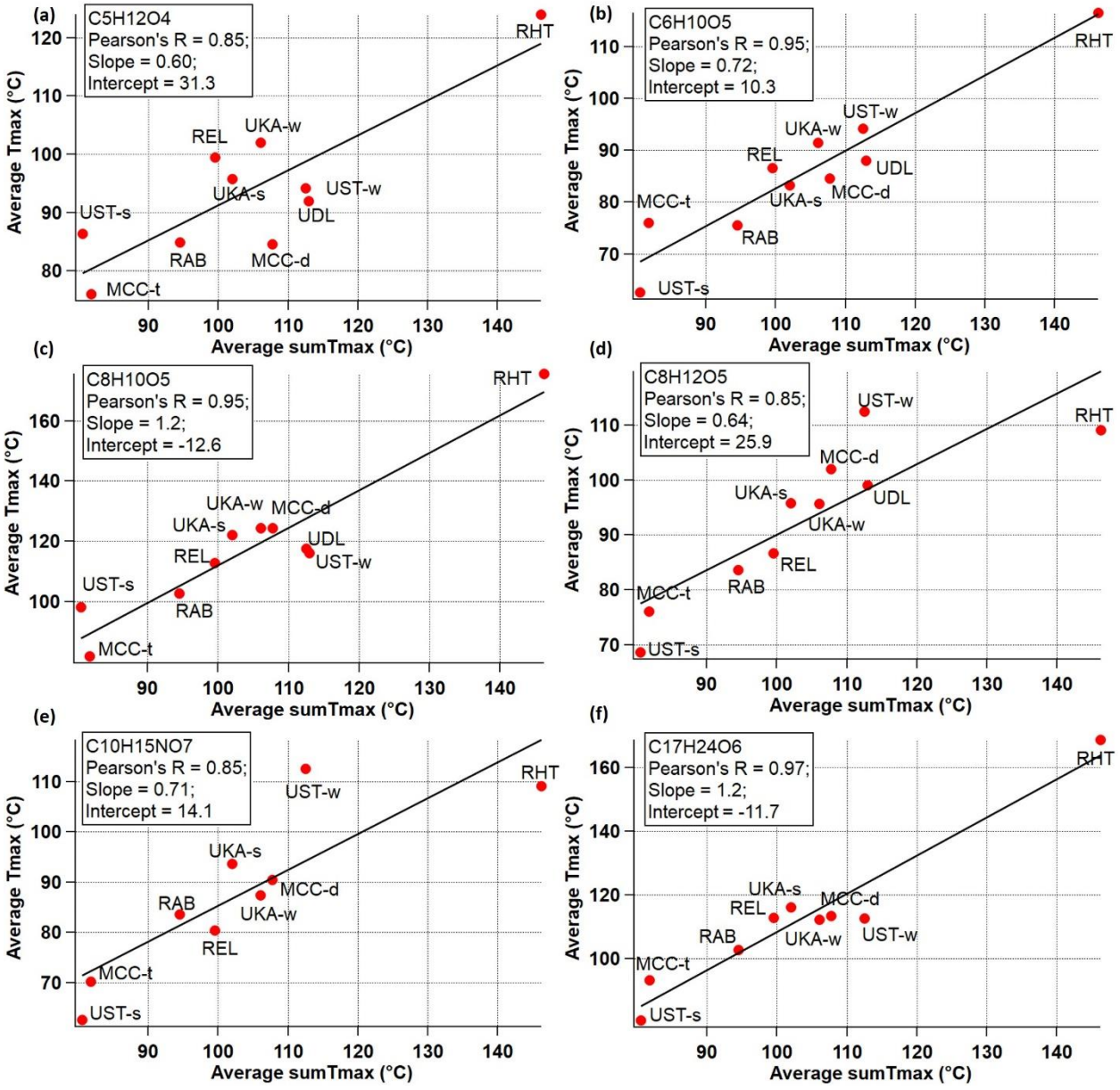

Figure ~~S7~~**S8.** Campaign-average T_{max} values for $C_5H_{12}O_4$ (a), $C_6H_{10}O_5$ (b), $C_8H_{10}O_5$ (c), $C_8H_{12}O_5$ (d), $C_{10}H_{15}NO_7$ (e), and $C_{17}H_{24}O_6$ (f) vs. the corresponding campaign-average $sumT_{max}$ values.

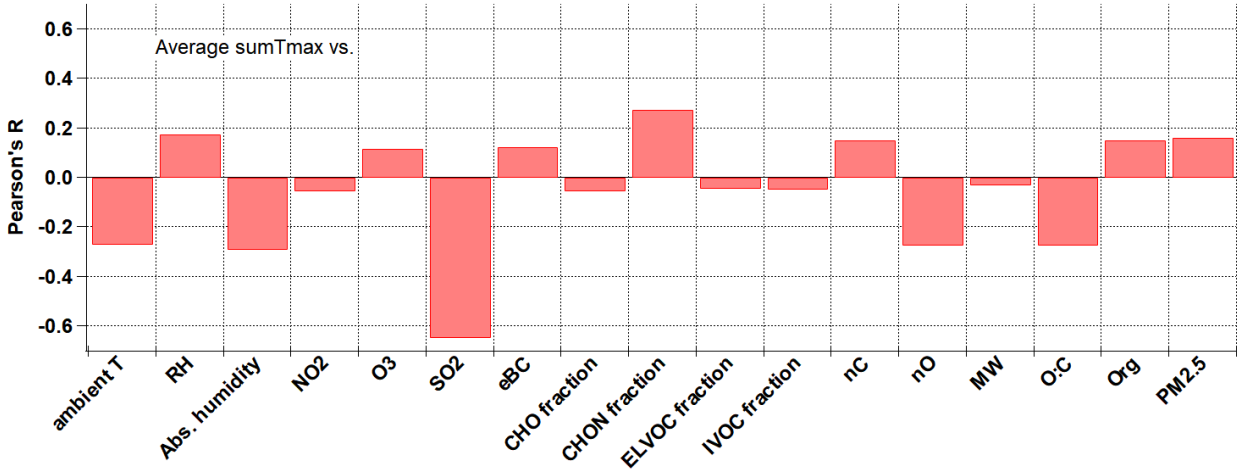

Figure ~~S8~~S9. Correlations of campaign-average sumT_{max} values vs. other parameters. Org and $PM_{2.5}$ data were total non-refractory mass concentration from a high-resolution time-of-flight aerosol mass spectrometer (HR-ToF-AMS, Aerodyne Research Inc.) or an aerosol chemical speciation monitor (ACSM, Aerodyne Research Inc.). The negative correlation with SO_2 (Pearson's R: -0.67) could be artificial as SO_2 would not react/condense directly onto aerosol particles and also less SO_2 data points were available for this correlation (see also Table S1). Levels of sulfur-containing organics (CHOS and CHONS) and non-refractory particulate sulfate show no correlations with sumT_{max} values as well.

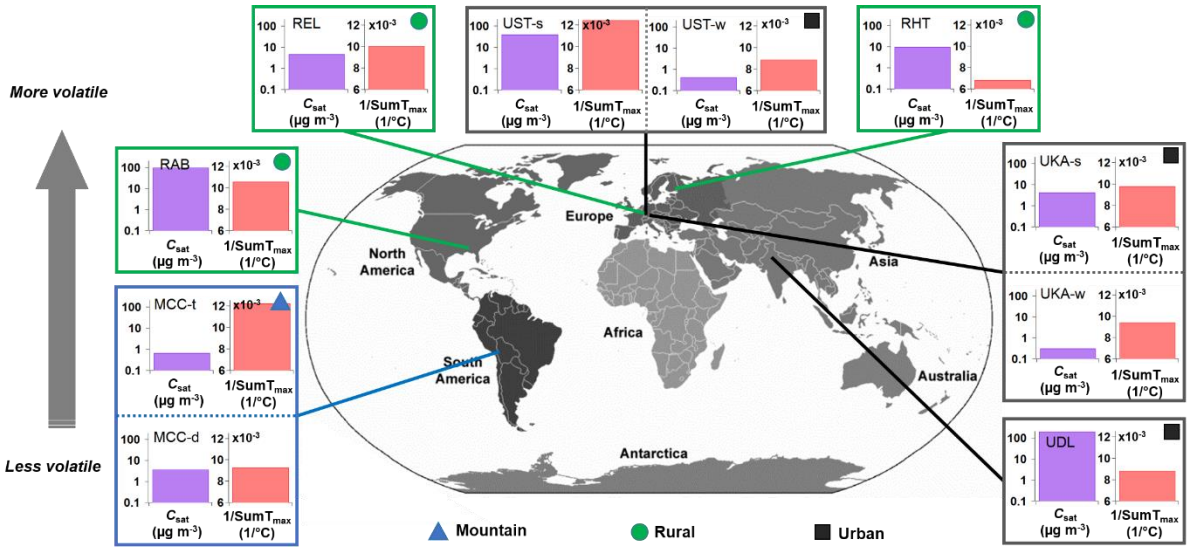

Figure ~~S9~~S10. Overview of the comparison of the average C_{sat} (T) (i.e, molecular composition-derived volatility) with the sumT$_{max}$ (i.e., thermal desorption-derived volatility) for different locations and seasons (Mountain sites in triangles, Rural sites in circles, and Urban sites in squares).

References

Daumit, K. E., Kessler, S. H., and Kroll, J. H.: Average chemical properties and potential formation pathways of highly oxidized organic aerosol, Faraday Discuss, 165, 181-202, https://doi.org/10.1039/C3FD00045A, 2013.

Donahue, N. M., Epstein, S. A., Pandis, S. N., and Robinson, A. L.: A two-dimensional volatility basis set: 1. organic-aerosol mixing thermodynamics, Atmos Chem Phys, 11, 3303–3318, https://doi.org/10.5194/acp-11-3303-2011, 2011.

Isaacman-VanWertz, G., and Aumont, B.: Impact of organic molecular structure on the estimation of atmospherically relevant physicochemical parameters, Atmos Chem Phys, 21, 6541–6563, https://doi.org/10.5194/acp-21-6541-2021, 2021.

Li, Y., Pöschl, U., and Shiraiwa, M.: Molecular corridors and parameterizations of volatility in the chemical evolution of organic aerosols, Atmos Chem Phys, 16, 3327–3344, https://doi.org/10.5194/acp-16-3327-2016, 2016.

Lopez-Hilfiker, F. D., Mohr, C., Ehn, M., Rubach, F., Kleist, E., Wildt, J., Mentel, T. F., Lutz, A., Hallquist, M., Worsnop, D., and Thornton, J. A.: A novel method for online analysis of gas and particle composition: description and evaluation of a Filter Inlet for Gases and AEROsols (FIGAERO), Atmos Meas Tech, 7, 983−1001, https://doi.org/10.5194/amt-7-983-2014, 2014.